ECONOMIC MANAGEMENT OF CONJUNCTIVE USE OF IRRIGATION WATER AND ROOT-ACCESSIBLE WATER TABLES

Report to the
WATER RESEARCH COMMISSION

by

B Grové[1], JH Barnard[2], JC Erasmus[1], MRM Hadebe[1]
[1] Department of Agricultural Economics, University of the Free State
[2] Department of Soil, Crop and Agricultural Science, University of the Free State

WRC Report No. 3118/1/23
ISBN 978-0-6392-0587-8

March 2024

WATER RESEARCH COMMISSION

UNIVERSITY OF THE FREE STATE
UNIVERSITEIT VAN DIE VRYSTAAT
YUNIVESITHI YA FREISTATA
UFS UV

Obtainable from
Water Research Commission
Bloukrans Building, Lynnwood Bridge Office Park
4 Daventry Street
Lynnwood Manor
PRETORIA

orders@wrc.org.za or download from www.wrc.org.za

This is the final report for WRC project no. C2019/2020-00209.

EXECUTIVE SUMMARY

BACKGROUND AND MOTIVATION

In South Africa, irrigated agriculture contributes significantly to the nation's field crop and horticultural production while exerting immense pressure on the country's water resources. Irrigated agriculture consumes approximately 64% of the available surface water in a country where water scarcity is prevalent (de Witt et al., 2021). The challenge of water scarcity is further compounded by projections suggesting intensified physical and economic water scarcity throughout Southern Africa by 2025 (Mabhaudhi et al., 2018).

Furthermore, the sector is troubled by low water use efficiency, prompting a pressing need for enhanced practices and optimal water use (Singels et al., 2019; de Witt et al., 2021). Research shows that current irrigation practices routinely overlook the significance of capillary rise from root-accessible water tables (Barnard et al., 2021) even though capillary rise from root-accessible water tables may contribute as much as 40% to crop evapotranspiration requirements (Jovanovic et al., 2004; Liu et al., 2022). This oversight might be the direct result of decision-makers' inability to comprehend the complexity of the interactions between irrigation scheduling decisions and the contribution of root-accessible water tables. Effective management of conjunctively using surface water, precipitation and root-accessible water tables requires information on the impact of irrigation scheduling decisions on water use and crop yield while acknowledging the necessity for irrigators to adjust their irrigation decisions to maximize the contribution of the most cost-effective water sources. The complexity of the interactions necessitates the use of integrated bio-economic optimisation models to provide the necessary information for decision support.

PROBLEM STATEMENT

Integrated bio-economic models that include enough detail to provide decision support to improve conjunctive use management of surface water and root-accessible water tables do not exist in South Africa, which hampers the conjunctive management of surface water and root-accessible water tables.

OBJECTIVES

The project's general objective was to develop and apply a bio-economic model to improve the conjunctive use and management of surface and shallow groundwater economically.

The following specific objectives were set to achieve the general objective of this research:

- To develop methods and procedures to calibrate complex soil-water-crop simulation models using inverse modelling.
- To develop methods and procedures to integrate a soil-crop-water simulation model with a financial accounting model with the purpose of simulating the economic impact of alternative conjunctive water use strategies.
- To develop an algorithm to optimise the conjunctive use of surface and shallow groundwater economically using the bio-economic simulation model.

APPROACH AND METHODS

The research team represents the scientific fields of Agricultural Economics and Crop and Soil sciences. The research commenced with reviewing the literature on bio-economic modelling to define a working conceptual framework to guide the responsibility assignments of the different scientific groupings. The review indicated that the choice of simulation to represent the biophysical component is extremely important to quantifying the impact of irrigation scheduling decisions on crop yield when root-accessible water tables are present. After reviewing several simulation models, AquaCrop and SWAP were chosen to represent the biophysical part of the bio-economic model.

The project team applied a Differential Evolution algorithm to calibrate both AquaCrop and SWAP using measured soil water content, seasonal biomass, and grain yield of maize. The measurements originate from lysimeter trials conducted by the Department of Soil, Crop and Climate Sciences of the University of the Free State to determine the contribution of root-accessible water tables to satisfying crop water requirements of maize.

The calibrated biophysical simulation models were linked to a financial model using Visual Basic to yield a bio-economic simulation model capable of simulating the financial impact of a predefined irrigation strategy. The bio-economic simulation model was then integrated with a differential evolution algorithm to optimise the contribution of root-accessible water tables to

satisfy crop water requirements by changing the irrigation decisions (i.e. timing and application).

The bio-economic optimisation models were applied to demonstrate the economic profitability of using root-accessible water tables as a water source by comparing a baseline irrigation strategy to an optimised one. The baseline irrigation strategy represents a situation where irrigators irrigate to satisfy crop water requirements. The optimised irrigation strategy represents irrigation decisions that will maximise the expected margin above the specified costs irrespective of the state of nature occurring. The research also evaluated a strategy where irrigators respond weekly to changing climatic conditions during the season.

SUMMARY OF RESULTS AND CONCLUSIONS

BIOPHYSICAL MODEL CALIBRATION AND VALIDATION

For AquaCrop, the DECAL calibration process showed good results, especially under non-limiting conditions. The validation results showed that AquaCrop could satisfactorily simulate soil water content, evapotranspiration, water table uptake and grain yield of maize grown on sandy soil. Measurements describing crop phenology, such as canopy cover, were not necessary for calibration using DECAL under these conditions. Instead, soil water content measurements were sufficient, while seasonal above-ground biomass played a crucial role in the objective function. The conclusion is that AquaCrop could be calibrated using inverse modelling when soil water measurements are available.

For SWAP, the results indicated that the calibrated model performed reasonably well, particularly in simulating soil water content and evapotranspiration. However, the validation results showed discrepancies in simulating above-ground biomass and grain yield, especially under shallow groundwater table conditions. This inconsistency might be due to the lack of calibration of soil hydraulic parameters, which were not considered in this study. The conclusion is that more complex models may require simultaneous calibration of soil properties and parameters determining crop water use and crop yield. In this regard, using sensitivity analysis to better understand parameter influences on modelling results can be vital for improving model outputs.

Overall, DECAL proved to be a valuable tool in fine-tuning calibration parameters.

BIO-ECONOMIC ANALYSES

The results of the baseline irrigation applications showed that water table uptake is negligible if the irrigators follow a strategy whereby crop water requirements are satisfied through irrigation and rainfall. The expectation is that such a strategy will result in an overirrigation of 19%. Water table uptake increased on average by 116 mm when water applications were reduced from 648 mm to 274 mm without affecting crop yield much. The maximum expected outcome of the irrigation strategy indicated substantial increases in water table uptake and reductions in water applications, which translate to notable increases in profitability (R2433 ha^{-1}), mainly due to increased water use efficiency. The conclusion is that the magnitude of water table uptake is a function of the decision maker's irrigation management decisions. Consequently, irrigators will forgo profits if they irrigate to satisfy crop evapotranspiration requirements because their conjunctive water use will be sub-optimal. Furthermore, irrigators must thoroughly understand the interrelated linkages between irrigation decisions and the state of the soil-water-atmosphere continuum in the presence of root-accessible water tables to optimise conjunctive water use. Such understanding requires soil water information and a mindset of not refilling the soil water back to field capacity when determining irrigation applications.

Results from the optimal sequential irrigation strategy showed negligible changes in the economic and biophysical indicators because the root-accessible water table acts as a buffer against climatic changes if the irrigation strategy is already devised to consider root-accessible water tables. The conclusion is that root-accessible water tables might be an important risk mitigation strategy in the presence of electricity load shedding and adverse climatic conditions.

SHORTCOMING

The evolutionary algorithm evaluates the biophysical system's current and possible future states and the time-of-use electricity tariff periods to devise an irrigation schedule (i.e. calendar of irrigations) to maximise expected profits. Since the evolutionary algorithm uses the “prescribed” irrigation scheduling option of the crop simulation model to optimise the irrigation schedule, providing a generic irrigation strategy defined by timing triggers and irrigation amounts is impossible. Consequently, no generic irrigation scheduling guideline could be devised to support better conjunctive water use strategies. However, solving the model recursively every week provides irrigation scheduling decision support for the upcoming week.

RECOMMENDATIONS

CALIBRATING BIOPHYSICAL MODELS

- Clarity on the objective of the calibration is essential when choosing calibration parameters. Some processes could be calibrated independently, while the parameters of interrelated processes must be calibrated simultaneously. Sensitivity analysis should target processes to identify the most influential parameters that need calibration.
- Automated calibration is a powerful tool to finetune calibration parameters. However, the calibration objective, selected calibration parameters and the bounds of these parameters must be carefully considered to produce realistic calibration parameters.

CONJUNCTIVE WATER USE

- Refilling the soil water content to field capacity is detrimental to maximising the contribution of root-accessible water tables to satisfying the evapotranspiration requirements of a crop. Irrigation strategies to maximise the contribution of root-accessible water tables must manage the soil water content so that the capillary fringe extends to its maximum level by leaving the soil dryer.
- Normal irrigation scheduling practices apply during the early stages of crop production while the roots have not reached the capillary fringe.
- Soil water measurements are essential for managing the contribution of root-accessible water tables to satisfy crop water requirements. Preferably, these measurements should include salinity indicators.
- Indirect estimates of crop water requirements (e.g. satellite imagery) must be supplemented with soil water measurements to maximise the contribution of root-accessible water tables to satisfy crop water requirements.
- Spatial monitoring of soil water content and water table depths is necessary to inform the water user association of any unintended hydrological consequences in the large-scale adoption of root-accessible water tables as a water source.

FURTHER RESEARCH

- The underlying information that the evolutionary algorithm uses to devise the optimal irrigation schedules needs to be further analysed using neural networks to develop

general guidelines to improve the conjunctive use of surface water and root-accessible water tables.

- The biophysical models' built-in irrigation scheduling options do not cater to irrigation strategies considering the contribution of root-accessible water tables. More research is necessary to develop generic strategies considering root-accessible water tables for these models.
- All indications are that maximising the contribution of root-accessible water tables to satisfy crop water requirements necessitated a lower soil water content. Research is necessary to understand fertiliser uptake and salinity buildup under these conditions.
- The research used Visual Basic for Applications to implement the DE algorithm to calibrate the biophysical models and optimise the contribution of root-accessible water tables to satisfy crop water requirements. The process could be done more efficiently using modern programming languages like Python. Such implementation will also allow capitalising on multithread processing.

ACKNOWLEDGEMENTS

The following reference group members supervised the project:

Dr L Nhamo	Water Research Commission (Chairman)
Prof. NS Mpandeli	Water Research Commission
Dr SN Hlophe-Ginindza	Water Research Commission
Prof. JG Annandale	University of Pretoria
Prof. T Mabhaudhi	University of KwaZulu-Natal
Dr H Oosthuizen	Optimal Agricultural Business Systems
Dr K Ndwambi	Khanimambo Innovative Solutions
Dr M Mutema	Agricultural Research Council
Dr SN Mokgehle	University of Mpumalanga
Dr MS Magombeyi	International Water Management Institute South Africa

The research team would like to sincerely thank the reference group members, especially the project chairman, for their guidance and valuable input and always being available to provide guidance and support when required.

Thanks to the farmers and specialists who were willing to discuss the project and project findings with the research team.

The team also wants to thank Dr MC du Plessis for his guidance in developing the genetic algorithm used for the study.

This page was intentionally left blank

TABLE OF CONTENTS

EXECUTIVE SUMMARY ..... **i**

ACKNOWLEDGEMENTS ..... **vii**

TABLE OF CONTENTS ..... **ix**

LIST OF TABLES ..... **xii**

LIST OF FIGURES ..... **xiv**

LIST OF ACRONYMS ..... **xvi**

LIST OF UNITS ..... **xvii**

CHAPTER 1: INTRODUCTION **1**

1.1 BACKGROUND AND MOTIVATION 1

1.2 PROBLEM STATEMENT 2

1.3 OBJECTIVES 2

1.4 STRUCTURE OF THE REPORT 3

CHAPTER 2: PROCESSES AND SCALE CONSIDERATION OF THE RESEARCH DOMAIN **4**

2.1 INTRODUCTION 4

2.2 REGIONAL, FARM AND FIELD SCALE 4

2.3 *IN SITU* FIELD DATA 7

2.4 RESEARCH IMPLICATIONS 9

CHAPTER 3: LITERATURE REVIEW **10**

3.1 BIO-ECONOMIC MODELLING DEFINED 10

3.2 CHARACTERISTICS OF BIO-ECONOMIC MODELS 10

3.2.1 POSITIVE OR NORMATIVE APPROACHES 10

3.2.2 UNIT OF ANALYSIS AND DECISION-MAKING UNIT 12

3.2.3 REPRESENTATION OF BIOPHYSICAL COMPONENT 12

3.2.3.1 Mathematical programming models 13

3.2.3.2 Evolutionary optimisation 15

3.2.4 DECISION-MAKING MODELLING 15

3.2.4.1 Objectives of the decision-maker 15

3.2.4.2 Responsive decision-making 16

3.2.4.3 Timing of decisions 17

3.3 BIOPHYSICAL MODELLING OF IRRIGATED FIELDS 20

3.3.1 RELEVANT MODELS 21
3.3.2 CROP GROWTH AND DEVELOPMENT MODELLING 24
3.3.3 WATER FLOW MODELLING 26
3.3.3.1 Soil water 27
3.3.3.2 Surface water 30
3.3.3.3 Subsurface water 31
3.3.3.4 Evaporation 31
3.3.3.5 Transpiration and root water uptake 33
3.4 RESEARCH IMPLICATIONS 34
CHAPTER 4: AQUACROP AND SWAP CALIBRATION AND VALIDATION 37
4.1 INTRODUCTION 37
4.2 SYNTHESIS OF PARAMETERS 38
4.2.1 AQUACROP 38
4.2.2 SWAP 41
4.3 EXPERIMENTAL DATA FOR CALIBRATION AND VALIDATION 44
4.4 MEASURED, DEFAULT AND PEDOTRANSFER PARAMETERS 46
4.5 DIFFERENTIAL EVOLUTION CALIBRATION ALGORITHM 51
4.6 RESULTS AND DISCUSSION 53
4.6.1 AQUACROP 53
4.6.2 SWAP 57
4.7 RESEARCH IMPLICATIONS 59
CHAPTER 5: BIO-ECONOMIC ANALYSIS OF CONJUNCTIVE WATER USE 61
5.1 INTRODUCTION 61
5.2 BIO-ECONOMIC OPTIMISATION MODEL 61
5.2.1 MODEL COMPONENTS AND INFORMATION FLOW 61
5.2.2 BIOPHYSICAL MODEL 63
5.2.3 ECONOMIC MODULE 63
5.2.4 DIFFERENTIAL EVOLUTION ALGORITHM 66
5.3 BIO-ECONOMIC ANALYSES 66
5.3.1 BASELINE 66
5.3.1.1 SWAP 66
5.3.1.2 AquaCrop 67
5.3.2 CONJUNCTIVE WATER USE OPTIMISATION 67
5.3.2.1 Expected outcome maximisation 68

5.3.2.2 Unfolding information maximisation 68
5.4 BIO-ECONOMIC MODEL SETUP AND DATA 69
5.4.1 SWAP DATA 69
5.4.2 AQUACROP DATA 70
5.4.3 ECONOMIC MODEL DATA 71
5.4.4 DIFFERENTIAL EVOLUTION ALGORITHM PARAMETERS 71
5.5 SWAP RESULTS 72
5.5.1 BIO-ECONOMIC ANALYSIS WITHOUT CONSIDERING WATER TABLE UPTAKE 72
5.5.2 BIO-ECONOMIC ANALYSIS OF CONJUNCTIVE WATER USE 73
5.5.2.1 Optimal Expected Outcome Irrigation Strategy 73
5.5.2.2 Optimal Sequential Irrigation Strategy 76
5.5.3 DISCUSSION 76
5.6 AQUACROP RESULTS 79
5.6.1 BIO-ECONOMIC ANALYSIS WITHOUT CONSIDERING WATER TABLE UPTAKE 79
5.6.2 BIO-ECONOMIC ANALYSIS OF CONJUNCTIVE WATER USE 80
5.6.3 DISCUSSION 82
CHAPTER 6: CONCLUSIONS, SHORTCOMINGS AND RECOMMENDATIONS 83
6.1 SUMMARY OF RESULTS AND CONCLUSIONS 83
6.1.1 BIOPHYSICAL MODEL CALIBRATION AND VALIDATION 83
6.1.2 BIO-ECONOMIC ANALYSES 83
6.2 SHORTCOMING 84
6.3 RECOMMENDATIONS 84
6.3.1 CALIBRATING BIOPHYSICAL MODELS 84
6.3.2 CONJUNCTIVE WATER USE 85
6.3.3 FURTHER RESEARCH 85
REFERENCES 87
APPENDIX A: CONSOLIDATED STUDENT CAPACITY BUILDING AND KNOWLEDGE DISSEMINATION 106
APPENDIX B: DATA ARCHIVING 110

LIST OF TABLES

Table 3.1: List of modelling studies for the past ten years specifically related to the presence of root-accessible water tables in crop systems 22

Table 3.2: Approaches applied by various crop models in simulating major processes determining crop growth and development as summarised by Palosuo et al. (2011) (Abbreviations are provided in the text) 24

Table 3.3: Number of crop parameters used to describe the various processes (Figure 4) as simulated by WOFOST (de Wit et al., 2019) 25

Table 3.4: Number of crop parameters used to describe the various processes as simulated by AquaCrop (Reas et al., 2018) 26

Table 3.5: Water flow processes simulated by various soil-crop water models 27

Table 4.1: Parameters required by AquaCrop for simulating crop growth, development, final yield and soil-crop-water flow processes under non-limiting conditions 39

Table 4.2: Parameters required by SWAP for simulating crop growth, development, final yield and soil-crop-water flow processes under non-limiting conditions 42

Table 4.3: Agronomic practices of maize for the lysimeter trials done by Ehlers et al. (2003) and Ehlers et al. (2007) 46

Table 4.4: Measured and pedotransfer function estimated parameters for the Clovelly soil used in AquaCrop 48

Table 4.5: Default parameters used in AquaCrop for simulating Trials 1 and 2 as provided in Annexes of the reference manual by Raes et al. (2022) 48

Table 4.6: Vertical discretization of the soil profile in SWAP 50

Table 4.7: Mualem-van Genuchten parameters of the three identified soil layers in the lysimeters describing the soil hydraulic functions used in SWAP 50

Table 4.8: Default parameters used in SWAP for simulating Trials 1 and 2 51

Table 4.9: DECAL estimated AquaCrop parameters for maize grown on the sandy Clovelly soil for the control treatment of Trial 1 54

Table 4.10: DECAL estimated SWAP parameters for maize grown on the sandy loam Bainsvlei soil for the control treatment of Trial 1 57

Table 5.1: Irrigated maize production cost estimates (2021) 71

Table 5.2: Economic and biophysical indicators when applying a state-specific full irrigation strategy without considering root-accessible water table uptake on a 30.1 ha pivot (2021) 73

Table 5.3: Economic and biophysical indicators for the optimal expected outcome strategy considering water table uptake and the changes relative to a state-specific full irrigation strategy for a 30.1 ha pivot (2021) 75

Table 5.4: Economic and biophysical indicators for a state-specific sequential strategy considering water table uptake and the changes relative to the optimal expected outcome irrigation strategy for a 30.1 ha pivot (2021) 77

Table 5.5: Expected simulation bio-economic indicators for the baseline irrigation strategies on a Clovelly soil with a 1.5 m constant groundwater table on a 30.1 ha pivot (2023) 79

Table 5.6: Expected bio-economic indicators for the optimal irrigation strategies on a Clovelly soil with a 1.5 m constant groundwater table and the changes relative to the baseline strategies of 274 mm and 648 mm on a 30.1 ha pivot (2023) 81

LIST OF FIGURES

Figure 2.1: Conceptualization of the water flow processes that influence root zone water availability on a regional and farm scale. 4

Figure 2.2: The domain of the study stretches from a plane just above the canopy to a plane in the shallow groundwater. 5

Figure 3.1: Forward recursive stochastic decision-making framework where solid squares represent fixed decisions, circles represent possible events to unfold, dashed squares represent decisions that will be optimised, triangles represent the outcome, A represents the area, I represents the irrigation decisions, T represents decision stage, and S represents the possible state of nature to unfold. 19

Figure 3.2: Visual illustration of the major processes and their linkage simulated by WOFOST (de Wit et al., 2019). 25

Figure 4.1: Weather data for the 2000-2001 and 2004-2005 maize growing seasons done by Ehlers et al. (2003) and Ehlers et al. (2007), respectively, at the lysimeter facility of the Department Soil, Crop and Climate Sciences, University of the Free State. 47

Figure 4.2: Illustration of soil water profile, at saturation (Sat), field capacity (FC) and adjusted field capacity (FCadj), in equilibrium with the groundwater as used in AquaCrop (Raes et al., 2022). 49

Figure 4.3: Comparison between measured and AquaCrop simulated soil water content and cumulative evapotranspiration (ET) using parameters in Tables 4.4, 4.5 and 4.6 without a water table. 54

Figure 4.4: Comparison between measured (ms) and AquaCrop simulated (sm) soil water content, cumulative evapotranspiration (ET) and cumulative water table uptake (WTU) using parameters in Tables 4.4, 4.5 and 4.6 under a constant water table at a depth of 1.5 and 1.2 m. 55

Figure 4.5: Comparison between measured (ms) and SWAP simulated (sm) soil water content and cumulative evapotranspiration (ET) using parameters in Tables 4.7, 4.8 and 4.10 in the absence of a groundwater table. 58

Figure 4.6: Comparison between measured (ms) and SWAP simulated (sm) soil water content, cumulative evapotranspiration (ET) and cumulative water table uptake (WTU) using parameters in Tables 4.7, 4.8 and 4.10 under a constant groundwater table at a depth of 1.5 and 1.2 m. 58

LIST OF ACRONYMS

$BM_{(s)}$	seasonal measured above-ground biomass
CWPF	Crop Water Production Function
DE	Differential Evolution
DECAL	Differential Evolution calibration
DEOPT	Differential Evolution Optimisation
EA	Evolutionary Algorithm
ET	Evapotranspiration
$ET_{(w)}$	weekly estimated evapotranspiration
FAO	Food and Agriculture Organisation
MAD	Mean Absolute Deviation
MAS	Margin above the specified costs
NRMSE	Normalised Root Mean Square Error
PE	absolute Percentage Error
WC	Water Content
$WC_{1.8(w)}$	weekly simulated soil water content over a depth of 1.8 m
WPF	Water Production Function
WRC	Water Research Commission
WTU	Water Table Uptake
WUA	Water User Association
$\theta_{(w)}$	weekly measured volumetric soil water content

LIST OF UNITS

°C	degree Celsius
%	percentage
% t^{-1}	percentage per growing degree day
bar	100 kilopascal
c kWh^{-1}	cent per kilowatt-hour
cm	centimetre
cm day^{-1}	centimetre per day
cm t^{-1}	centimetre per growing degree day
cm^2	square centimetre
cm^3 cm^{-3}	cubic centimetre per cubic centimetre
g m^{-2}	gram per square metre
h	hours
ha	hectare
ha kg^{-1}	hectare per kilogram
kg ha^{-1}	kilogram per hectare
kg ha^{-1} $hour^{-1}$	kilogram per hectare per hour
kg J^{-1}	kg per joule
kg kg^{-1} day^{-1}	kilogram per kilogram per day
kPa	kilopascal
kVAR	kilovar
kW	kilowatt
m	metre
m^2 m^{-2}	square metre per square metre
m^2 m^{-2} day^{-1}	square metre per square metre per day
m^3 m^{-3}	cubic metre per cubic metre
m^3 h^{-1}	cubic metre per hour
mm	millimetre
mm day^{-1}	millimetre per day
mSm^{-1}	millisiemens per metre
plants ha^{-1}	plants per hectare
R	Rand
R $1000h^{-1}$	Rand per 1000 hours
R h^{-1}	Rand per hour
R ha^{-1}	Rand per hectare

R $kVARh^{-1}$	Rand per kilovarhour
R kWh^{-1}	Rand per kilowatthour
R mm^{-1}	Rand per millimetre
R t^{-1}	Rand per ton
t	growing degree days
t ha^{-1}	ton per hectare

CHAPTER 1: INTRODUCTION

1.1 BACKGROUND AND MOTIVATION

The National Development Plan 2030 (National Planning Commission of South Africa, 2102) identifies the need for rural communities to participate fully in the country's economic, social and political life. In this regard, irrigated agriculture has been identified as a major role player in achieving an integrated rural economy. The Irrigation Strategy for South Africa has set a target to increase irrigated land by more than 50% in South Africa (DAFF, 2015). Water availability is the major limiting factor in the growth of this sector. On the contrary, the government argues that irrigated agriculture, as the largest water user in the country, may provide large amounts of water by using irrigation water more efficiently.

The Water Research Commission (WRC) of South Africa has funded research on the efficient use of surface irrigation water, completed over several decades. Annandale et al. (2011) offer an excellent review of past irrigation scheduling experiences in South Africa. In particular, four irrigation scheduling modelling efforts stand out, namely SAPWAT (Van Heerden and Walker, 2016), BEWAB (Bennie et al., 1988), PUTU (De Jager et al., 2001), SWB (Annandale et al., 1999a) and MyCanesim (Singels and Smit, 2009). Several studies also showed the economic benefits of alternative irrigation water use strategies to improve surface irrigation water use efficiency (Oosthuizen et al., 1996; Venter et al., 2017; Grové et al., 2019). None of the studies evaluated the economic benefits of the conjunctive use of surface water and shallow groundwater, even though it is estimated that the contribution of shallow groundwater to crop water demand may be as large as 65% (Ehlers et al., 2003). According to Ayar et al. (2006), shallow groundwater is routinely overlooked when water management alternatives are considered in irrigated agriculture. The last mentioned is corroborated by research done by Barnard et al. (2017), who showed that irrigation farmers in Vaalharts irrigate according to their crop water requirements without considering the contribution of shallow groundwater through capillary rise.

Devising irrigation management strategies to maximise the use potential of shallow groundwater is complicated as capillary rise from shallow groundwater is affected by groundwater depth, groundwater quality, crop growth stage, crop salt tolerance, irrigation frequency and depth of irrigation applications. The complexity of the problem makes it impossible to conduct experiments that will cover all the factors at once (Ayar et al., 2006). Simulation models provide a powerful means to analyse complex systems and develop water

management strategies. In most cases, all the input parameters necessary to model a system with a particular model are unavailable. The application of sophisticated models that model all the essential processes to maximise the contribution of shallow groundwater to crop growth in South Africa is, therefore, scarce. Šimůnek and de Vos (1999) proposed an estimation method of unknown parameters using inverse optimisation modelling. Inverse modelling uses information from easily measured variables to estimate soil properties, which are usually very difficult to obtain. Recently, Sedaghatdoost et al. (2019) applied inverse modelling to estimate the SWAP model's soil hydraulic and solute transport parameters satisfactorily.

Even though a well-calibrated simulation model might be available to simulate conjunctive irrigation and shallow groundwater usage, it might still be challenging to optimise conjunctive use strategies economically. The interrelated linkages between irrigation management decisions, soil water dynamics, water application costs, and the resulting crop yield make the problem very complex. The complexity of the problem renders the application of standard optimisation methods infeasible. Several researchers (Schutze et al., 2012; Lehmann and Finger, 2014; Grové and du Plessis, 2019) have recently demonstrated the feasibility of evolutionary algorithms to optimise agricultural water use by integrating biophysical simulation models and economic models.

1.2 PROBLEM STATEMENT

Integrated bio-economic models that include enough detail to provide decision support to improve conjunctive use management of surface water and root-accessible water tables do not exist in South Africa, which hampers the conjunctive management of surface water and root-accessible water tables.

1.3 OBJECTIVES

The project's general objective was to develop and apply a bio-economic model to improve the conjunctive use and management of surface and shallow groundwater economically.

The following specific objectives were set to achieve the general objective of this research:

- To develop methods and procedures to calibrate complex soil-water-crop simulation models using inverse modelling.
- To develop methods and procedures to integrate a soil-crop-water simulation model with a financial accounting model with the purpose of simulating the economic impact of alternative conjunctive water use strategies.

- To develop an algorithm to optimise the conjunctive use of surface and shallow groundwater economically using the bio-economic simulation model.

1.4 STRUCTURE OF THE REPORT

Chapter 1 provides the background and motivation for the research as well as the problem statement and objectives of the research.

Chapter 2 contextualises the research domain by providing information regarding the hydrological processes governing soil water flow to clarify the necessary modelling assumptions made during the research.

A literature review on bio-economic modelling is done in Chapter 3 to inform the development of the bio-economic optimisation model to evaluate conjunctive irrigation water use strategies. Special attention is given to different models for simulating the interaction between irrigation management decisions, soil water dynamics in the presence of root-accessible water tables and crop yields.

Chapter 4 discusses the calibration and validation of AquaCrop and SWAP to represent the bio-physical component of the bio-economic optimisation model. The first part discusses the data and methods used, while the latter discusses the results.

Chapter 5 discusses the development of the bio-economic optimisation model and the results from applying the bio-economic optimisation model to evaluate the conjunctive use of surface and root-accessible water tables.

The conclusions and recommendations for further research are given in Chapter 6.

CHAPTER 2: PROCESSES AND SCALE CONSIDERATION OF THE RESEARCH DOMAIN

2.1 INTRODUCTION

This WRC project is a modelling study. Hence, Chapter 2 provides background regarding the soils, groundwater table depths, crop, irrigation volumes, and initial and boundary conditions used during modelling. Chapter 2 will also explain why specific assumptions were made during modelling.

2.2 REGIONAL, FARM AND FIELD SCALE

Figure 2.1 conceptualizes the water flow processes influencing root zone water availability on a regional and farm scale. Confined and unconfined (does not have a confining layer on top) aquifers are groundwater reservoirs saturated with water composed of confining units such as sand and gravel, sandstone, limestone and fractured, crystalline rocks. Groundwater above unsaturated rock formations or clay layers is referred to as a perched aquifer because of a discontinuous impermeable layer.

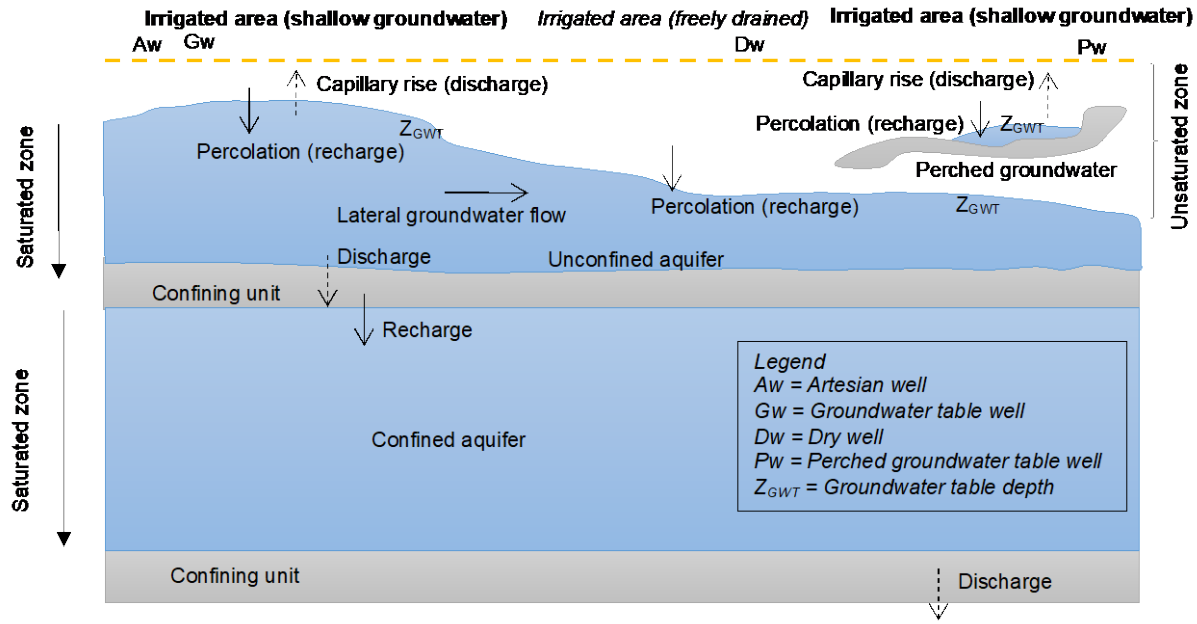

Figure 2.1: Conceptualization of the water flow processes that influence root zone water availability on a regional and farm scale.

Typically, four scenarios (or conditions) occur at the farm scale where shallow groundwater tables are present and accessible to roots through capillary rise. The first scenario is where groundwater below the root zone of the irrigated field flows laterally to lower-laying fields. In addition, there will be an artificial drainage flux from the installed subsurface drainage system. Local recharge to the groundwater below the irrigated field includes percolation of rain and/or irrigation beyond the root zone. Regional recharge is from higher laying areas and fields due to leakage of irrigation and/or drainage canals, irrigation dams and over-irrigation of fields. Discharge from the groundwater below an irrigated field is through the artificial drainage flux and groundwater flow to lower laying areas. No artificial drainage system is present in the second scenario, but lateral groundwater flow to lower laying areas is possible. The third and fourth scenarios represent a worse case where the groundwater below the root zone is stagnant (with no lateral movement possible) with and without an artificial drainage system.

The field scale stretches from a plane just above the canopy to a plane in the shallow groundwater and defines the domain of the study (Figure 2.2).

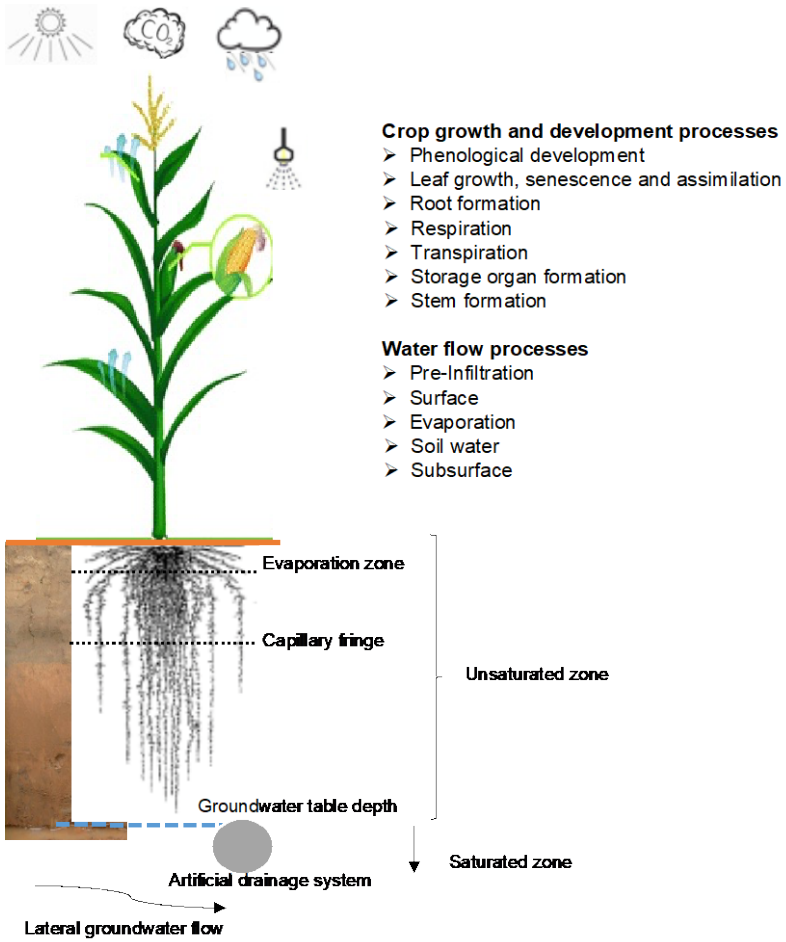

Figure 2.2: The domain of the study stretches from a plane just above the canopy to a plane in the shallow groundwater

Potential crop growth and development: Light interception and carbon dioxide assimilation are primary crop growth-driving processes. Light interception by the leaf canopy during the day depends on the incoming radiation, the crop leaf area, and the photosynthetic leaf characteristics. Carbon dioxide assimilation is possible because of the contra-flow gas exchange of carbon dioxide (atmosphere) and water vapour (inside of the leaf) through stomates, namely transpiration (Ehlers and Goss, 2003). These processes determine the potential gross assimilation rate, i.e. potential photosynthesis. Crops with a root system for water uptake and leaves from which water is lost to the atmosphere regularly experience a slight water shortage in their tissue during the day. This water shortage is caused by the time lag between leaf transpiration and root water uptake, a prerequisite for water flow in the soil-plant-atmosphere system. As long as this time lag remains small and the root zone water content is not depleted below a specific level (i.e. soil water potential decreased), transpiration is determined by atmospheric conditions and crop characteristics, namely potential transpiration or non-limiting soil conditions.

Soil-crop water flow: The volume of water arriving at the soil surface (pre-infiltration pool) in semi-arid regions (snow is generally limited in these regions) is determined by rainfall and irrigation after subtracting evaporation losses from canopy and mulch surfaces. Stem flow (gravitational flow through plant surfaces) and surface run-on are also part of the pre-infiltration pool. Effective infiltration is the fraction of the infiltration pool entering the soil at each timestep. The remaining fraction causes ponding or surface runoff. Ponding water can evaporate or infiltrate in the following timesteps, while surface conditions and topographic characteristics influence runoff. Soil evaporation is driven by atmospheric conditions and/or soil water flow, with the latter determined by soil hydraulic properties. Soil water flow processes include infiltration, redistribution, percolation (drainage) and capillary rise (from shallow groundwater table). When the soil is saturated with water (root-accessible water table conditions), lateral flow and subsurface artificial drain discharge (when installed) also occur. A part of the downward vertical flux that passes the root zone (percolation) can be redirected upward into the root zone, i.e. internal recirculation (Kroes et al., 2009). Hence, capillary rise has two sources, namely groundwater and recirculated percolation. Soil water decreases from saturation just above the groundwater table to approximately a value equal to field capacity at the capillary fringe. Hence, soil water between the capillary fringe and the groundwater table is above field capacity, allowing no room for water storage.

Actual crop growth and development: Water flows in the soil-plant-atmosphere system because of differences in water potential, i.e. a water potential gradient. The water potential of soils and plants includes the component matric, osmotic, gravimetric and pressure

potentials. During the early afternoon, crops often experience a more distinct temporary water shortage because root water uptake does not compensate for the accelerated transpiration rate, i.e. the total water potential gradient between soil and leaves is small. As soil water is depleted (due to evaporation and transpiration), the water shortage will become more severe if soil water is not replenished. This is because soil water depletion causes a reduction in soil water potential through a decrease in the component soil matric potential (Ehlers and Goss, 2003). Unfortunately, irrigation and capillary rise from shallow groundwater also transport salts into the root zone (salts added through rainfall are assumed negligible). Excessive salt in the root zone will also decrease the soil water potential by reducing the osmotic potential. Hence, water shortage experienced by crops is due to the combined decrease in matric and osmotic potential of soil water (i.e. matric and osmotic stress). A temporary water shortage that continues for a longer period will cause tension in plants with an associated reduction in potential transpiration (i.e. actual transpiration), which causes the potential gross assimilation rate to decrease, yielding actual gross assimilation (actual photosynthesis). Subsequently, the first plant process to slow down is cell enlargement and leaf growth (at a water potential of around $\pm$ -4 bar), followed by transpiration and carbon dioxide assimilation (at around $\pm$ -7 bar). Part of the actual assimilates (photosynthesis) is used to maintain living biomass, i.e. maintenance respiration. The remaining assimilates are used for growth respiration. In this process, carbohydrates are converted into structural plant material, which takes a certain amount of energy (de Wit et al., 2019). Partitioning of dry matter among roots, leaves, stems, and storage (grain yield) organs is a function of phenological development, with the fraction partitioned to leaves determining its development and light interception. Respiration and translocation of assimilates are the last processes to slow down (at a water potential of around $\pm$ -9 and -12 bar, respectively). Part of the living biomass dies during the growing season due to senescence.

2.3 *IN SITU* FIELD DATA

Root-accessible water tables within or just below a depth of 2 m from the soil surface occur extensively in irrigated regions worldwide, including the Lower Vaal River Basin, central South Africa. Weekly and seasonal measurements over four production seasons (2 years) on 19 farms (34 measurement points) located in Vaalharts and Orange-Riet revealed the following (Van Rensburg et al., 2012; Barnard et al., 2021), which informed the modelling conditions and assumptions of our study.

- Vaalharts (± 40 000 ha) and Orange-Riet Irrigation Schemes (± 17 000 ha) are located in the Lower Vaal River basin and receive its irrigation water from the Vaal River

through numerous gravity-fed canals, while Orange-Riet utilizes water originating from the Orange River.

- Both areas are classified as semi-arid, summer rainfall regions with an approximate annual rainfall of 427 mm (Vaalharts) and 450 mm (Orange-Riet).
- Most of the irrigated fields at Vaalharts have a permanent shallow groundwater table. At Orange-Riet, localised periodic root-accessible water tables also exist.
- No evidence was found that soil water content, water table depth, and root zone salt content explain the variation in yield over the measuring period. However, there was a significant variation in the yields of maize, groundnuts, wheat, barley, and lucerne, which can be attributed to other factors.
- The mean volumetric soil water content over a depth of about 1.8 m fluctuated between a matric potential of -6 kPa and -30 kPa, representing field water capacity.
- Evidence of waterlogging, namely a water table depth of less than 1 m for long periods, was limited to 3 fields. At only two fields, the soil's salt content was higher than the relevant crop threshold.
- An evaluation of the pivot points showed that the average water distribution under the system (> 85%) was good. For most of the pivot points, more than 85% of the pumped water ended up in the field at the crop. The variation in the combined effect, namely the system efficiency, was high, with a lower-than-expected average value (only 78%). Factors contributing to this atmospheric water loss include an incorrect nozzle package and excessive pump pressure.
- Lucerne received a mean irrigation of 1000 mm. However, there was a significant variation in application, around 400 mm. The mean irrigation for the two winter crops (barley and wheat) was approximately 600 mm, again with significant variation (± 215 mm). Maize and groundnuts received a mean of 511 mm and 424 mm, respectively. The variation was ± 220 mm.
- At 59% of the measurement points, the annual irrigation averaged 34% more than the irrigation quota. When rainfall is added to irrigation, the average increases to 55% more than the quota.
- Producers did not consider rainfall as a source of water when irrigation scheduling took place. This statement is confirmed by a conservative calculation of crop water requirements (namely only transpiration), given the measured biomass and atmospheric evaporation demand for the season. There was no evidence that producers used less irrigation to use the capillary rise of shallow water tables (<2 m from the ground surface) as an additional water source.

- Overirrigation (rainfall plus irrigation) caused a large amount of leaching. Between 0.9 and 3 tons of salts per hectare, applied by irrigation, were leached each season. It has been found that these salts do not accumulate in shallow water tables, provided they can flow laterally from higher to lower parts of the landscape. Where a shallow water table is stagnant, the salt content increases dramatically.

2.4 RESEARCH IMPLICATIONS

Maize grown in a semi-arid area on sandy-to-sandy loam soils with a groundwater table that varies between 1 and 1.8 m from the surface will be the focus of the modelling study. Furthermore, the project team argue that the higher rainfall during a maize growing season (summer rainfall region) compared to wheat provides an alternative dynamic to the economic investigation of conjunctive water use. The impact of rainfall is important as the measured data showed that irrigators did not consider rainfall in irrigation management. Consequently, it is important to inform irrigators of the importance of considering rainfall in irrigation management decisions. The groundwater table's mean depth and electrical conductivity were > 1.2 m from the surface and < 250 mS m^{-1} in sandy loam, loamy and sandy soils. The effect of excessive salt in the root zone on soil water availability, i.e. the osmotic potential of soil water, which reduces soil water availability, is not part of the study. However, The project team acknowledges that the salt load associated with irrigation is important. Monitoring salts in the root zone will be necessary when considering conjunctive water use strategies. Sound irrigation strategies should ideally aim to i) manage soil matric (water stress) and osmotic (salinity stress) potential to maintain optimum yields, ii) reduce the amount of irrigation by utilizing rainfall and capillary rise from root-accessible water tables to supplement crop water requirements and iii) minimize salt additions and irrigation-induced drainage and leaching (Barnard et al., 2021). Hence, our modelling study will focus on non-limiting conditions to economically investigate the conjunctive use of irrigation water and root-accessible water tables.

CHAPTER 3: LITERATURE REVIEW

"All models are wrong, but some are useful."
George E.P. Box.

3.1 BIO-ECONOMIC MODELLING DEFINED

Bioeconomic modelling integrates biology with economic decision-making to study the interrelated linkages between biological systems and economic decisions while considering the consequences of these management decisions on the environment. The multi-disciplinary nature of bioeconomic modelling efforts has resulted in a magnitude of models that range in their level of integration. On the one end of the continuum of bioeconomic modelling efforts are biological systems models that include an economic analysis component. In contrast, on the other end, you have economic optimisation models that include some representation of the biological system (Brown, 2000). Biophysical systems models that only include an economic analysis component do not include decision-making capabilities and are mainly used to simulate predefined behaviour. Optimisation models optimise a decision-maker's decisions according to an objective function but usually have simplified representations of the biophysical system to enable the application of first-order conditions to optimise the system. According to Flichman and Allen (2015), the bioeconomic models between the two poles are worthy of being called "bioeconomic" models as these models integrate the biophysical and economic modules sufficiently.

No bioeconomic model applies to all situations, and researchers have developed different bioeconomic models to suit their goals. The following section describes the characteristics that distinguish different bioeconomic models.

3.2 CHARACTERISTICS OF BIO-ECONOMIC MODELS

3.2.1 POSITIVE OR NORMATIVE APPROACHES

The researcher/analyst should consider the purpose of the bioeconomic modelling efforts before integrating biophysical models with economic models, as the purpose of the modelling effort will determine the general approach that is followed. Two broad strands of bioeconomic models have developed in literature based on the approach that is followed to pursue the goal

of the analyst. Bioeconomic models could be positive or normative (Janssen and Van Ittersum, 2007).

Positive economic modelling efforts intend to develop models that can simulate the observed behaviour of decision-making units and predict how decision-makers will behave in future (Louhichi et al., 1999). Statistical inference is commonly used to justify econometric models of observed behaviour (Flichman, 1997). From a farming systems point of view, well-calibrated biophysical models that can describe how the agricultural system behaves given external environmental drivers and the decisions or policies under consideration are invaluable for analyses of such choices or policies (Jones et al., 2017). In essence, positive models try to describe observed behaviour without any reference to the appropriateness of the behaviour.

Contrary to positive models, normative models include *a priori* objective functions that are optimised to determine optimal behaviour according to the included objective function (Graveline, 2016). Consequently, normative models are not calibrated to observed behaviour as these models predict how decision-makers "ought" to respond, not "how" they respond. Typically, normative bioeconomic models are based on linear or non-linear mathematical programming approaches (Graveline, 2016). Purely normative models are criticized for their prediction ability and usefulness in policy assessment (Janssen and Van Ittersum, 2007). However, several options are available to calibrate normative models. Therefore, calibrated normative models could be applied positively (Flichman, 1997; Graveline, 2016).

According to Flichman (1997), calibrating mathematical programming models requires careful consideration of the model specification and the utility function used. Proper model specification requires a deep understanding and appropriate representation of production possibilities, while the utility function implies knowing the objectives of the decision-maker. The calibration process is not exact, and the calibration results could be evaluated with the Finger and Kreinin similarity index (Finger and Kreinin, 1979). Precise calibration of mathematical programming models could be achieved through the positive mathematical programming approach developed by Howitt (1995). Positive mathematical programming, however, is not without criticism, as some researchers argue that farmer response might be distorted if not within the observed initial calibration area (Graveline, 2016).

3.2.2 UNIT OF ANALYSIS AND DECISION-MAKING UNIT

The scope of a bio-economic model is dependent on the questions being asked and the decisions and policies being studied (Jones et al., 2017). Consequently, the spatial scale of bio-economic models varies from field to regional or landscape scales.

Field scale or enterprise bio-economic models are concerned with choosing management practices that will maximise profits, meet production targets or minimise environmental consequences for a specific field or enterprise. Typically, production conditions are assumed to be spatially homogeneous across the field while modelling the impact of management changes on production with detailed crop models (e.g. Lehmann et al., 2014). However, some models that support precision agriculture take spatial heterogeneity of field conditions into account through multiple crop models (e.g. Basso et al., 2012).

Farm scale models integrate different fields into one decision-making unit. Consequently, farm-scale bio-economic modelling allows for the interaction between fields or enterprises to be modelled while allocating scarce resource endowments of the farm firm between enterprises. An advantage of farm scale modelling is that results could be interpreted in terms of equity and address distribution effects (Graveline, 2016). From a development economics perspective, farm-scale modelling parallels household modelling.

Bio-economic modelling at larger scales requires some form of aggregation, which may lead to bias (Graveline, 2016). Preserving the farm as an essential modelling unit typically involves the construction of typical farms since data availability does not allow for the inclusion of a farm model for each farm. Alternatively, aggregate regional models are developed to evaluate alternative scenarios. The results of these models are then downscaled to smaller areas using maximum entropy (Howitt and Reynaud, 2003) or farm scale using a Bayesian framework (Gocht and Britz, 2010). Graveline (2016) argues that downscaling approaches do not explicitly consider farm-specific conditions and structural changes that might interest policymakers. Consequently, farm-scale models might be more appropriate in specific settings.

3.2.3 REPRESENTATION OF BIOPHYSICAL COMPONENT

Two broad approaches have developed in the literature to model agricultural systems (Brown, 2000; Jones et al., 2017). The most comprehensive methods try to model the underlying biological processes based on the current theoretical understanding. These methods are referred to as “mechanistic” or “process-based” approaches. On the other hand, reduced-form

approaches estimate empirical functions that summarise the biophysical processes. These types of methods are commonly referred to as “functional” approaches. According to Brown (2000), a decision needs to be made on the specific processes that need to be modelled and the level of detail. Economists have developed various methods to represent the biophysical component of the agricultural system being modelled within mathematical programming[1] models or optimisation models that use near-optimal solution techniques[2]. Irrespective of the approach followed, decision-maker responses should allow for intensive and extensive margin adjustments (Graveline, 2016). Intensive margin adjustments refer to input combinations per hectare, while extensive margin relates to changes in the areas allocated to different crops. Next, the methods used to represent the biophysical component in bio-economic mathematical programming models and near-optimal models are discussed in more detail.

3.2.3.1 Mathematical programming models

The use of mathematical programming as the basis for developing a bio-economic model implies that the developer must decide on the representation of the biophysical component within a constraint optimisation framework.

The production function forms the basis of the study of production economics. A production function represents the physical transformation of inputs into output. As such, it provides a reduced-form approach to modelling the biophysical component of bio-economic models. When concerning irrigation water use, it is essential to distinguish between a water production function (WPF) and a crop water production function (CWPF). The former depicts the relationship between applied irrigation water and crop yield (Li, 1998), while the latter is the relationship between consumptively used water (evapotranspiration) and crop yield (Stewart and Hagan, 1973; Vaux and Pruitt, 1983). The distinction is essential since the decision-maker controls applied irrigation water, not evapotranspiration per se. The implication is that the crop does not consume all the applied water due to different hydrological processes that result in inefficiencies. Consequently, CWPF ignores the processes that cause inefficiencies and is therefore more or less independent of the irrigation systems, soils and other factors that influence the management of applied irrigation water (English et al., 2002).

The linear relationship between ET and crop yield over a season or within a specific crop growth stage has made it a widely applied methodology to directly incorporate the impact of

[1] Mathematical programming models refer to the use of linear programming, non-linear programming and integer programming.

[2] Near optimal solution techniques refer to the use of evolutionary algorithms.

crop water use into mathematical programming models. The relationship between applied irrigation water and crop yield is typically incorporated into CWPF by assuming constant inefficiencies (Ghahraman and Sepaskhah, 2004; Sadati et al., 2014) or by taking a specific level of inefficiency for the level of water availability as a fraction of the required amount (Homayounfar et al., 2014). The assumptions mentioned above oversimplify the processes of deep percolation and runoff losses that cause inefficient water applications. Consequently, the impact of varying irrigation applications on water use is modelled unrealistically (English and Raja, 1996). A popular approach to incorporate the non-linear relationship between applied water and crop yield is to account for the uniformity with which irrigation water is applied by assuming some statistical distribution (Reca et al., 2001; Ortega et al., 2005). The production function (WPF or CWPF) approach is criticized by researchers, arguing that the onset and duration of ET deficits are a function of the status of the soil water store. Consequently, the production function approach is unsuitable for modelling typical intraseasonal irrigation decisions regarding the timing and magnitude of irrigation events. Explicit water budget calculations are necessary to model intraseasonal water management decisions. A tipping bucket approach is typically used to simplify water budget calculations in mathematical programming models. However, Grové (2019) has shown that the free-from specification used to model water budget calculations that are employed by numerous researchers (Ghahraman and Sepaskhah, 2004; Kanooni and Monem, 2014; Sadati et al., 2014) may malfunction under certain conditions. Proper functioning water budget calculations result when applying a square root approximation of the MIN function inherent in water budget modelling (Grové, 2019).

Metamodeling provides an alternative method to establish the relationship between management actions and the impact thereof on the biophysical system being modelled without empirical observations. In bio-economic modelling, a metamodel of the biophysical system results when the output of detailed process-based agricultural systems models is summarised using the statistical estimation of response functions. Within a South African context, Mathews and Grové (2017) used a metamodeling approach to model the economic and environmental trade-offs of nitrate pollution by estimating metamodels based on the output from SWB (Van der Laan et al., 2009).

Another approach that utilises the output of validated process-based agricultural system models is where the output from these models is directly included as activities in mathematical programming models to represent an “engineering” production function (Flichman, 1997; Flichman and Allan, 2015). The engineering production function approach emphasises the technical processes that result in the production of outputs and externalities. The programming model needs to include several activities to allow for non-linear production presentations

(Graveline, 2016) and for substitution between inputs (Hazell and Norton, 1986). Researchers who use only a few activities to represent alternative production processes (e.g. Oosthuizen, 2014) may not appropriately capture the substitution effects. The necessity to include multiple alternatives when applying the engineering production function approach creates a strong information demand which suits the use of a validated processed-based agricultural systems model (Flichman and Allan, 2015). Applying the engineering production function approach may require software development to systematically generate alternative activities for the mathematical programming model (Dogliotti et al., 2003). The burden of developing large mathematical programming models is softened with modern mathematical programming languages such as GAMS (GAMS Development Corporation, 2017).

3.2.3.2 Evolutionary optimisation

Evolutionary algorithms (EAs) do not rely on first-order optimisation conditions to optimise bio-economic models. Instead, EAs rely on metaheuristic procedures based on an iterative exploration of the search space by a structured means inspired by biological evolution to find near-optimal solutions efficiently (Maier et al., 2014). The metaheuristic nature of the algorithms does not require simplification of biological processes before commencing optimisation. Consequently, EAs can optimise complex agricultural system models. Such bio-economic models that use EAs to optimise the system could indeed be classified as integrated bio-economic models because no simplification of the biophysical processes is necessary. Recently, several researchers (Schutze et al., 2012; Lehmann and Finger, 2014; Grové and Du Plessis, 2019) have demonstrated the feasibility of EAs to optimise agricultural water use by integrating irrigation simulation models and economic models.

The application of EAs is compatible with the engineering production function approach since the agricultural systems model represents the production process during optimisation. The implication is that a simulation model setup is required for each production function, increasing the computational time required to solve the model. However, applying EAs is perfectly suited for parallel processing, which will reduce computation time (Maier et al., 2014).

3.2.4 DECISION-MAKING MODELLING

3.2.4.1 Objectives of the decision-maker

The main objective of the economic component of the bio-economic model is to determine the set of activities that will satisfy the goals of the decision-maker. Optimisation is core to modelling decision-making, which entails specifying the objective function that needs to be

maximised (Janssen and Itersum, 2007). Biological processes are subject to variable weather and environmental conditions. Consequently, the outcome of these processes on which decision-makers depend to achieve their objectives is uncertain. Under such risky conditions, modellers have applied expected utility theory as the most generally accepted basis to guide decision analysis considering risk (Hardaker and Lien, 2010). Application of expected utility theory requires quantifying the decision-maker's subjective beliefs (probabilities) about the risky outcome variable and determining the preferences (utility) of the decision-maker over those outcomes. Biophysical process-based simulation models are essential in quantifying the risk of producing under different states of nature (Finger, 2013). Probability and value assessments are then integrated to determine choices between risky prospects based on expected utility maximization. Risk-neutral behaviour resolves to maximise expected outcomes.

Decision-makers might not always be classified as economically rational and may not always try to maximise profit, whether the expected profit or profit adjusted for risk aversion. Instead, decision-makers might have multiple objectives derived from different dimensions, i.e. economic, environmental, biophysical and social (Janssen and Itersum, 2007). Multi-criteria decision-making methods (Rehman and Romero, 1993) are relevant when multiple objectives need to be considered. Multi-criteria decision-making methods either incorporate different goals directly into the objective function using weights or in the constraint set. An example of multiple objectives is where an irrigation farmer tries to maximise profits while simultaneously trying to end the growing season with a targeted soil water content.

3.2.4.2 Responsive decision-making

Risk decision-making is frequently modelled based on the assumption that decisions are made before the resolution of the risk and that production is instantaneous (Boisvert and McCarl, 1990; Dorward, 1999). Consequently, these models do not allow the possibility of managing risk sequentially through the season as the risk unfolds and more information is available. Modelling adaptive decisions under risk requires a dynamic sequential decision-making framework incorporating interactive linkages between the decisions being made and the state of the modelled biophysical system.

Modelling adaptive sequential decision-making is especially important in irrigation agriculture, where irrigators need to make weekly irrigation decisions within a dynamic stochastic environment (Robert et al. 2016, 2017). From a South African perspective, Madende and Grové (2020) have shown that the profit margins are higher while the variability thereof is lower when sequential decisions are included in their bio-economic irrigation model compared

to a model that ignores sequential decision-making. Representing sequential dynamic decisions in optimisation models results in large models depending on the number of decision nodes and states of nature included. The problem above is referred to in the literature as the "curse of dimensionality" (Boisvert and McCarl, 1990; Blanco and Flichman, 2002). Blanco and Flichman (2002) developed a solution method to overcome the "curse of dimensionality" by applying forward recursion in contrast to the typical backward recursion methods.

3.2.4.3 Timing of decisions

The decision-making environment could be static or dynamic (Janssen and Ittersum, 2007). Static models ignore the influence of time on decision-making. Static models are typically constructed for a single season or year, while dynamic models explicitly account for time by dividing the planning horizon into several periods. Robert et al. (2016) argue in favour of using dynamic models to model the impact of farmer decision-making on biophysical systems. Blanco and Flichman (2002) distinguish between different dynamic modelling approaches, as depicted in Figure 3.1.

Intertemporal models optimise decisions that maximise the objective function over the entire planning horizon while considering intertemporal trade-offs between periods. Discount rates are used to indicate relative preference for current income generation above future income. Intertemporal models do not explicitly consider the interactions between decisions made in one period and those made in the next.

Recursive models include several periods in the planning horizon, with the end values of one period being the starting values of the following period. The optimisation is, however, carried out period by period. Thus, the decisions made in the current period depend on the outcome of previous periods and are independent of future conditions. Dynamic recursive models also include multiple periods, with the end values of one period being the start values of the next period. However, one optimisation is done over the whole planning horizon, implying that the interaction of decisions between periods is explicitly considered. Dynamic recursive models assume complete knowledge of how the biophysical system will react to management changes.

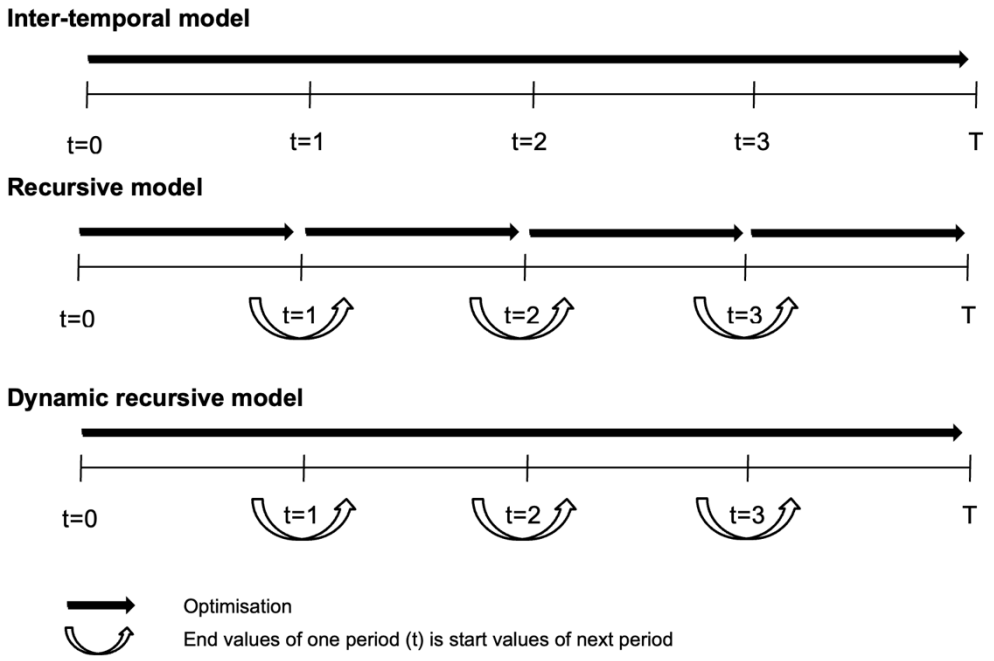

Figure 3. 1: Different types of dynamic models (Blanco and Flichman, 2002)

Stochastic programming models acknowledge that some decisions are made before the uncertain future unfolds and are made sequentially over the planning period. Cognisance should be taken that stochastic programming models have short planning horizons subdivided into several decision stages. The planning horizon is typically a season or a year. Different states of nature are included in the model as discrete distributions of outcomes, and the adaptive decision-making process that is modelled could be presented as a decision tree (Boisvert and McCarl, 1990). Stochastic programming models are subject to the curse of dimensionality since including more states of nature may result in very large models. Belhouchette et al. (2012) developed a recursive solution procedure (Figure 2) to overcome the problems of solving large models.

Madende and Grové (2020) applied the solution procedure to solve the irrigation problem where the irrigator needs to decide on the area to plant and how to schedule his limited irrigation water over the season, as depicted in Figure 3.2.

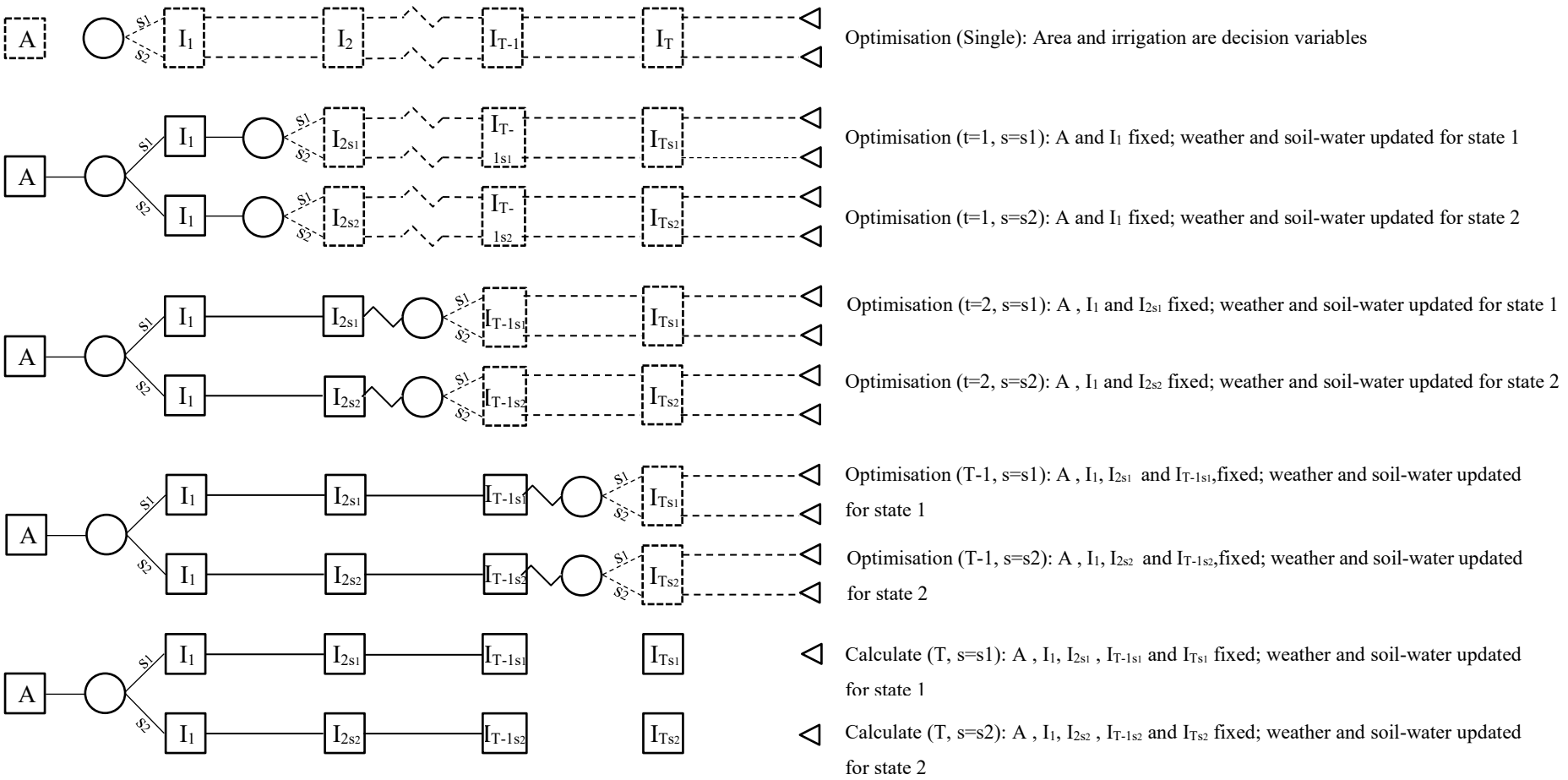

Figure 3.1: Forward recursive stochastic decision-making framework where solid squares represent fixed decisions, circles represent possible events to unfold, dashed squares represent decisions that will be optimised, triangles represent the outcome, A represents the area, I represents the irrigation decisions, T represents decision stage, and S represents the possible state of nature to unfold.

Within the forward recursive stochastic decision-making framework, the area decision is made in the first stage, and the irrigation scheduling decisions are made sequentially in subsequent stages as more information becomes available weekly. Figure 3.2 shows that the first optimisation optimises irrigation area and amounts regardless of the state of nature. The optimised values will result in the best average outcome across all the states of nature. After the first optimisation, the area and the first irrigation decisions are fixed. Subsequent optimisations are carried out at each decision stage (week) conditional on information on the unfolding state of nature by updating the biophysical model with the state-specific information and the optimised irrigation decision of the previous week. Consequently, a separate optimisation is done at each irrigation decision stage for each unfolding state of nature.

The time scale over which decisions are modelled within integrated bio-economic models is of utmost importance because the timing of decisions dictates the key decision points in the biophysical models (Brown, 2000). Consequently, the time scale of decisions significantly affects the level of integration and complexity of the model structure necessary to model the impact of decisions on the biophysical system being modelled.

3.3 BIOPHYSICAL MODELLING OF IRRIGATED FIELDS

Section 3.3 of the literature review provides a synopsis of transient-state mathematical biophysical models that allow for potential crop production, for example, temperature, radiation, crop characteristics, etc., and the growth limiting factor of water. The review focuses on biophysical models specifically applied when producing field crops in irrigated production systems on soils with a shallow groundwater table within or below a depth of 2 m.

Hydrology-based models generally emphasize water flow dynamics in the soil-plant-atmosphere system at different scales. The effect of growth-defining factors (radiation, temperature, etc.) and soil water availability on crop growth and development are generally the focus of crop models. Models in these two families are sometimes grouped as cropping systems, agroecosystems, soil water or soil hydrological models. The complexity and detail with which the relevant processes are simulated vary considerably between models, with no clear-cut distinction between mechanistic and empirical approaches. Generally, there is a continuum between the two approaches, “with mechanistic models always having some empirical components” (Tenreiro et al., 2020).

3.3.1 RELEVANT MODELS

Popular crop growth models in chronological order that were developed after 1980 include, for example, WOFOST, DSSAT, DAISY, APSIM, STICS, AquaCrop and MONICA. The popular hydrology-based models are HYDRUS1D, MIKE-SHE, SWAP, SWIM and HYDRUS-2D. Table 3.1 provides a list of modelling studies for the past ten years specifically related to the presence of root-accessible water tables in cropping systems.

SWAP (Kroes et al., 2009; Kroes et al., 2017) and HYDRUS-1D (Šimunek et al., 2012) are popular models for studying water flow under these conditions. WOFOST, a detailed model for the dynamic growth of arable crops, is fully integrated into SWAP (a simple module for static crop growth is also part of SWAP). WOFOST has been used for over 25 years and shares many algorithms and approaches with SUCROS. A clear difference between WOFOST and SUCROS is the “myriad of SUCROS versions differing slightly in approach and output” compared to “clear version control and proper documentation of WOFOST” (de Wit et al., 2019). WOFOST also allows the simulation of an extensive range of crop types with a single code base by only changing parameter values (de Wit et al., 2019). As an alternative combination, SWAP has been successfully combined with EPIC (calibrated and validated) to analyse groundwater recharge processes and capillary rise in the Hetao Irrigation District of the upper Yellow River basin (Xu et al., 2015). In addition, SWAP was integrated into the groundwater flow model MODFLOW2000 and tested using a two-dimensional saturated-unsaturated groundwater table recharge experiment (Xu et al., 2012). Kroes et al. (2018) used SWAP to quantify upward flow and recirculated separately percolation water as well as the contribution of capillary rise and recirculated water to crop yield and groundwater recharge (this was with grass, maize and potato grown in the Dutch delta).

HYDRUS-1D was coupled with the FAO-56 dual crop coefficient approach by Ren et al. (2016). After calibration and validation, a simulation was done for maize, sunflower and watermelon grown in the command area of a typical irrigation canal system in Hetao Irrigation District. Results showed that large volumes of irrigation water percolated due to over-irrigation. The reuse of percolated irrigation water through capillary rise was considerable. Han et al. (2015) coupled HYDRUS-1D with a simplified crop growth module from SWAT. The coupled model was calibrated and validated using field observations. Namely, soil water content, leaf area index, plant height, above-ground biomass and cotton yield grown on soils with root-accessible water tables at the Aksu water balance station in Xinjiang, northwest of China.

Table 3.1: List of modelling studies for the past ten years specifically related to the presence of root-accessible water tables in crop systems

Model	coupled	Crops	Title of paper	Reference
SWAP	-	grass, maize, potato	Impact of capillary rise and recirculation on simulated crop yields	Kroes et al. (2018)
	MODFLOW	-	Integration of SWAP and MODFLOW-2000 for modelling groundwater dynamics in shallow water table areas	Xu et al. (2012)
	EPIC	-	Groundwater recharge and capillary rise in irrigated areas of the Upper Yellow River Basin assessed by an agro-hydrological model	Xu et al. (2015)
	-	date palms	Soil salinization and critical shallow groundwater depth under saline irrigation conditions in a Saharan irrigated land	Haj-Amor et al. (2017)
	-	-	Irrigation regime and salt dynamics for rise with brackish water irrigation in the coastal region of North Jiangsu Province	Wang et al. (2014)
	-	-	Assessing the effects of water table depth on water use, soil salinity and wheat yield: Searching for a target depth for irrigated areas in the upper Yellow River basin	Xu et al. (2013)
	-	-	Simulation of hydrology following various volumes of irrigation to soil with different depths to the water table	Huo et al. (2012)
HYDRUS-1D	FAO56 (dualKc)	maize, sunflower, watermelon	Modeling and assessing field irrigation water use in a canal system of Hetao, upper Yellow River basin: Application to maize, sunflower and watermelon	Ren et al. (2016)
	FEFLOW-3D	cotton, wheat and vegetables	A GIS-based approach for up-scaling capillary rise from field to system level under soil-crop-groundwater mix	Awan et al. (2014)
	EPIC	maize	Modeling soil water-salt dynamics and maize yield responses to groundwater depths and irrigations	Hao et al. (2014)
	-	wheat	Effect of climate change on the contribution of groundwater to the root zone of winter wheat in the Huaibei Plain of China	Gao et al. (2020)
	-	maize	Simulation of maize (Zea mays L.) water use with the HYDRUS-1D model in the semi-arid Hailiutu River catchment, Northwest China	Hou et al. (2017)
	simplified crop growth module from SWAT	cotton	Evaluating the impact of groundwater on cotton growth and root zone water balance using Hydrus-1D coupled with a crop growth model	Han et al. (2015)
	DSSAT	soybean	Coupling DSSAT and HYDRUS-1D for simulations of soil water dynamics in the soil-plant-atmosphere system	Shelia et al. (2018)
DRAINMOD	-	canola	Evaluating Drainmod-s to predict drainage water salinity and groundwater table depth during winter cropping in heavy-textured paddy soils	Davoodi et al. (2019)
	-	cotton	The effect of natural rainfall on salt leaching under water table management	Li et al. (2018)
	-	-	Impact of accurate evapotranspiration estimates on DRAINMOD simulation in North Dakota	Niaghi et al. (2017)
	-	-	Shallow groundwater use and salinity buildup based on DRAINMOD predicted field hydrology in irrigated areas	Li et al. (2015)
SWAT	DRAINMOD	-	Shallow water depth algorithm in SWAT: Recent developments	Moriasi et al. (2011)
AquaCrop	-	maize	Evaluating the effect of groundwater table on summer maize growth using the AquaCrop model	Zhao et al. (2020)
	-	wheat	Improving irrigation scheduling of wheat to increase water productivity in shallow groundwater conditions using Aquacrop	Goosheh et al. (2018)
AWPM-SG	-	-	Modeling contribution of shallow groundwater to evapotranspiration and yield of maize in an arid area	Gao et al. (2017)

Model	coupled	Crops	Title of paper	Reference
APSIM	-	soybean	Enhancing APSIM to simulate excessive moisture effects on root growth	Ebrahimi-Mollabashi et al. (2019)
Unique vadose zone model	-	maize	A unique vadose zone model for shallow aquifers: the Hetao irrigation district, China	Liu et al. (2019)
DSSAT	-	wheat, maize	Estimating of groundwater use by crop production simulated by DSSAT-wheat and DSSAT-maize models in the piedmont	Yang et al. (2006)
new model	-	-	Optimizing irrigation and drainage by considering agricultural hydrological process in arid farmland with shallow groundwater	Li et al. (2020)
new model	-	-	Development and application of long-term root zone salt balance model for predicting soil salinity in arid shallow water table area	Sun et al. (2019)
new model	-	-	Untangling the effects of shallow groundwater and deficit irrigation on irrigation water productivity in arid region: New conceptual model	Xue et al. (2018)

HYDRUS-1D was also coupled with the EPIC crop growth module by Hao et al. (2014) to simulate crop height, leaf area index, above-ground biomass and crop yield. A new soil evaporation module was added to describe better soil evaporation where root-accessible water tables are present. After calibration and validation, the model assessed groundwater table and irrigation impacts on soil water-salt dynamics and maize yields. Awan et al. (2014) used HYDRUS-1D to simulate capillary rise at field scale for cotton, wheat and vegetables grown on six different hydrological response units in the Shomakhulum Water Users Association, Uzbekistan. A simple aggregation approach was used to up-scale capillary rise from these hydrological response units to Water User Association levels. FEFLOW-3D was used in parallel to simulate groundwater table depths under four improved irrigation schedules, which were then used in HYDRUS-1D to quantify the impact of improved irrigation schedules on the contribution of capillary rise. Gao et al. (2020) studied how climate change (20111-2100) will impact groundwater table depths and crops. This was done with a circulation model HadGEM2-AO (which performed best in simulating precipitation in the study area) and HYDRUS-1D. Simulations showed that the most significant groundwater contribution and deep drainage occurred at a groundwater table depth of 1.5 m and that climate change could alter the distribution of groundwater contribution during each growing season. Simulations of maize grown on shallow groundwater table soils in the semi-arid Hailiutu River catchment of the Maowusu Desert, China, with HYDRUS-1D were done by Hou et al. (2017). Results revealed that increased groundwater table depth would increase irrigation water requirements. Below a depth of 1.57 m, the contribution of groundwater to maize water use was insignificant under these conditions.

The FAO model AquaCrop was also used in shallow groundwater table studies by Goosheh et al. (2018) and Ahmadi et al. (2015). In the former study, various irrigation schedules for

wheat were simulated for 12 years, and the water and salt balance were evaluated under shallow groundwater table conditions. The latter study focused on simulations of maize growth and soil water content under full and deficit irrigation schedules. DRAINMOD was also a popular model for water flow dynamics concerning root-accessible water tables and artificial drainage, while new models were also developed recently (Table 3.1).

3.3.2 CROP GROWTH AND DEVELOPMENT MODELLING

Palosuo et al. (2011) grouped 8 (WOFOST, DSSAT, DAISY, STICKS, CROPSYST, APES, FASSET, HERMES) crop models in terms of the detail with which they treat the major crop growth processes (Table 3.2). Leaf area development and light interception are simulated with a simpler approach by CROPSYST and DSSAT through a specific leaf area at emergence and biomass partitioning factors or a "forcing function with an exogenously defined maximum leaf area index" (Palosuo et al., 2011). For example, WOFOST, STICS and DAISY adopt a more detailed approach for simulating the effect of temperature and light on leaf expansion at different phenological stages. Light utilization simulations by DAISY, FASSET, and WOFOST are explanatory descriptions of photosynthesis, respiration, and partitioning of assimilates in various growth stages. DSSAT, STICS and CROPSYST employ the descriptive (simpler) radiation use efficiency approach. Yield formation, used by the multiple models that depend on a fixed harvest index, above-ground biomass, number of grains and partitioning during reproductive stages are listed in Table 3.2.

Table 3.2: Approaches applied by various crop models in simulating major processes determining crop growth and development as summarised by Palosuo et al. (2011) (Abbreviations are provided in the text)

Model	Leaf area development and light interception	Light utilization	Yield formation	Crop phenology	Root distribution
APES	D	RUE	Y (Prt)	f (T, DL, V)	exponential
CROPSYST	S	RUE	Y (HI, B)	f (T, DL, V)	linear
DAISY	D	P-R	Y (Prt)	f (T, DL, V)	exponential
DSSAT	S	RUE	Y (HI(Gn), B)	f (T, DL, V)	exponential
FASSET	D	RUE	Y (HI, B)	f (T, DL)	exponential
HERMES	D	P-R	Y (Prt)	f (T, DL, V)	exponential
STICS	D	RUE	Y (HI(Gn), B)	f (T, DL, V)	sigmoidal
WOFOST	D	P-R	Y (Prt, B)	f (T, DL)	linear

D detailed approach; S simple approach; RUE radiation use efficiency; P-R gross photosynthesis-respiration
Y yield; Prt reproductive stages; HI harvest index; B biomass
Gn number of grains; f crop phenology; T temperature; DL day length
V vernalization

Crop phenology as a function of temperature, day length and vernalization are also included. Roots are distributed linearly over depth by CROPSYST and WOFOST, exponentially by APES, DAISY, DSSAT, FASSET and HERMES and sigmoidal by STICS. Figure 3.3 shows,

as an example, a visual illustration of the major processes and their linkage simulated by WOFOST, while Table 3.3 provides the number of parameters required (de Wit et al., 2019). The authors distinguish between single-value parameters (scaler) and parameters where the value depends on another state, i.e. tabular parameters (usually development stage and temperature). Table 3.4 provides the parameters required by AquaCrop. An indication is provided whether the various parameters are 1) conservative generally applicable, 2) conservative for a given specie but can or may be cultivar specific, 3) depend on environment or management and 4) cultivar specific (Raes et al., 2018).

Table 3.3: Number of crop parameters used to describe the various processes (Figure 4) as simulated by WOFOST (de Wit et al., 2019)

Process	Scalar	Tabular	Total
Phenological development	13	2	15
Leaf growth, senescence and assimilation	9	3	12
Root formation	4	2	6
Respiration	5	1	6
Transpiration	5	0	5
Storage organ formation	2	1	3
Stem formation	2	2	4

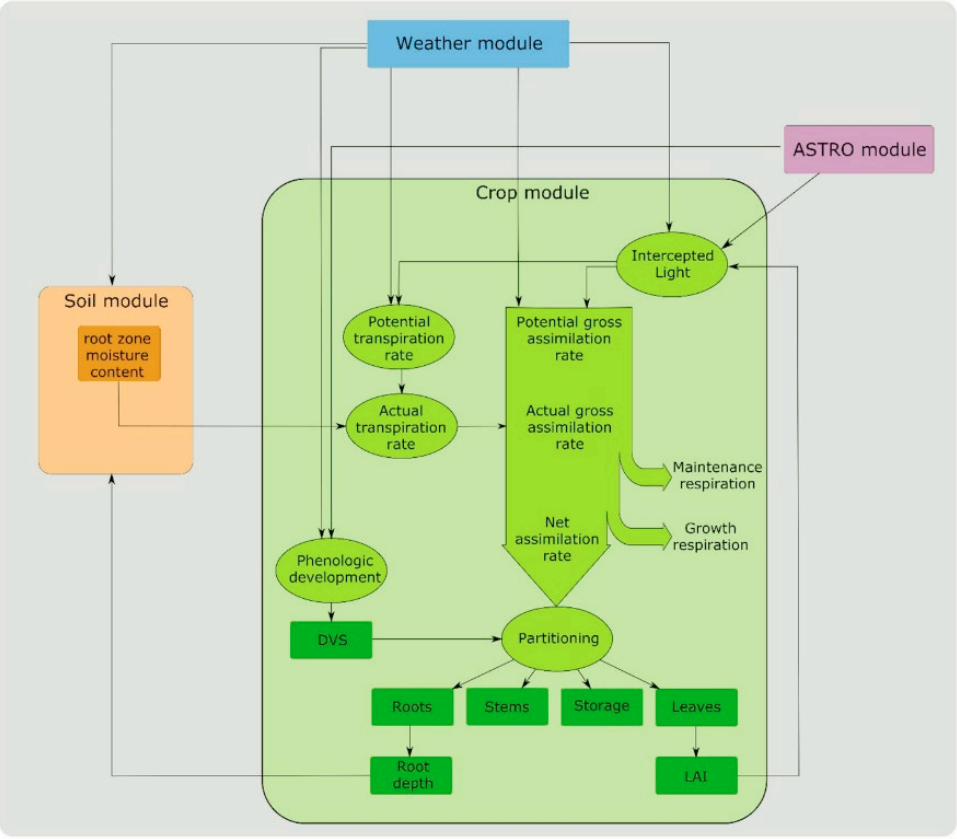

Figure 3.2: Visual illustration of the major processes and their linkage simulated by WOFOST (de Wit et al., 2019).

Table 3.4: Number of crop parameters used to describe the various processes as simulated by AquaCrop (Reas et al., 2018)

Process	Conservative [1]	Conservative [2]	Management [3]	Cultivar [4]
Crop phenology	6	1	5	4
Transpiration	2	-	-	-
Biomass production	2	-	-	-
Yield formation	4	1	-	1
Water stress	8	-	1	
Salinity stress	2	-	-	-

3.3.3 WATER FLOW MODELLING

Tenteiro et al. (2020) conducted a review in which soil-crop water processes were "structured following the fate of water in a hypothetical hydrological unit". The authors described every water flow process (including the fundamentals of modelling approaches) adopted by various popular crop models (WOFOST, DSSAT, DAISY, APSIM, STICS, AquaCrop and MONICA). Hydrology-based models like HYDRUS1D, MIKE-SHE, SWAP, SWIM and HYDRUS2D were also included. The project team believes such a comprehensive review of water flow modelling approaches adopted by popular soil-crop water models is limited. Hence, the review paper of Tenteiro et al. (2020) will form the basis for understanding the various soil-crop water flow approaches and data requirements of relevant popular models.

Water flow processes above the soil surface are shown in Table 3.5. A model like MIKE-SHE, which operates at a catchment scale, can allow for run-on as part of the infiltration pool. Generally, irrigation must be set up within a management module, assuming no losses (DSSAT, APSIM, DAISY, AquaCrop, MONICA, HYDRUS, SWAP, SWIM) or subtracting application losses (STICS). Models that allow for canopy or mulch interception and evaporation from plant surfaces, i.e. the interception pool, are limited to STICS, HYDRUS, SWAP and MIKE-SHE. AquaCrop provides some interception control, allowing users to define the fraction of soil surface wetted by irrigation. Intercepted water from the canopy or mulch can be part of the direct evaporation pool or recovered in the infiltration pool through stem flow, with the latter process simulated by STICS.

Stemflow is simulated as a function of leaf area index, light extinction coefficient, and an empirical crop coefficient that depends on the architecture and wettability of plant surfaces, rainfall, and/or irrigation (Brisson et al., 2003). HYDRUS and SWAP use the method of Braden (1985) and von Hoyningen-Huene (1981) to simulate the fraction of intercepted water. Variables and parameters required include the leaf area index, an empirical coefficient (a, assumed as 0.25 by default), b, the soil cover fraction (assumed as 0.33 of leaf area index) and the 'above canopy pool'. The effect of mulch residues on modelling water interception

dynamics can be done with STICS. Empirical equations that estimate the quantity of soil cover with time are used.

3.3.3.1 Soil water

Darcy's and Richard's equations are used for a complex mechanistic approach to model soil water processes (hydraulic and hydrodynamic behaviour and continuous water flow in unsaturated and saturated soil). Darcy's and Richard's equations are used. Richard's equation is a non-linear partial differential equation (solved numerically) that combines Darcy's and the continuity equations. The former relates the soil water flux density to hydraulic conductivity and soil water potential gradient (which include both the matric and gravimetric potentials) over a vertical coordinate. Matric potential is expressed negatively, equivalent to soil water tension (positive) or soil water pressure head (negative).

Table 3.5: Water flow processes simulated by various soil-crop water models

Process	Models	Method / Approach
Surface run-on	MIKE-SHE	-
Irrigation	DSSAT, APSIM, DAISY, AquaCrop, MONICA, HYDRUS, SWAP, SWIM, STICS	User-defined schedule (i), constant or variable volumes when soil water content threshold is reached (ii) and planned schedule based on growth stage, soil water content and availability constraints (iii)
Interception pool	STICS, HYDRUS, SWAP and MIKE-SHE	Braden (1985) and von Hoyningen-Huene (1981)
Stemflow	STICS	Brisson et al. (2003)
Effective infiltration	MONICA, WOFOST	Capacity model
	DSSAT, APSIM, STICS, AquaCrop	Curve number
	DAISY, HYDRUS-1D, HYDRUS-2D, SWAP, MIKE-SHE, SWIM	Richard's
Ponding infiltration	DAISY	Darcy
	HYDRUS, SWAP, MIKE-SHE	Green-Ampt
Redistribution and drainage	WOFOST, DSSAT, APSIM, STICS, AquaCrop, MONICA	Tipping bucket
	HYDRUS-1D, HYDRUS-2D, SWAP, MIKE-SHE, SWIM	Richard's
Hysteresis	*HYDRUS-1D/2D, SWAP*	
Preferential flow	*DAISY, HYDRUS-1D, HYDRUS-2D, SWAP, MIKE-SHE*	
Capillary rise	STICS, MONICA	Predefined
	DSSAT, AquaCrop,	Without updating the groundwater table
	DAISY, HYDRUS-1D, HYDRUS-2D, SWAP, MIKE-SHE, SWIM	Update groundwater table
Surface water flow	WOFOST, DSSAT, APSIM, AquaCrop, MONICA, HYDRUS-1D, SWAP	HRTf and SATf
	DAISY, STICS	HRTf, SATf, THRf
	DAISY, HYDRUS-1D, SWAP	Out

Process	Models	Method / Approach
Subsurface lateral flow	HYDRUS-2D	Out, In
Solute transport	HYDRUS-1D/2D, SWAP, SWIM	convection-dispersion equation
	AquaCrop	program parameter that describes the global capacity for salt diffusion
Evaporative demand	WOFOST, DSSAT,	Penman
	WOFOST, APSIM, DAISY, STCTS, AquaCrop, MONICA, HYDRUS-1D, HYDRUS-2D, SWAP	Penman-Monteith
	DSSAT, APSIM, STICS, MONICA	Priestly and Taylor
	DAISY, HYDRUS-1D, HYDRUS-2D	Hargreaves
	MIKE-SHE, SWIM	Soil vegetation atmosphere transfer scheme
Soil evaporation	WOFOST, DSSAT, APSIM, DAISY, STICS, MONICA, HYDRUS-1D, HYDRUS-2D, SWAP, SWIM	Integrated through Beer-Lambert equation
	AquaCrop, HYDRUS-1D, HYDRUS-2D, SWAP, MIKE-SHE, SWIM	Soil cover method
	APSIM, SICTS, AquaCrop, SWAP, SWIM	Two-stage method
Atmospheric demand for transpiration	-	Penman
	WOFOST, DSSAT, APSIM, DAISY, STICS, AquaCrop, MONICA, HYDRUS-1D/2D, SWAP	Penman-Monteith
	DSSAT, APSIM, STICS, MONICA	Priestly and Taylor
	DAISY, HYDRUS-1D/2D	Hargreaves
	MIKE-SHE, SWIM, DAISY, STICS	Soil vegetation atmosphere transfer scheme
Actual transpiration (root water uptake)	DSSAT, APSIM, STICS, AquaCrop	Water stress coefficients (Ks)
	WOFOST, DSSAT, APSIM, DAISY, STICS, AquaCrop, MONICA, HYDRUS-1D/2D, MIKE-SHE	Linear extraction sink term (Si)
	APSIM	Exponential extraction sink term (Si)
	HYDRUS-1D/2D, SWIM	Non-linear differential equations for extraction sink term (Si)
	HYDRUS-1D/2D	Compensatory uptake

Hydraulic conductivity is a function of soil matric potential. The continuity equation represents the water balance of an infinitely small soil volume. Namely, the change in volumetric soil water content over time is determined by the change in soil water flux density over the vertical coordinate and a sink term. The sink term generally represents the root water extraction rate. The extraction rate by drain discharge in the saturated zone and exchange rate with macro pores are sometimes included in models adopting Richard's equation (SWAP). Darcy's equation is sometimes used without the continuity equation for steady-state flow modelling (Richard's equation is used for transient flows).

Models that employ this mechanistic approach to simulate soil water flow processes are data intensive. Highly non-linear soil hydraulic functions are required, i.e. functions relating to volumetric soil water content, matric potential (soil pressure head) and hydraulic conductivity. Parameters like saturated hydraulic conductivity, residual and saturated volumetric soil water content, and empirical m, n and α shape parameters are required to describe these functions. Different water retentivity and hydraulic conductivity functions or adaptations to the same relationships can be used. For example, with SWAP, typically α, *n* and *m* parameters will be required for a specific soil to describe the relationship proposed by Van Genuchten (1980). In HYDRUS, any of four relationships with different parameters can be chosen, i.e. Van Genuchten-Mualem, modified Van Genuchten, Brooks-Corey or Kosugi (Šimůnek et al., 2012). Software packages that could be used to estimate parameters for water retention and hydraulic conductivity functions from soil texture and/or bulk density measurements include SWCT, SOILPAR, ROSETTA and NEUROPACK (Schaap 2004).

Solving Richard's equation (for example, finite-difference and finite-element methods) is difficult due to the hyperbolic nature, rapidly changing boundary conditions and nonlinearity of the soil hydraulic functions. As emphasised by Kroes et al. (2017), the “structure of the numerical scheme, the applied time and space discretizations, and the procedure for the top boundary condition (Van Genuchten, 1982; Milly, 1985; Celia et al., 1990; Warrick, 1991; Zaidel and Russo, 1992)” can significantly affect soil water fluxes.

Infiltration: Effective infiltration (i.e. the fraction of water arriving at the soil surface that infiltrates into the soil) is generally simulated with three methods/approaches (Table 3.5). The most straightforward approach is the capacity model, which defines maximum infiltration capacity as the difference between volumetric soil water at saturation and actual volumetric soil water. A popular alternative approach is the “infiltration-loss based method” (Allen, 1991), referred to as the USDA curve number method. Potential maximum retention is estimated from an empirical parameter determined from tabled values according to land cover and soil hydrological group. Probability distribution curves of measured infiltration rates were used to classify soil hydrological groups. The third approach for effective infiltration can be defined by unsaturated soil water flow, simulated by numerically solving Richard’s equation (DAISY, HYDRUS-1D/2D, SWAP, MIKE-SHE and SWIM). Ponding infiltration (when water accumulates at the soil surface) can be simulated by, for example, DAISY, HYDRUS-1D/2D, SWAP and MIKE-SHE. Theoretically, this happens when the infiltration pool increases at a higher rate than the maximum infiltration capacity of the soil. Ponded infiltration is simulated through a solution of Darcy’s equation (DAISY) or with the Green-Ampt approach (HYDRUS-1D/2D, SWAP, MIKE-SHE). According to Tenteiro et al. (2020), effective infiltration

approaches “that are based on the hydraulic conductivity of the top soil layer assume that after infiltrating into the soil, water is stored in successive layers downward according to a physical constraint that is imposed by the drainage ability of the soil (APSIM, STICS, AquaCrop)”.

Redistribution and drainage: Darcy’s or Richard's equations and a simpler fixed number of soil layers cascading (or tipping bucket) approach can be used to simulate redistribution (Table 3.5). With the latter approach, the volumetric soil water content at field capacity; drained upper limit or upper limit of plant available water) and permanent wilting point; lower limit of plant available water) are required as parameters. Generally, for the tipping bucket models, a drainage coefficient relates internal drainage to the volumetric soil water content above field capacity. With Darcy’s and Richard's equation 2D and 3D soil water flow is possible because the flow term q can be defined as one, two or three-dimensional vectors. This will require, however, different calibration requirements and computing times. An important phenomenon to consider in soil water flow modelling is hysteresis, i.e. the wetting/drying history of the specific soil. Hysteresis retard in general water flow, while preferential flow (macropore flow) enhances it. The effect of hysteresis is modelled (HYDRUS-1D/2D, SWAP) by using multiple soil matric potential and volumetric soil water content relationships.

*Capillary rise: STICS and MONICA us*e capillary rise as an input defined by a lower boundary condition where the flux is a function of time. DSSAT and AquaCrop simulate it with relationships between groundwater table depth, soil hydraulic properties and actual soil water content (or matric potential) (Raes et al., 2017). Capillary could be simulated modelled as a function of soil water content (Dirichlet type) and as a function of groundwater table depth (Cauchy type). The models above do not simulate the feedback between the unsaturated zone and the groundwater table. DAISY, HYDRUS-1D, HYDRUS-2D, SWAP, MIKE-SHE, and SWIM use Richard's equation to simulate capillary rise with different approaches while updating groundwater table depth (Table 3.5).

3.3.3.2 Surface water

Most of the models mentioned above consider surface water flow as a water loss from the system. Ponce and Hawkins (1996) distinguished five types of surface water flow loss (as described by Tenreiro et al., 2020):

- Hortonian overland flow is when rainfall and/or irrigation exceeds the infiltration capacity of the soil;
- saturation overland flow is when the soil profile is saturated with water, i.e. a post-infiltration process;

- throughflow is horizontal water flow beneath the soil surface under saturated conditions;
- the direct channel interception flow is runoff that refers to the spatial redistribution of rainfall directly intercepted by channels and
- surface phenomena flow is all the flow driven by crust development, hydrophobic layers and frozen ground that do not allow vertical flow.

The DSSAT, APSIM, STICS and AquaCrop models mostly simulate surface water flow loss (HRTf, SATf, THRf) through empirical approaches based on the curve number method. DAISY, HYDRUS-1D/2D, SWAP and SWIM use Richard's-based approaches (Table 3.5). Surface water flow can also be an inflow to the water balance of neighbouring fields (redistribution flow) or a channel inflow. Still, it is not simulated by the models mentioned above.

3.3.3.3 Subsurface water

Among the models, only Richard's equation-based models simulate subsurface water flow (DAISY, HYDRUS-1D, SWAP, MIKE-SHE, SWIM). These simulations are also limited to lateral drainage processes of lateral outflow between the simulated plot and neighbouring artificial drainage systems (Table 3.5). This lateral flow to drains is simulated by the Hooghoudt equation (Ritzema, 1994) and is assumed to be a system water loss but not a redistributive process (Tenreiro et al., 2020).

3.3.3.4 Evaporation

Definitions related to evaporation and transpiration are provided below to enhance the readability of the relevant sections.

- Evapotranspiration is the actual transfer of moisture from the surface, i.e. bare soil, intercepted water on vegetation, open water and transpiration from within vegetation to the atmosphere.
- Potential evapotranspiration is evapotranspiration that would take place from a well-watered surface under ambient atmospheric conditions (a synthetic measure of evaporative demand).
- Reference evapotranspiration is evapotranspiration from a well-watered reference crop under specific surface moisture conditions by ambient atmospheric conditions (synthetic measure of evaporative demand).
- Crop evapotranspiration is evapotranspiration estimated from a crop surface assuming well-watered and stress-free conditions.

- Evaporative demand is the “thirst” of the atmosphere for given ambient atmospheric conditions (radiation and advective drivers) but with unlimited moisture supply (i.e. maximal rate of evapotranspiration). It can be measured by pan evaporation or lysimeter or modelled by potential or reference evapotranspiration.

Models like DSSAT and MONICA do not simulate direct evaporation of water intercepted by crop canopy from the soil surface and mulches separately (Tenreiro et al. 2020). This is because evaporative demand may include all the components together depending on the calculation procedure. Five approaches can be used to calculate the evaporative demand of which the Penman-Monteith equation is used by most models (Table 3.5). The remaining approaches include Penman, Priestly and Taylor, Hargreaves and the Soil Vegetation Atmosphere Transfer Scheme (SVAT).

WOFOST, APSIM, AquaCrop, DAISY, HYDRUS and SWAP first calculate evaporative demand, which is then partitioned according to the evaporative surface area (i.e. the fraction of crop canopy, fraction of uncovered soil, fraction of mulch). The models WOFOST, DSSAT, APSIM, DAISY, STICS, MONICA, HYDRUS-1D/2D, SWAP and SWIM follow a Beer-Lambert type approach through the leaf area index and an extinction coefficient to calculate an evaporation coefficient (Ke, for wet surfaces) to estimate evaporation from soil (Table 3.5). An alternative option used by AquaCrop, HYDRUS-1D/2D, SWAP, MIKE-SHE and SWIM is to use soil cover through a soil-cover-based method. Some models provide options for both approaches; the evaporative demand is required for both approaches. DSSAT can also use an adaptation to the original Penman's equation to derive both daily evaporations intercepted by crop canopy and soil evaporation, while STICS can simulate evaporation from mulches with a similar approach. MIKE-SHE simulated total evaporation (all three components included) with the SVAT approach.

Models that use the Beer-Lambert or soil-cover based (soil cover) approaches integrate soil evaporation into a single formulation. However, the models APSIM, STICS, AquaCrop, SWAP, MIKE-SHE and SWIM divide soil evaporation into two consecutive stages. Ritchie (1972) proposed the “two-stage method”, which is based on Philip and De Vries (1957), where soil evaporation is limited in the first stage by energy availability and the second stage by water availability. AquaCrop calculates a Kr factor to reduce soil evaporation through an exponential relation that depends on a decline factor related to relative soil water content. APSIM empirically relates the second evaporation stage to the square root of time. A parameter that relates soil type to time is required. SITCS simulate the second stage of soil evaporation with an empirical parameter that depends on the aerodynamic resistance, the latent heat of

vaporization, the water vapour pressure, air temperature, and a diffusion coefficient that is related to the bulk density of the evaporative soil layer and the surface temperature (Brisson and Perrier, 1991). SWAP and MIKE-SHE, for example, model the second stage of soil evaporation as a function of soil water flux density. In this case, a simplified form of the numerical solution of Richard's equation is used to limit (boundary) the maximum upward flow rate (van Dam and Feddes, 2000).

3.3.3.5 Transpiration and root water uptake

The atmospheric demand for transpiration is conceptually the same as the evaporative demand. Models like DSSAT, APSIM, DAISY, STICS, AquaCrop, MONICA and HYDRUS-1D/2D can be separated into two different calculation procedures. Similar to evaporative demand, transpiration demand can be estimated with five different approaches (Table 3.5). Potential crop transpiration is simulated by, for example, MONICA by multiplying transpiration demand with a crop-specific coefficient. At the same time, AquaCrop uses a transpiration coefficient (which is equal to the crop basal coefficient). As with evaporation approaches, potential crop transpiration is adjusted to the transpiration surface through a Beer-Lambert type integrated approach (using leaf area index) or a green canopy soil cover-based method (AquaCrop). SWAP uses an alternative approach, which assumes that the water evaporation from the wet canopy reduces potential transpiration.

Actual transpiration or root water uptake is simulated by DSSAT, APSIM, STICS and AquaCrop with a stress coefficient (Table 3.5). The relative stress level at the upper and lower threshold, a rate factor and a curve shape factor are used in AquaCrop to determine the stress coefficient, which reduces potential transpiration. An alternative approach is "actual crop transpiration is limited by a water uptake (extraction) sink term, which, in the case of multi-layer models, is computed separately for each soil layer" (Tenreiro et al., 2020). The water uptake sink term depends on a reduction coefficient, which is a function of matric potential or volumetric soil water content and a maximum water uptake rate (Ritchie, 1972, 1981; Feddes et al., 1978). The maximum water uptake rate depends on the rooting depth and can be employed in discrete or continuous schemes. With discrete schemes, the maximum water uptake rate is a product of actual transpiration and root density, which can be determined separately for each layer or entire root zone. Continued schemes define the maximum water uptake rate through an integral equation where the root length density is defined as a function of space and time (van Dam et al., 1997; Šimůnek and Hopmans, 2009).

APSIM provides an alternative exponential approach for describing the water uptake sink term, which requires a diffusivity constant, the root length density, time and the beginning time

of water extraction. The dimensionless water stress reduction coefficient can be postulated for matric and osmotic stress. To combine the matric and osmotic stresses, either an additive or a multiplicative approach is used (Skaggs et al., 2006). In addition to the modelling approaches described above HYDRUS-1D/2D also allows for compensated water uptake, i.e. crops can extract more water from non-stressed parts of the root zone.

3.4 RESEARCH IMPLICATIONS

The aim of the research is to provide field scale decision-support regarding the conjunctive use of irrigation water and root-accessible water tables, which implies a normative approach to modelling decision-making. Applying mathematical programming to optimise irrigation water use is infeasible due to the complexity of the interaction between irrigation management and root-accessible water table dynamics. Consequently, the research must adopt an evolutionary optimisation approach to optimise conjunctive irrigation water use by developing a bio-economic evolutionary optimisation model. The response of the biophysical environment to farmer decision-making needs to be valid, suggesting a positive approach to modelling the system. The implication is that the biophysical component of the bio-economic optimisation model needs to be calibrated and valid while the proposed management strategy needs to be feasible. Crop simulation models typically provide alternative means to trigger the timing of irrigation events and to specify the irrigation intensity once an irrigation event is triggered. The research team will explore these options to devise the optimal conjunctive irrigation management strategy.

The recursive stochastic decision-making framework of Madende and Grové (2020) suggests two decision-making stages where different states of nature represent weather risk. The first stage is at the beginning of the season when irrigators must decide the area to irrigate based on the expected weather conditions across different states of nature. Since our focus is on demonstrating the economic value of considering root-accessible water tables as a water source to satisfy crop evapotranspiration requirements partly, the area irrigated is assumed to be fixed. Therefore, irrigation water availability does not constrain crop production. During the second phase, irrigators devise irrigation schedules based on the current status of the biophysical system and expected weather conditions across different weather states while simultaneously considering time-of-use electricity tariffs. The bio-economic model must be solved weekly during the growing season to account for dynamic decision-making. The assumption is that irrigators will maximise expected profits across different weather states. Consequently, irrigators' risk preferences are assumed to be neutral.

A critical part of the bio-economic optimisation model is the biophysical component. The project team decided to concentrate on AquaCrop and SWAP after assessing the i) required model inputs and parameters, ii) details with which important processes are simulated, and iii) integration capabilities with economic and optimisation algorithms. SWAP is considered data-intensive as many inputs and model parameters are required, while AqauCrop is less so. Important differences between the models include:

- AquaCrop adopts the cascading (also called the tipping bucket) approach for soil water flow. The relationships between groundwater table depth, soil hydraulic properties and actual soil water content (or matric potential) are used to simulate capillary rise. AquaCrop, however, does not simulate the feedback between the unsaturated zone and the water table (saturated zone).
- SWAP deals with soil water flow in the unsaturated zone and the upper part of the saturated groundwater. The model focuses primarily on one-dimensional vertical upward and downward soil water flow by numerically solving Richard's partial differential equation. Three-dimensional interactions with groundwater and artificial drains are modelled as additional sinks (drains) and sources (infiltration from ditches and drains), which makes SWAP a quasi-3D model.
- AquaCrop has a water-driven growth engine which is based on the "conservative" nature of the relationship between above-ground biomass and transpiration (normalised water productivity, WP*) when normalized for atmospheric evaporative demand (effect of different climates) (Steduto et al., 2007). The model does not calculate biomass partitioning into various organs (e.g. leaves, roots, etc.). Instead, a reference harvest index (crop-specific) is used.
- WOFOST (de Wit et al., 2019), a detailed model for the dynamic growth of arable crops, is fully integrated into SWAP. The model uses a radiation-driven growth engine and adopts a detailed approach for simulating the effect of temperature and light on leaf expansion at different phenological stages. Light utilization simulations by WOFOST are explanatory descriptions of photosynthesis, respiration and partitioning of assimilates in various growth stages.
- The Penman-Monteith equation applied to a well-watered reference grass surface (ET_o, Allen et al., 1998) is used by AquaCrop as an index for the evaporating power of the atmosphere.
- AquaCrop simulates soil evaporation by decreasing ET_o with a soil evaporation coefficient (related to the fraction of soil surface not covered by the canopy) and

an evaporation reduction coefficient. The latter reduces soil evaporation when soil water is insufficient to respond to the evaporative demand of the atmosphere.

- AquaCrop uses daily ETo and the maximum crop basal coefficient (as defined in FAO56 and FAO66) to simulate potential crop transpiration, which is adjusted to the transpiration surface through the simulated canopy cover.
- SWAP uses crop and soil factors to convert ET_o to potential evapotranspiration of uniform surfaces, namely a dry crop canopy (ET_{p0}), wet crop canopy (ET_{w0}) and wet bare soil (E_{p0}). These crop factors are different from the well-known FAO56 crop factors that depend on the crop development stage and soil cover. Hence, the crop factors in SWAP relate to uniform, cropped surfaces and can be larger than the well-known crop factors.
- Potential crop transpiration and soil evaporation fluxes of partly covered soils are then determined using the simulated leaf area index and the fraction of the day that the crop is wet.

CHAPTER 4: AQUACROP AND SWAP CALIBRATION AND VALIDATION

4.1 INTRODUCTION

After Wallach et al. (2021), calibration is defined as “adjusting model parameters to reduce the error between model results and measured data”. The first step often involves deciding which measured variables should be included in the calibration process. Wallach et al. (2021) highlighted that, in general, as many variables as possible should be included, i.e. to prevent “getting the right answer for the wrong reason”. Measurements of seasonal above-ground biomass and grain yield are popular choices. Canopy cover, leaf area index and above-ground biomass measurements during the growing season are also sometimes used. This also applies to soil water and evapotranspiration measurements.

In the second step of calibration, a decision must be made regarding which parameters to adjust and the default values of the remaining parameters. Seidel et al. (2018) found that 66% of respondents in a web-based survey of crop model calibration practices calibrated less than ten parameters. More than half of the cases (61%) involved fitting the model to crop phenology data. Wallach et al. (2021) found that the choice of which phenology parameters to adjust is based on expert opinion. The authors also found that crop modellers generally aim to adjust parameters until some error measure between simulated and measured values is minimised, i.e. a frequentist method.

In this project, we refer to the trial-and-error approach for the search of values as the ‘determination’ of parameters. Furthermore, estimation of optimal parameters refers to using an algorithm, also sometimes called inverse modelling. Two methods can be used for model parameter estimation. The first is where posterior probability distributions of model parameters are provided through general likelihood uncertainty estimation (He et al., 2010; Sun et al., 2016). Unfortunately, no direct recommendation regarding the optimal solution can be made. With the second method, global optimal or near-optimal parameters can be found with an optimization algorithm. In any case, the objective function is vital to estimate accurate parameters. A single objective function, for example, the mean error between measured and simulated grain yield, is often used to estimate crop model parameters, as highlighted previously.

Until now, to the best of our knowledge, studies where an optimization algorithm was used to calibrate AquaCrop and SWAP are rare. Optimization algorithms, however, have been applied successfully to assimilate values for specific variables (e.g. canopy cover and above-ground biomass) from remote sensing data (e.g. vegetation indices) when calibrating AquaCrop (Jin et al., 2016; Silvestro et al., 2017; Wagner et al., 2020). These algorithms have also been combined with AquaCrop to determine optimal irrigation schedules at regional and local scales (Li et al., 2018; Mwiya et al., 2020; Liu et al., 2021; Guo et al., 2021; Wang et al., 2022). Guo et al. (2021) is the only study where an optimization (elite genetic) algorithm was used to calibrate AquaCrop. Measured variables in the objective functions for calculating the minimum error included in-season canopy cover, above-ground biomass, and seasonal grain yield. Three different calculations of the weight factors for these variables were investigated.

The project team decided to use measurements of weekly soil water content, evapotranspiration, and seasonal above-ground biomass in an objective function to estimate essential parameters for AquaCrop and SWAP. These measurements are available for the modelling conditions in the research domain outlined in Chapter 2. After successful calibration and validation, the two models were applied in Chapter 5 to evaluate the economic benefit of conjunctive use of irrigation water and root-accessible water tables.

4.2 SYNTHESIS OF PARAMETERS

4.2.1 AQUACROP

A description of AquaCrop is available in Steduto et al. (2009), Raes et al. (2009) and Steduto et al. (2012). This section will highlight the parameters required by AquaCrop for simulating crop growth, development, final yield, and soil-crop-water flow processes under non-limiting conditions (Table 4.1).

Simulation of the final yield by AquaCrop happens in four steps on a daily time step. AquaCrop simulates the development of green canopy cover using three parameters (Step 1), namely initial canopy cover (CCo), a canopy growth coefficient (CGC) and maximum canopy cover (CC_x). If no values for CCo are available, the user can determine this parameter from the soil surface covered by an individual seedling at 90% emergence ($CC_{seedling}$, cm^2) and the plant density. Simulations can be done in calendar days (CD) or growing degree days (GDD), i.e. time (t) = CD or t = GDD. To simulate a decline in the green canopy cover due to senescence, the model requires a canopy decline coefficient (CDC) and time to the start of senescence (t_{sc}). AquaCrop can simulate until a defined date or the time to reach physiological maturity

(t_{mt}). Some crops can mature before complete canopy decline is achieved. The user can also decide to use the time to maximum canopy cover (t_{mc}) instead of CGC.

Table 4.1: Parameters required by AquaCrop for simulating crop growth, development, final yield and soil-crop-water flow processes under non-limiting conditions

Process	Parameters	Units
Green canopy cover	CCo	%
	t_{em}	t
	t_{sc}	t
	t_{mt}	t
	CCx	%
	CGC (or t_{mc})	% t^{-1} (t)
	CDC	% t^{-1}
Root expansion	TAW_g	%
	Z_n	m
	Z_x	m
	n	-
	Z_{er} (or t_{Zx})	cm t^{-1} (t)
Transpiration and root water uptake	$Kc_{Tr\,x}$	-
	f_{age}	% t^{-1}
	a	-
	extraction pattern	%
	$S_{x\,top}$	m^3 m^{-3}.t
	$S_{x\,bottom}$	m^3 m^{-3}.t
Biomass production	WP*	g m^{-2}
	f_{yield}	%
Yield formation	HIo	%
	t_{fl}	t
	$t_{flperiod}$	t
Soil water flow	PWP	%
	FC	%
	SAT	%
	Ksat	mm day^{-1}
Soil evaporation	Ke_x	-
	f_{cc}	%
	f_m	%
	f_w	%
	REW	mm
	E_{stage2}	-

At the start of the season, a minimum soil water content expressed as a percentage of total available water (TAW_g) in the minimum effective rooting depth (Z_n) determines germination's success. The root zone will expand under non-limiting soil moisture conditions until the maximum rooting depth (Z_x), which depends on the soil depth, while the root zone expansion curve describes the rate of root deepening. The curve depends on a shape factor (n) and

average root zone expansion rate (Z_{er}). Alternatively, the user can use the time to maximum rooting depth (t_{Zx}).

To simulate daily transpiration (step 2), a crop coefficient at maximum transpiration ($Ks_{Tr,x}$) is required. AquaCrop does adjust the canopy cover for micro-advective effects (CC*), which needs no parameters because an empirical function based on the work of Adams et al. (1976) and Villalobos and Fereres (1990) are used. $Ks_{Tr,x}$ is adjusted for ageing effects, which requires a f_{age} crop parameter (reduction expressed as a fraction per day of CC_x). Similarly, AquaCrop uses a factor (f_{sen}) to adjust $Ks_{Tr,x}$ once senescence is triggered. To determine $f_{sen,}$ the user can use a shape program parameter (a) to accentuate or minimise the effect of senescence on $Ks_{Tr,x}$. For the simulation of root water uptake (soil water extraction) due to transpiration, the user must set the pattern for water extraction throughout the root zone. AquaCrop divides the root zone into four equal parts, each of which the user must specify the contribution (%) to total extraction. In addition, the user must specify a maximum root extraction parameter for the top ($S_{x\,top}$) and bottom ($S_{x\,bottom}$) parts of the root zone.

AquaCrop uses a water-driven growth engine and requires a normalised crop water productivity parameter (WP*) to simulate biomass production (step 3). When yield formation starts, the user can reduce WP* for products rich in lipids or proteins with a coefficient (f_{yield}, % of WP*). These high lipid or protein products require much more energy per dry weight unit than synthesising carbohydrates. The WP* parameter is considered conservative and independent of climate. Partitioning biomass into yield (step 4) requires a reference harvest index (HIo) and a crop- and cultivar-specific parameter. The time until flowering starts (t_{fl}) and duration of the flowering period ($t_{flperiod}$) are required; both parameters are crop and cultivar-specific.

The user can specify up to five soil horizons or layers in AquaCrop. Essential parameters for each soil layer include volumetric soil water content at the permanent wilting point (PWP), field capacity (FC) and saturation (SAT), as well as the saturated hydraulic conductivity (Ksat). In addition, the user can specify the stoniness and penetrability of each horizon, which the model uses to adjust the total available water (TAW) and the maximum rooting depth, respectively. From the entered Ksat, AquaCrop determines the drainage coefficient (α) for each layer, an important parameter to simulate redistribution and deep soil water percolation. The relationships between groundwater table depth, soil hydraulic properties and actual soil water content (or matric potential) are used to simulate capillary rise. Important capillary rise parameters include an a and b parameter, which are determined from Ks. The model,

however, does not simulate the feedback between the unsaturated zone and groundwater table (saturated zone).

Simulation of soil evaporation requires a maximum coefficient for fully wet and non-shaded surfaces (Ke_x), which, together with canopy cover (1-CC, i.e. exposed soil surface), determines evaporation during stage 1, i.e. energy limiting stage. AquaCrop allows adjustment of the fraction of soil surface not covered by the green canopy for micro-advective effects (1-CC*). No parameter is required because an empirical function is used based on data from Adams et al. (1976) and Villalobos and Fereres (1990). Users can adjust the Ke_x parameter for the sheltering effect of the withered canopy (f_{cc}), the presence of mulches (f_m) and partial wetting (f_w) of soil through irrigation. In addition, during stage 1 of evaporation, a parameter representing readily evaporable water (REW) is required. To simulate soil evaporation during stage 2 (dry soil surface), AquaCrop uses a decline factor (E_{stage2}).

4.2.2 SWAP

Table 4.2 provides the parameters required by SWAP for simulations under non-limiting conditions. The date of sowing or crop emergence is a critical management input in SWAP. Germination is represented by the start of the simulation or can be simulated, which requires three parameters, namely lower threshold temperature for emergence (TBASEM), temperature sum from sowing to emergence (TSUMEMEOPT) and maximum effective temperature for emergence (TEFFMX).

The temperature sum from emergence to anthesis (TSUMEA), temperature sum from anthesis to maturity (TSUMAM) and effective temperature (DTSM) are required to simulate the length of the growth period and phenological development stage ($1 < DVS < 2$). The latter is a tabular function of average daily temperature (TAV) and needs to be specified. SWAP also allows the simulation of the effect of day length on development. A parameter for the minimum day length for optimum crop development (DLO) and the shortest day length for any development (DLC) is required. The project team chose the option where crop development before anthesis depends on temperature only. Potential daily biomass production depends on the intercepted amount of irradiation. Hence, the time course of green leaf mass, the resulting leaf area index, the fraction of irradiation intercepted by the canopy, and the time course of total above-ground biomass production are essential. Changing the lower specific leaf area parameter (SLATB) can simulate a higher or lower leaf area index. Biomass production is primarily determined by the daily photosynthesis rate, simulated with a photosynthesis-light response curve.

Table 4.2: Parameters required by SWAP for simulating crop growth, development, final yield and soil-crop-water flow processes under non-limiting conditions

Process		Parameters	Units
Germination		TBASEM	°C
		TSUMEMEOPT	°C
		TEFFMX	°C
Length of growth period and Phenology		TSUMEA	-
		TSUMAM	-
		TAV vs DTSM	°C
		DLO	Hours
		DLC	Hours
Light interception and potential biomass production	Green leaf area	SLATB vs DVS	ha kg^{-1}
	Assimilation	EFF	kg CO_2 J^{-1} adsorbed
	Assimilation	AMAXTB vs DVS	kg ha $hour^{-1}$
	Initial value	LAIEM	m^2 m^{-2}
	Initial value	RGRLAI	m^2 m^{-2} day^{-1}
	Green leaf area	SPAN	Day
	Initial value	TDWI	kg ha^{-1}
	Green leaf area	TBASE	°C
	Assimilation	KDIF	-
	Assimilation	KDIR	-
	Assimilation	TMNFTB vs Min T	°C
	Assimilation	TMPFTB vs Ave T	°C
	Green leaf area	SPA	ha kg^{-1}
	Green leaf area	SSA	ha kg^{-1}
	Assimilate conversion	CVL	kg ha^{-1}
	Assimilate conversion	CVO	kg ha^{-1}
	Assimilate conversion	CVR	kg ha^{-1}
	Assimilate conversion	CVS	kg ha^{-1}
	Maintenance respiration	Q10	/10 °C
	Maintenance respiration	RML	kg CH_2O kg^{-1} day^{-1}
	Maintenance respiration	RMO	kg CH_2O kg^{-1} day^{-1}
	Maintenance respiration	RMR	kg CH_2O kg^{-1} day^{-1}
	Maintenance respiration	RMS	kg CH_2O kg^{-1} day^{-1}
	Maintenance respiration	RFSETB vs DVS	-
Grain yield (assimilate distribution between organs)	Partitioning	FRTB vs DVS	kg kg^{-1}
	Partitioning	FLTB vs DVS	kg kg^{-1}
	Partitioning	FSTB vs DVS	kg kg^{-1}
	Partitioning	FOTB vs DVS	kg kg^{-1}
Root density distribution and growth		RDCTB vs Rdepth	cm^3 cm^{-3}
		RDI	cm
		RRI	cm day^{-1}
		RDC	cm
Soil water flow	upward and downward	θ_r	cm^3 cm^{-3}
		θ_s	cm^3 cm^{-3}
		α	cm^{-1}
		n	-
		l	-
		Ks	cm day^{-1}
Potential soil evaporation		CFBS	-
		KDIF	-
		KDIR	-
Actual soil evaporation		COFRED	-
Potential evapotranspiration of dry or wet canopy		CF vs DVS	-

The initial angle (EFF, light use efficiency for real leaf) is generally constant. At the same time, the maximum (AMAXTB, maximum CO_2 assimilation rate) is often crop variety specific and can decrease due to nutrient shortage and canopy ageing. AMAXTB is specified for a particular stage of development (DVS). Leaf area index and light interception at the start and end of the growing season may also be calibrated by the leaf area index at emergence (LAIEM) and maximum relative increase in leaf area index (RGRLAI) parameters. Both parameters affect the initial increase in leaf area index and the duration until the linear growth phase starts. During the linear growth phase, a complete light interception occurs. The life span of the leaves (SPAN) influences the simulated time course of the leaf area index during the final growth period.

The SPAN value must be increased to simulate a more extended period of green leaves and a higher leaf area index, thus biomass production near crop maturity. Other parameters that may influence light interception and potential biomass production include initial total crop dry weight (TDWI), lower threshold temperature for the ageing of leaves (TBASE), extinction coefficient for diffuse visible light (KDIF), extinction coefficient for direct visible light (KDIR), a reduction factor of AMAX as a function of average daily temperature (TMPF) and a reduction factor of AMAX as a function of minimum day temperature (TMNF). The first two parameters are specially for simulating green leaf area, while the latter four parameters are associated with assimilation. The specific pot (SPA) and stem area (SSA) parameters are related to crops other than maize. For the conversion of assimilates into biomass, four parameters that represent the efficiency of conversion into leaves (CVL), storage organs (CVO), roots (CVR) and stems (CVS) are required. The six parameters used in simulating maintenance respiration include the increase in respiration rate with temperature (Q10), the maintenance respiration rate of leaves (RML), storage organs (RMO), roots (RMR) and stems (RMS), and the reduction factor of senescence (RFSETB) as a function of the development stage.

Parameters used to allocate the produced assimilates to the different organs are important because they determine leaf mass, light interception, and economical products (i.e. the grain). These parameters are the fraction of total dry matter increase partitioned to the roots (FRTB), leaves (FLTB), stems (FSTB) and storage organs (FOTB), which are all a function of the development stage.

The specific crop's root density (RDCTB), the initial rooting depth (RDI), the maximum daily increase in rooting depth (RRI) and the maximum rooting depth of the crop or cultivar (RDC) need to be specified.

SWAP deals with soil water flow in the unsaturated zone and the upper part of the saturated groundwater. The model focuses primarily on the one-dimensional vertical upward (capillary rise) and downward soil water flow by numerically solving Richard's partial differential equation. Highly non-linear soil hydraulic functions are required, i.e. functions that relate volumetric soil water content to soil pressure head (also known as matric potential) and hydraulic conductivity. SWAP uses the Mualem-Van Genuchten functions, which are described by six parameters, namely saturated hydraulic conductivity (K_s), residual (θ_r) and saturated volumetric soil water content (θ_s), and empirical *m*, n and *α* shape parameters, where $m = 1 - \frac{1}{n}$.

The Penman-Monteith equation applied to a well-watered reference grass surface (Allen et al., 1998) is used in SWAP as an index for the evaporating power of the atmosphere. SWAP uses a soil factor (CFBS) to convert ET_o to the potential evaporation rate of a wet, bare soil (E_{p0}). Potential evaporation (E_p) is then simulated from the leaf area index as well as an extinction coefficient for diffuse (KDIF) and direct (KDIR) visible light. The actual evaporation rate is simulated according to Darcy's law using average hydraulic conductivity between the soil surface and the first node, the soil water pressure head in equilibrium with the air relative humidity, the soil water pressure head of the first node, and the first node's soil depth. Hence, the soil hydraulic parameters (as mentioned above) describing the relationship between volumetric soil water content and soil pressure head will be necessary. SWAP also has the option to use the empirical evaporation functions of either Black (1969) or Boesten and Stroosnijder (1986) in combination with the Darcy flux, which requires a soil evaporation coefficient (COFRED). In addition, crop factors (CF) are used to convert ET_o to potential evapotranspiration of a uniform dry (ET_{p0}) or wet (ET_{w0}) crop canopy. These crop factors are different from the well-known FAO56 crop factors that depend on the crop development stage and soil cover. Hence, the crop factors in SWAP relate to uniform, cropped surfaces and can be larger than the well-known crop factors. Potential transpiration is then simulated using ET_{p0} and E_p. Under non-limiting conditions, actual transpiration simulated by both AquaCrop and SWAP will be close to potential transpiration.

4.3 EXPERIMENTAL DATA FOR CALIBRATION AND VALIDATION

Two datasets of WRC-funded projects done on the same lysimeter facility (i.e. the Department of Soil, Crop and Climate Sciences, University of the Free State, Bloemfontein, South Africa) were used in calibration and validation. Trial 1 was conducted by Ehlers et al. (2003), and Trial 2 by Ehlers et al. (2007). The facility is located on the experimental farm of the University of the Free State (Department of Soil, Crop and Climate Sciences) in South Africa. The

experimental area is 0.245 ha with 30 static lysimeters (1.8 m diameter and 2 m deep, with rims of 0.05 m above the soil surface) situated in the middle, i.e. arranged in 2 parallel rows of 15 each. The one row of lysimeters contains a homogenous sandy soil (mean 8% silt-plus-clay) classified as Clovelly Setlagole (according to Soil Classification Working Group, 1991), which qualifies as Quartzipsament (according to Survey Staff, 2003). The other row of 15 lysimeters contains a sandy loam (mean 18% silt-plus-clay) Bainsvlei Amalia soil (according to Soil Classification Working Group, 1991), which qualifies as Plinthustalf (according to Survey Staff, 2003). Two neutron access tubes in each lysimeter allow soil water measurements (0.3 m intervals up to 1.8 m). In contrast, the inner walls and bottom of the lysimeters can be accessed through an underground chamber (1.8 m wide, 2 m deep and 30 m long). A monometer and bucket at the bottom of each lysimeter allow recharging and regulation of root-accessible water tables (< 1.8 m from the surface) and drainage measurement. A randomised split-plot experiment was conducted with three replications during both trials. Soil type was applied at two levels as the main-plot treatments, namely Bainsvlei and Clovelly.

The sub-plot control treatment for Trial 1, which is no groundwater table, was used to calibrate AquaCrop and SWAP. The control data for the Clovelly soil were used for AquaCrop and the Bainsvlei soil for SWAP. The treatment with a constant groundwater table depth of 1.5 m was used for validation. Root water uptake from the groundwater was recorded daily and then added through the bottom of the lysimeter to recharge the groundwater table and keep it at a depth of 1.5 m. The sub-plot treatments for Trial 2 consisted of four irrigation and groundwater table salinities (irrigation and groundwater had the same salinity, i.e. 0.2 to 6.0 dS m^{-1}). A shallow ground water table was kept constant at a depth of 1.2 m from the soil surface with the same procedure described above. Only data from the non-saline control treatment for the Bainsvlei soil, with a constant groundwater table at 1.2 m from the surface, were used as additional validation.

All the data in the trials, used for calibration and validation, represent optimum conditions for crop growth, allowing for maximum root water uptake and grain yield. Measured weekly (w) volumetric soil water content ($\theta_{(w)}$) and evapotranspiration ($ET_{(w)}$), and seasonal (s) above-ground biomass ($BM_{(s)}$) were used in the calibration of AquaCrop and SWAP. In Section 4.5, the calibration algorithm is explained. Simulations of weekly soil water content over a depth of 1.8 m ($WC_{1.8(w)}$), cumulative evapotranspiration, cumulative water table uptake (WTU, mm) and seasonal grain yield were used to validate both models. The same maize cultivar was grown during both trials with the agronomic practices listed in Table 4.3.

Table 4.3: Agronomic practices of maize for the lysimeter trials done by Ehlers et al. (2003) and Ehlers et al. (2007)

Trial	**1 | Ehlers et al. (2003)**		**2 | Ehlers et al. (2007)**	
Cultivar	PAN 6335		PAN 6335	
Planting date	6 December 2000		15 December 2004	
Planting depth (cm)	2.5		2.5	
Row width (m)	0.9		0.9	
Planting density (plants ha^{-1})	50 000		50 000	
Fertilization	At planting	Top dressing	At planting	Top dressing
Nitrogen (kg ha^{-1})	217	50	217	50
Phosphorous (kg ha^{-1})	49	-	49	-
Potassium (kg ha^{-1})	-	-	50	-
Pest control	Curater		Decus	

4.4 MEASURED, DEFAULT AND PEDOTRANSFER PARAMETERS

Daily minimum and maximum temperatures and ET_o values, as shown in Figure 4.1, during the maize growing season of both trials were entered into both models. In addition, default carbon dioxide values for AquaCrop were used, while daily radiation measurements were entered for SWAP. Rainfall during the growing season of Trial 1 was entered as part of irrigation. During Trial 2, the rain shelter was closed; hence, no rainfall values were entered.

The measured, default and pedotransfer function estimated parameters used in AquaCrop are shown in Tables 4.4 and 4.5. Soil parameters were entered for five layers, each 0.3 m thick, except the last layer, 0.6 m thick. Volumetric soil water at saturation and field capacity were obtained from an internal drainage experiment done on each lysimeter (Barnard et al., 2010). Field capacity generally refers to the soil water content in the field after 2 to 4 days following thorough rainfall and/or irrigation. After two days of drainage, from initial saturated soil profiles, the bottom of the various lysimeters was wet, i.e. volumetric soil water content was close to saturation, as shown in Table 4.4. This does not reflect these soils' natural drainage condition and is typical of lysimeters or pot trials where there is an abrupt, discontinuous boundary from the bottom soil layer to the gravel, i.e. soil water at saturation equals lysimeter saturation and water content at field capacity equals lysimeter capacity. Under these conditions, a small water table develops at the bottom, from where the pressure head must be high enough to transport water to the gravel layer beneath. Hence, the saturation and field capacity values entered in AquaCrop under lysimeter conditions approximate a soil water profile in equilibrium with the groundwater table, illustrated in Figure 4.2.

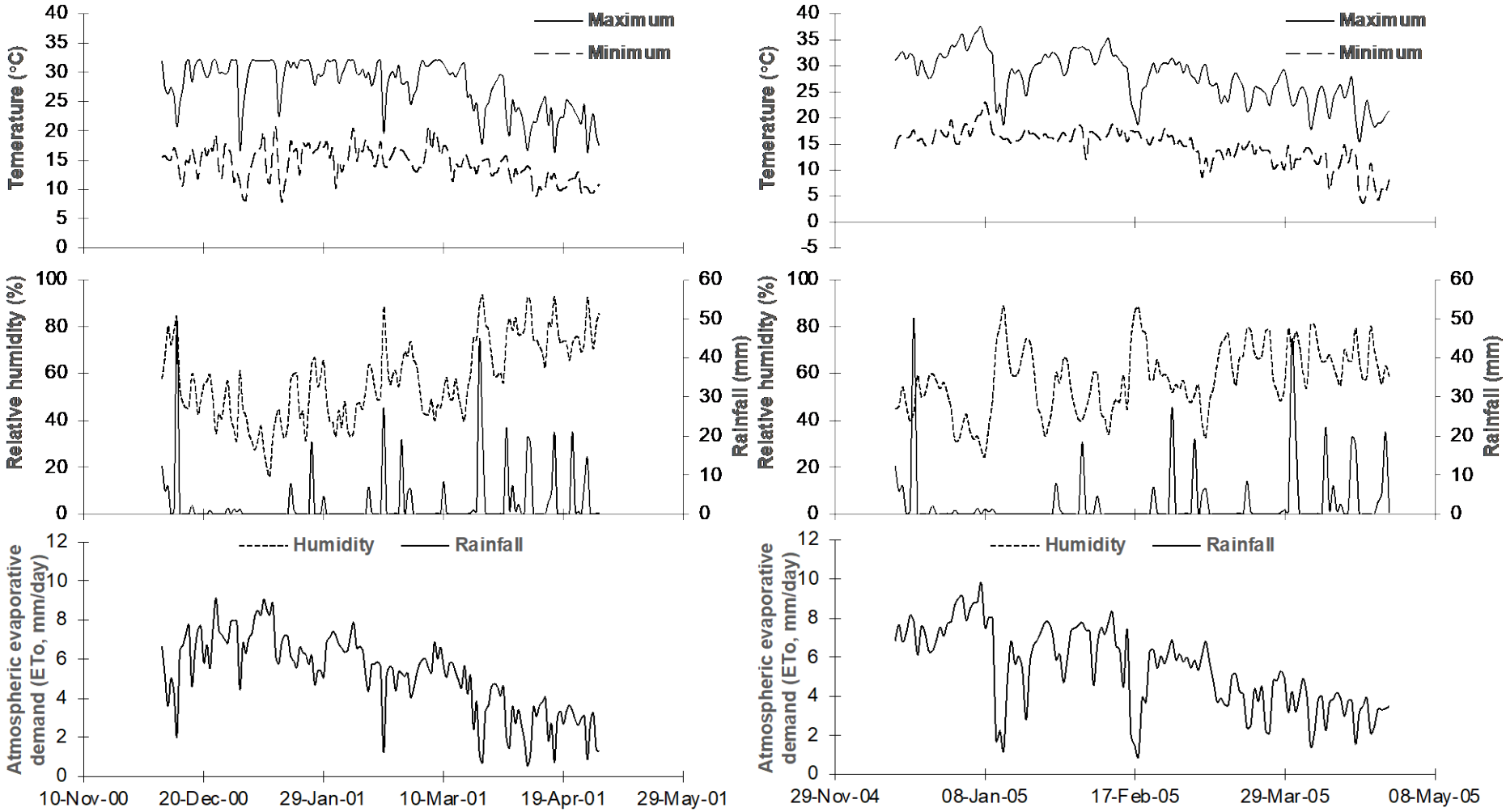

Figure 4.1: Weather data for the 2000-2001 and 2004-2005 maize growing seasons done by Ehlers et al. (2003) and Ehlers et al. (2007), respectively, at the lysimeter facility of the Department Soil, Crop and Climate Sciences, University of the Free State.

Table 4.4: Measured and pedotransfer function estimated parameters for the Clovelly soil used in AquaCrop

Soil	Thickness (m)	Silt (%)	Clay (%)	$\theta_{LSat} = \theta_{Sat}$ (%)	$\theta_{LC} = \theta_{FC}$ (%)	θ_{PWP} (%)	K_s mm day^{-1}
Sandy (Clovelly)	0-0.3	4	5	29.5	10.5	4.80	1004.38
	0.3-0.6	3	5	32.2	16.5	4.40	1131.07
	0.6-0.9	3	5	28.8	18.4	4.40	1131.07
	0.9-1.2	3	5	31.0	20.3	4.40	1131.07
	1.2-1.8	3	5	31.9	28.8	4.40	1131.07
	Mean	3	5	30.9	20.6	4.50	1099.40

Table 4.5: Default parameters used in AquaCrop for simulating Trials 1 and 2 as provided in Annexes of the reference manual by Raes et al. (2022)

Process	Parameters	Units	Values
Green canopy cover	CCo	%	0.33
	t_{em}	t	DECAL
	t_{sc}	t	DECAL
	t_{mt}	t	DECAL
	CCx	%	0.95
	CGC (or t_{mc})	% t^{-1} (t)	DECAL
	CDC	% t^{-1}	DECAL
Root expansion	TAW_g	%	20
	Z_n	m	0.3
	Z_x	m	1.75
	n	-	1.5
	Z_{er} (or t_{Zx})	cm t^{-1} (t)	2.3 (980)
Transpiration and root water uptake	$Kc_{Tr\,x}$	-	DECAL
	f_{age}	% t^{-1}	0.150
	a	-	1
	extraction pattern	%	40, 30, 20, 10
	$S_{x\,top}$	$m^3\ m^{-3}.t$	0.0480
	$S_{x\,bottom}$	$m^3\ m^{-3}.t$	0.0120
Biomass production	WP*	g m^{-2}	33
	f_{yield}	%	100
Yield formation	HIo	%	44
	t_{fl}	t	DECAL
	$t_{flperiod}$	t	DECAL
Soil evaporation	Ke_x	-	DECAL
	f_{cc}	%	60
	f_m	%	0
	f_w	%	100
	REW	mm	DECAL
	E_{stage2}	-	DECAL

DECAL = **D**ifferential **E**volution **Cal**ibration algorithm

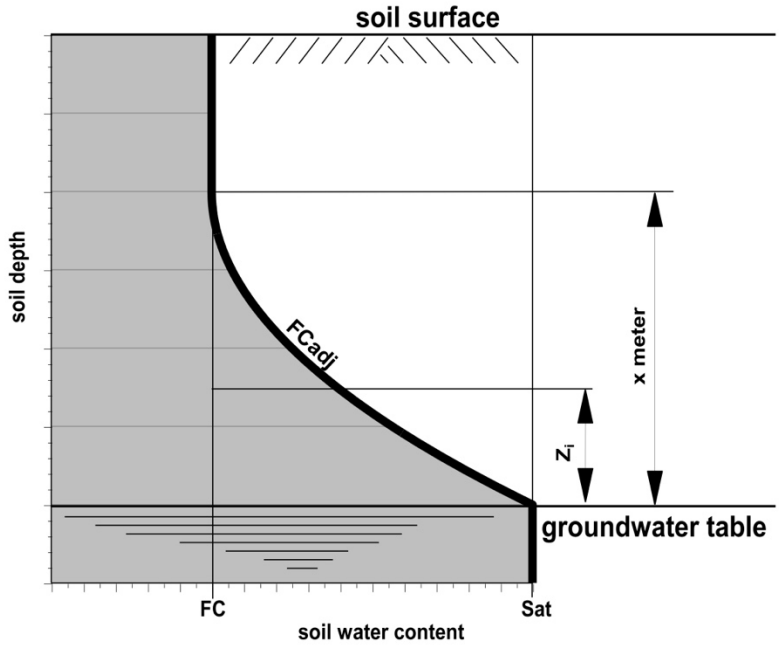

Figure 4.2: Illustration of soil water profile, at saturation (Sat), field capacity (FC) and adjusted field capacity (FCadj), in equilibrium with the groundwater as used in AquaCrop (Raes et al., 2022).

Under shallow groundwater table conditions, the field capacity within the capillary fringe x m is referred to as adjusted field capacity in AquaCrop (FCadj) (Raes et al., 2022). A locally developed pedotransfer function, RETEN (Streuderst, 1985), was used to estimate volumetric soil water at -1500 kPa from silt-plus-clay, i.e. permanent wilting point (PWP). Saturated hydraulic conductivity was determined with Equation 4.1 from silt-plus-clay, developed by Ehlers et al. (2003) for the two soils. The initial volumetric soil water at the start of the growing season was entered. Default a and b parameters used to simulate capillary rise were estimated by AquaCrop from Ks values. Table 4.5 shows the default maize parameters used in AquaCrop (i.e. annexes of the reference manual by Reas et al. 2022).

$$K_s = 2925.8\, e^{-0.1188(silt-plus-clay)} \quad (4.1)$$

Vertical discretization of the soil profiles that were used in SWAP are shown in Table 4.6, i.e. six sub-layers of 30 cm each, with 30 compartments of 1 cm each in the first layer and six compartments of 5 cm each in the remaining five sublayers. The first sub-layer represents soil physical layer 1, sub-layers 2, 3 and 4 soil physical layer two and sub-layers 5 and 6 soil physical layer 3. Table 4.7 provides the Mualem-van Genuchten soil parameters used in SWAP. Three physical soil layers were identified based on the silt-plus-clay measurements of the Bainsvlei soil, namely 10%, 18% and 24% as physical soil layers 1, 2 and 3. RETEN was used to establish the relationship between volumetric soil water and matric suction (pressure

head) for the three physical layers from silt-plus-clay measurements. These values were then entered in the RETC software package (version 6.02, van Genuchten et al., 1991), which estimated the Mualem-van Genuchten parameters, while the saturated hydraulic conductivity was determined with Equation 4.1. The measured initial volumetric soil water at the start of the growing season was entered.

Table 4.6: Vertical discretization of the soil profile in SWAP

Sub layer	Soil physical layer	Sub layer thickness (cm)	Compartment Thickness (cm)	Number of compartments
1	1 ^{Bv} 1 ^{Cv}	30	1	30
2	2 ^{Bv} 1 ^{Cv}	30	5	6
3	2 ^{Bv} 1 ^{Cv}	30	5	6
4	2 ^{Bv} 1 ^{Cv}	30	5	6
5	3 ^{Bv} 1 ^{Cv}	30	5	6
6	3 ^{Bv} 1 ^{Cv}	30	5	6

Bv = Bainsvlei soil; Cv = Clovelly soil

Table 4.7: Mualem-van Genuchten parameters of the three identified soil layers in the lysimeters describing the soil hydraulic functions used in SWAP

Soil parameters	Physical soil layer		
	1	2	3
Residual volumetric water content (θ_r, cm^3 cm^{-3})	0.033	0.046	0.061
Saturated volumetric water content (θ_s cm^3 cm^{-3})	0.336	0.354	0.369
Alfa of main drying curve (α, cm^{-1})	0.0181	0.0196	0.0215
Parameter n	1.447	1.352	1.315
Exponent in hydraulic conductivity function (l)	1.795	-3.501	-6.112
Saturated hydraulic conductivity (K_s, cm d^{-1})	115.57	56.84	34.02

Table 4.8 shows the default parameters for maize used in SWAP. These parameters were obtained from the WOFOST database for maize.

Table 4.8: Default parameters used in SWAP for simulating Trials 1 and 2

Parameters	Units	Values
TBASEM	°C	6
TSUMEMEOPT	°C	DECAL
TEFFMX	°C	30.0
TSUMEA	-	DECAL
TSUMAM	-	DECAL
TAV vs DTSM	°C	DECAL
DLO	Hours	1.0
DLC	Hours	0.0
SLATB vs DVS	ha kg^{-1}	DECAL
EFF	kg CO_2 J^{-1} adsorbed	DECAL
AMAXTB vs DVS	kg ha^{-1} $hour^{-1}$	DECAL
LAIEM	m^2 m^{-2}	DECAL
RGRLAI	m^2 m^{-2} day^{-1}	DECAL
SPAN	day	DACAL
TDWI	kg ha^{-1}	50.00
TBASE	°C	10.00
KDIF	-	0.60
KDIR	-	0.75
TMNFTB vs Min T	°C	0.00 (5.00); 1.00 (8.00)
TMPFTB vs Ave T	°C	0.10 (0); 0.8 (16); 1.00 (20); 0.95 (36); 0.56 (42)
SPA	ha kg^{-1}	0.0
SSA	ha kg^{-1}	0.0
CVL	kg ha^{-1}	0.6800
CVO	kg ha^{-1}	0.6710
CVR	kg ha^{-1}	0.6900
CVS	kg ha^{-1}	0.6580
Q10	/10 °C	2.00
RML	kg CH_2O kg^{-1} day^{-1}	0.03
RMO	kg CH_2O kg^{-1} day^{-1}	0.01
RMR	kg CH_2O kg^{-1} day^{-1}	0.015
RMS	kg CH_2O kg^{-1} day^{-1}	0.015
RFSETB vs DVS	-	1.00 (0); 1.00 (1.50); 0.75 (1.75); 0.25 (2.00)
FRTB vs DVS	kg kg^{-1}	0.40 (0); 0.34 (0.20); 0.23 (0.50); 0.10 (0.8); 0 (1); 0 (2)
FLTB vs DVS	kg kg^{-1}	0.62 (0); 0.62 (0.33); 0.15 (0.88); 0.10 (1.10); 0 (1.2); 0 (2)
FSTB vs DVS	kg kg^{-1}	0.38 (0); 0.38 (0.33); 0.85 (0.88); 0.40 (1.10); 0 (1.2); 0 (2)
FOTB vs DVS	kg kg^{-1}	0.00 (0.95); 0.50 (1.10); 1.0 (1.2); 1.0 (2)
RDCTB vs Rdepth	cm^3 cm^{-3}	1 (0); 0.74 (0.2); 0.30 (0.4); 0.17 (0.6); 0.9 (0.8); 0.05 (1)
RDI	cm	5.00
RRI	cm day^{-1}	2.20
RDC	cm	75
CFBS	-	1.25
KDIF	-	0.60
KDIR	-	0.75
COFRED	-	DECAL
CF vs DVS	-	DECAL

DECAL = **D**ifferential **E**volution **Cal**ibration algorithm

4.5 DIFFERENTIAL EVOLUTION CALIBRATION ALGORITHM

The main purpose of the Differential Evolution Calibration algorithm (DECAL) is to determine the value of the calibration parameters listed in Tables 4.5 and 4.8 for AquaCrop and SWAP, which will minimise the simulation error, i.e. the difference between the measured and the simulated outcome variables. Three measured variables were used to estimate the composite simulation error to be minimised by DECAL. When calculating the composite simulation error,

equal weights were assigned to each simulation error. The measured variables that were included in the calculation of the composite simulation error in the objective function were $WC_{1.8(w)}$, $ET_{(w)}$ and $BM_{(s)}$, as explained in Section 4.3. The normalised root mean square error (NRMSE) determined the simulation error of $WC_{1.8(w)}$ and $ET_{(w)}$, while the simulation of $BM_{(s)}$ was assessed with the absolute percentage error (PE).

DECAL evolves an initial population of candidate solutions through an iterative mutation, crossover, and selection process to generate an updated generation of candidate solutions with better performance indicators than the previous generation. During the population initialisation phase, a population of NP vectors of different levels of the D calibration parameters are randomly generated. Each vector of calibration parameter levels is referred to as an individual and represents a candidate solution to the minimised composite simulation error. Let's symbolise each individual in a generation by $X_i^g = [x_{i,1}^g,\ x_{i,2}^g\ \cdots\ x_{i,D}^g]$, for i = 1, 2, … NP vectors of d = 1, 2, … D AquaCrop calibration parameters, where g = 0, 1, … G represents different generations with g=0 indicating the initial population. Large heterogeneity in the initial population (g=0) is key to ensuring that the search space is covered as much as possible. A uniform distribution is used to generate the initial search space with Equation 4.2.

$$x_{i,d,min}^0 + \left(x_{i,d,max}^0 - x_{i,d,min}^0 \right) U(0,1) \tag{4.2}$$

Where $U(0,1)$ represents a uniformly distributed random number in the range [0,1], where $x_{i,d,min}^0$ and $x_{i,d,max}^0$ are the minimum and maximum levels of the respective calibration parameters. The upper and lower bounds on the calibration parameter levels were taken as ± 20% of the default values. These bounds ensure that compensating errors that may occur between parameters are controlled.

Next, the initial population evolves through a process of mutation and crossover. For each target vector, X_i^g, a mutant vector V_i^g is created with Equation 4.3.

$$V_i^g = X_{r1}^g + F \cdot \left(X_{r2}^g - X_{r3}^g \right) \tag{4.3}$$

Where r1, r2 and r3 are randomly chosen indexes from $i \in [1, \ldots NP]$ which need to be different from the current generation index i, and F is a constant scaling factor. The exploration capability of the mutant generation strategy employed is strong since both the base (r1) and the difference vectors (r2 and r3) are randomly generated. Crossover increases the diversity

of the population by combining the mutant vector with the target vector to create a trial vector $U_i^g = [u_{i,1}^g, u_{i,2}^g \cdots u_{i,D}^g]$ using Equation 4.4.

$$u_{i,j}^g = \begin{cases} v_{i,\mathrm{j}}^g & \text{if } \mathrm{U}(0,1) \leq \mathrm{CR} \text{ or } \mathrm{j}=\mathrm{r} \\ x_{i,j}^g & \text{otherwise} \end{cases} \quad (4.4)$$

Where $CR \in [0,1]$ defines the crossover probability and $r \sim U[1, \mathrm{D}]$ selects a random index to identify a random calibration parameter. The composite simulation errors of the trial vector (U_i^g) are compared to the composite simulation errors of the current generation (X_i^g) to determine whether an individual in the trial vector should replace an individual in the current population when the trial vector's composite simulation error was smaller. The processes of mutation and crossover are repeated until the stopping criterium is met. Visual Basic for Application© code was developed to automate the implementation of DECAL using the AquaCrop plug-in program, ACsaV60.EXE, which allows for the automation of multiple simulations, i.e. the program executes a list of projects while saving the results in output files. The SWAP executable was used to implement DECAL with SWAP.

4.6 RESULTS AND DISCUSSION

4.6.1 AQUACROP

The DECAL estimated parameters for the control treatment showed a high consistency level between different Clovelly soil replications. Replication 3, however, had the best NRMSE (< 5%) for simulations of $WC_{1.8(w)}$ and $ET_{(w)}$, while the simulation of $BM_{(s)}$ had the lowest PE (< 5%). Table 4.9 provides the DECAL estimated parameters for maize grown on the Clovelly soil for replication three without a shallow groundwater table. A visual comparison between measured and simulated $WC_{1.8(w)}$ and cumulative ET, using the parameters in Tables 4.4, 4.5 and 4.9 and the mean irrigation of the three replications, confirms that AquaCrop was reasonably well calibrated with DECAL (Figure 4.3). $BM_{(s)}$ and grain yield were over-simulated by less than 3% and 1.5%, respectively.

Table 4.9: DECAL estimated AquaCrop parameters for maize grown on the sandy Clovelly soil for the control treatment of Trial 1

Process	Parameters	Units	DECAL values
Green canopy cover	t_{em}	t	51
	t_{sc}	t	1519
	t_{mt}	t	1805
	CGC (or t_{mc})	% t^{-1} (t)	1.499
	CDC	% t^{-1}	1.987
Transpiration and root water uptake	$Kc_{Tr\,x}$	-	1.28
	t_{fl}	t	974
	$t_{flperiod}$	t	186
Soil evaporation	Ke_x	-	1.30
	REW	mm	6
	E_{stage2}	-	4

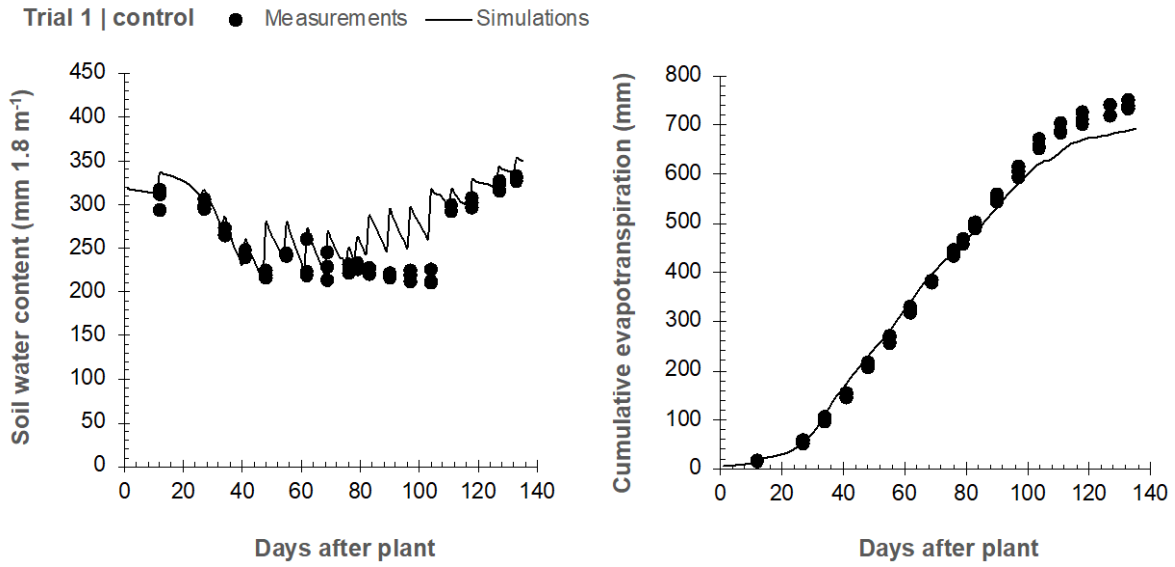

Figure 4.3: Comparison between measured and AquaCrop simulated soil water content and cumulative evapotranspiration (ET) using parameters in Tables 4.4, 4.5 and 4.6 without a water table

Figure 4.4 shows the validation results, i.e. where simulations were done in the presence of a groundwater table at a depth of 1.5 and 1.2 m. $WC_{1.8(w)}$ and cumulative ET were expected to be simulated reasonably accurately for the 1.5 m groundwater table depth because this treatment was part of Trial 1. Simulations of $WC_{1.8(w)}$ and cumulative ET were also acceptable for the 1.2 m groundwater table depth, considering that it was done under different conditions, namely Trial 2. Seasonal simulated WTU amounted to 182 and 323 mm for the 1.5 and 1.2 m groundwater table depth, which were 28 mm more and 9 mm less than the measured values, respectively. $BM_{(s)}$ and grain yield were over-simulated by less than 6% for the 1.5 m groundwater table depth and 25% for the 1.2 m groundwater table depth.

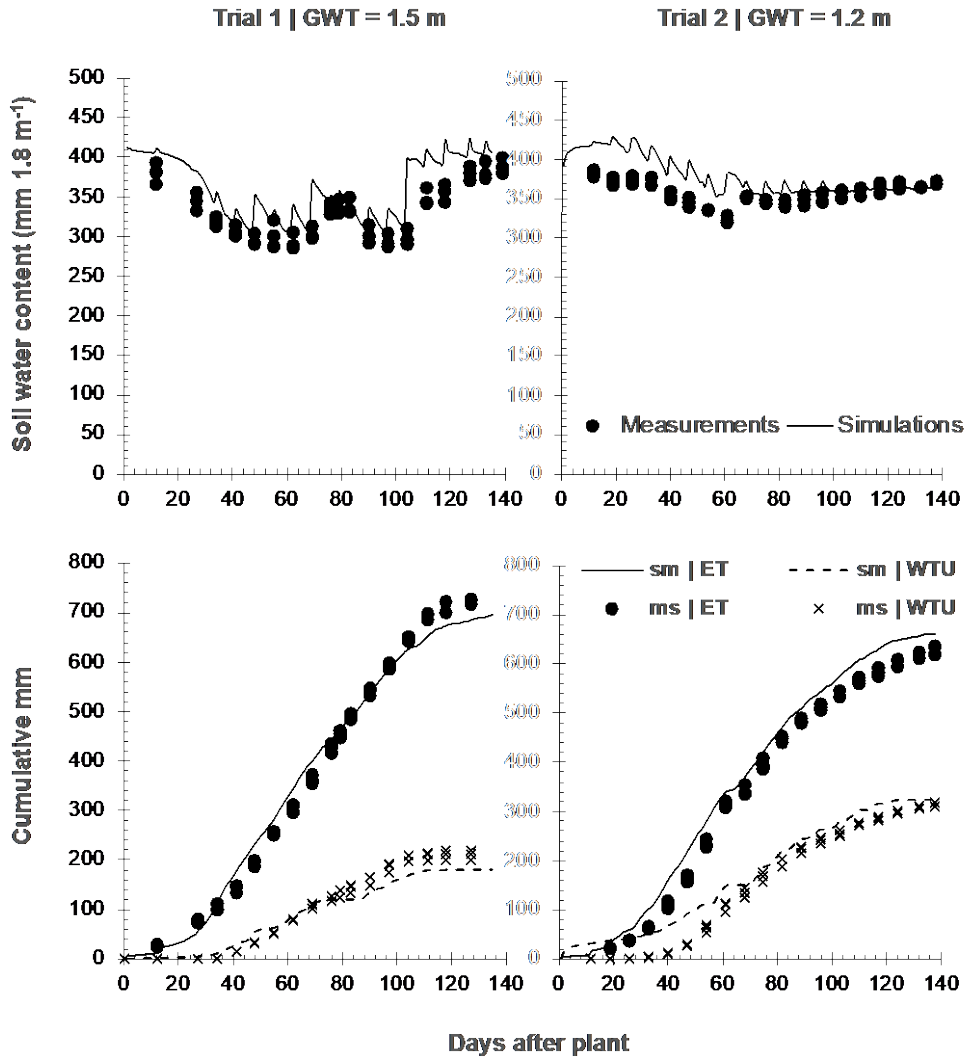

Figure 4.4: Comparison between measured (ms) and AquaCrop simulated (sm) soil water content, cumulative evapotranspiration (ET) and cumulative water table uptake (WTU) using parameters in Tables 4.4, 4.5 and 4.6 under a constant water table at a depth of 1.5 and 1.2 m

Under non-limiting conditions, the simulated grain yield will compare well to measured values when users calibrate AquaCrop to simulate BM(s) accurately. The specified reference harvest index and $BM_{(s)}$ determine grain yield. AquaCrop does not reduce the selected harvest index due to water, salinity, or fertility stress under non-limiting conditions. Our results revealed that no measurements describing crop phenology, for example, green canopy cover or time of various development stages, are required to calibrate AquaCrop under non-limiting conditions with DECAL. Either $WC_{(w)}$ or $ET_{(w)}$ measurements will suffice. However, $BM_{(s)}$ should be part of the objective function. According to Seidel et al. (2018), crop modellers generally use data that describe crop phenology in the calibration process. For AquaCrop and maize, specifically, canopy cover is primarily used in the calibration process, for example, Abedinpour et al. (2012), Shrestha et al. (2013), Hassanli et al. (2016) and Shirazi et al. (2021). The project team acknowledge that the accuracy of WC and ET measurements in the objective function

is vital in calibration where no crop phenology measurements are available. Under lysimeter conditions, researchers can reasonably accurately apply irrigation and quantify drainage beyond the measured soil depth. In addition, runoff cannot occur as the lysimeter rims were 5 cm above the soil surface. This accurate quantification of the soil water balance components improves the determination of ET.

The DECAL estimated parameters compare well to the literature. This finding, however, is expected as we included bounds, which ensured that the estimated parameter could not differ more than 20% from the default values. We believe that including $BM_{(s)}$ measurements in the objective function when calibrating AquaCrop improves the separation of ET in evaporation and transpiration. The latter is better simulated because of the relationship between seasonal BM and transpiration, characterised through a normalised water productivity parameter (Steduto et al. 2009).

WTU of maize grown in a sandy soil was simulated well with the DECAL estimated parameters for a groundwater table depth of 1.5 and 1.2 m. This result is satisfactory, considering that no calibration of the parameters required to simulate WTU (i.e. capillary rise) was done. The capillary rise parameters are determined by AquaCrop using the input saturated hydraulic conductivity of the soil. Goosheh *et al*. (2018) and Zhao *et al*. (2020), respectively, simulated WTU of maize and wheat accurately with AquaCrop. The latter authors used AquaCrop to improve the irrigation scheduling of wheat and increase water productivity under shallow groundwater table conditions.

An essential step in calibrating mathematical bio-physical models is a sensitivity analysis of parameters, which was not done in this project. Essential parameters for accurately simulating green canopy cover, transpiration, and evaporation with AquaCrop were calibrated using DECAL. The project team argue that evapotranspiration must be simulated reasonably well to have a good chance of simulating WTU accurately. The global sensitivity analysis method EFAST (extended Fourier amplitude sensitivity test) has become very popular when analysing AquaCrop parameters (Vanuytrecht et al. 2014; Guo et al. 2020). Lu et al. (2021) highlight that determining parameter ranges is critical for robust and trustworthy sensitivity results. Parameter ranges should be physically valid and locally reasonable and hence application-dependent. Parameter sensitivities also depend on the target output, e.g. grain yield, transpiration, green canopy cover, evaporation, etc. Lu et al. (2021) found that WP* and time of yield formation, i.e. essential parameters for biomass and yield formation, do not influence total transpiration. Parameter sensitivities also depend on environmental conditions. A sensitivity analysis should be carried out before each model calibration and application. Under

low water stress conditions for dryland maize grown near Mean, eastern Nebraska, Monze in southern Zambia and Xiaotangshan in northern China, Lu et al. (2021) identified CCx, t_{fl}, duration of yield formation, t_{mt}, t_{sc} and f_{yield} as parameters that have a major influence on yield. For simulations of transpiration CCx, CGC, t_{sc} and base temperature below which crop growth does not occur were identified as the most influential. Guo et al. (2020) found that t_{sc} and t_{mt} were the most influential parameters when simulating $BM_{(s)}$ under non-limiting conditions. The authors also indicated that CGC and CCx were insensitive to $BM_{(s)}$ but were sensitive to BM production during the maize's early and middle growth period. Parameters such as Kc_{Trx}, WP* and t_{sc} also strongly influence BM during different maize growth periods. In addition, it was found that CCx, t_{sc} and CGC were sensitive to green canopy development during different growth stages. Guo et al. (2020) concluded that these sensitive parameters had a stronger influence on green canopy development than BM production during the growing season.

4.6.2 SWAP

Table 4.10 provides the DECAL estimated parameters for SWAP. The values represent the mean over three replications for the control treatment of the sandy loam Bainsvlei soil. The NRMSE for simulations of $WC_{1.8(w)}$ was < 5% and for $ET_{(w)}$ < 20%. Simulated $WC_{1.8}$ and cumulative ET during the growing season are provided in Figure 4.5 and compared well to the measurements. $BM_{(s)}$ and grain yield of maize grown on the Bainsvlei soil were over and under-simulated by 8.9% and 5.9%, respectively.

Table 4.10: DECAL estimated SWAP parameters for maize grown on the sandy loam Bainsvlei soil for the control treatment of Trial 1

Parameters	Units	Values
TSUMEMEOPT	°C	94
TSUMEA	-	994
TSUMAM	-	798
TAV vs DTSM	°C	8 (0); 32 (24); 45 (24)
SLATB vs DVS	ha kg^{-1}	0.0024 (0.0); 0.00220 (0.78); 0.00150 (2.00)
EFF	kg CO_2 J^{-1} adsorbed	0.49
AMAXTB vs DVS	kg ha $hour^{-1}$	80 (0.0); 80 (1.25); 78 (1.50); 78 (1.75); 56 (2.00)
LAIEM	m^2 m^{-2}	0.04836
RGRLAI	m^2 m^{-2} day^{-1}	0.03530
SPAN	day	38
COFRED	-	0.60
CF vs DVS	-	0.21 (0.30); 0.95 (0.50); 1.34 (0.7); 1.38 (1.00); 1.21 (1.40); 0.93 (2)

The validation results, namely where the parameters in Tables 4.7, 4.8 and 4.10 were used for simulations done under a 1.5 m and 1.2 m constant groundwater table, are shown in Figure 4.6.

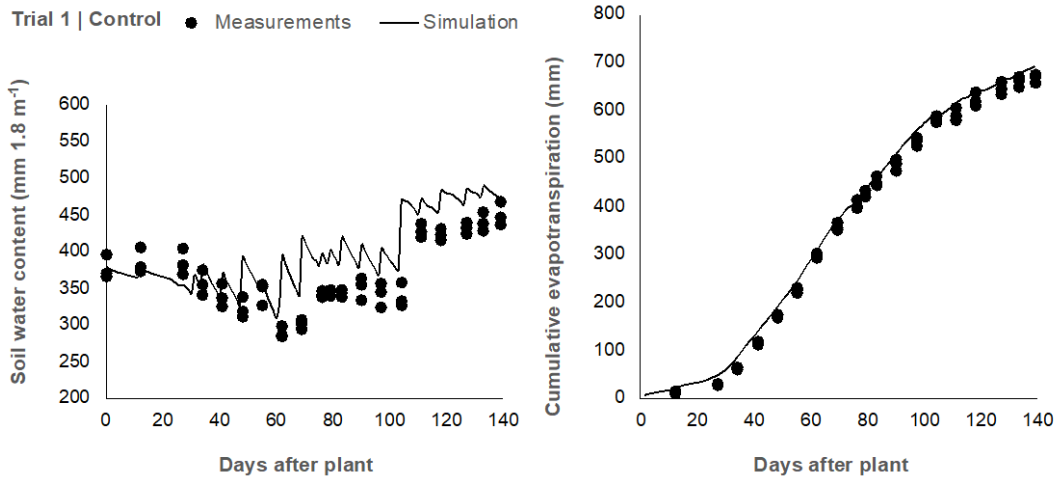

Figure 4.5: Comparison between measured (ms) and SWAP simulated (sm) soil water content and cumulative evapotranspiration (ET) using parameters in Tables 4.7, 4.8 and 4.10 in the absence of a groundwater table

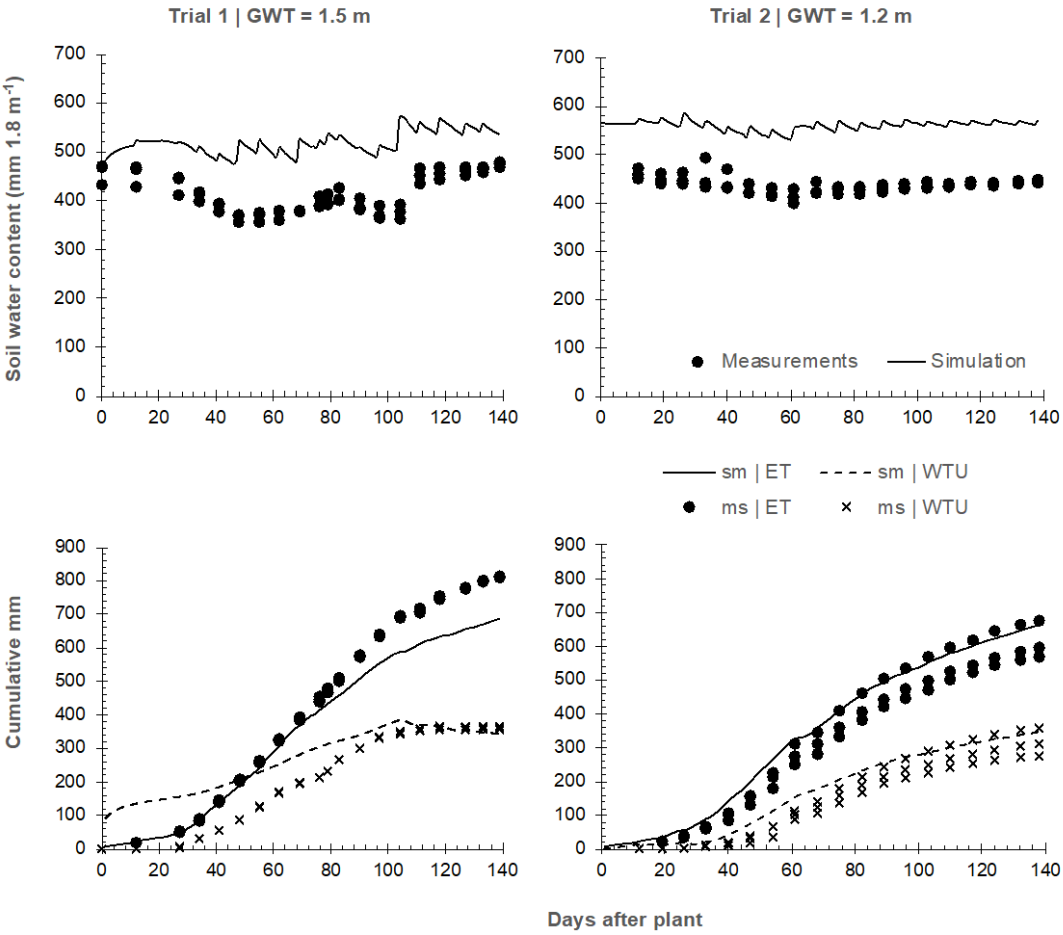

Figure 4.6: Comparison between measured (ms) and SWAP simulated (sm) soil water content, cumulative evapotranspiration (ET) and cumulative water table uptake (WTU) using parameters in Tables 4.7, 4.8 and 4.10 under a constant groundwater table at a depth of 1.5 and 1.2 m

$BM_{(s)}$ was under-simulated by about 20% for the 1.5 m groundwater table depth and over-simulated by about 7% for the 1.2 m groundwater table depth. The difference between

measured and simulated grain yield amounted to 15% and -26%, respectively. Cumulative ET and WTU were simulated worst for the 1.5 m groundwater table depth compared to the 1.2 m depth. Up until about 80 days after plant cumulative WTU was over-simulated by SWAP compared to the measured values. From 80 days after plant to the end of the season, cumulative ET was under-simulated by SWAP. The comparison between measured and simulated cumulative ET and WTU were much better at the 1.2 m groundwater table depth. At both groundwater table depths, however, the simulation of $WC_{1.8}$ was poor. The difference between the mean simulated $WC_{1.8}$ over the growing season and the measured value amounted to 105 and 123 mm for the 1.5 m and 1.2 m groundwater table depth, respectively. SWAP was, however, able to simulate the trend in $WC_{1.8}$ relatively well during the growing season for both groundwater table depths.

Li and Ren (2019) found after an extensive sensitivity analysis of SWAP-WOFOST that n, α and θ_S were the most influential when simulating soil water content. The project team did not calibrate any of the soil hydraulic parameters in this study, which could explain the over-simulation of soil water content compared to the measurements for both the 1.5 m and 1.2 m groundwater tables. Wang et al. (2023) highlight several issues related to parameter sensitivity analysis, including sampling size, parameter variation range, temporal characteristics of sensitivity analyses and multi-variable output. The authors found that for WOFOST parameters important to leaf expansion, light interception, assimilation and phenological development play a key role in simulation outputs. The project team decided to estimate the parameters listed in Table 4.10 with DECAL after consulting the many technical documents of SWAP and WOFOST. In a variance-based sensitivity analysis of WOFOST, Confalonieri (2010) found that seven out of 34 parameters, primarily related to CO_2 assimilation and the conversion of photosynthates into plant organs, accounted for approximately 90% of the total output variability. No significant differences were observed in the relevance of the WOFOST parameters. Hence, parameters with significantly higher relevance compared to others were limited.

4.7 RESEARCH IMPLICATIONS

For AquaCrop, the DECAL calibration process showed good results, especially under non-limiting conditions. It was observed that AquaCrop could accurately simulate soil water content, evapotranspiration, water table uptake and grain yield of maize grown on sandy soil. Measurements describing crop phenology, such as canopy cover, were not necessary for calibration using DECAL under these conditions. Instead, soil water content measurements

were sufficient, while seasonal above-ground biomass played a crucial role in the objective function.

For SWAP, the results indicated that the model performed reasonably well, particularly in simulating soil water content and evapotranspiration. However, there were discrepancies in simulating above-ground biomass and grain yield, especially under shallow groundwater table conditions. This inconsistency might be due to the lack of calibration of soil hydraulic parameters, which were not considered in this study.

Sensitivity analysis was emphasized, as understanding parameter influences can improve model outputs. Although no sensitivity analysis was conducted in this project, previous studies have highlighted the significance of specific parameters for simulating variables like soil water content, evapotranspiration and yield.

CHAPTER 5: BIO-ECONOMIC ANALYSIS OF CONJUNCTIVE WATER USE

5.1 INTRODUCTION

Chapter 5 discusses the bio-economic optimisation model, the application of the model to improve conjunctive water management and the results from the bio-economic analyses. Procedures were developed to link AquaCrop and SWAP to a differential evolutionary algorithm to optimise the conjunctive use of surface and root-accessible water tables. Consequently, the setup and bio-economic analyses are discussed for both models.

5.2 BIO-ECONOMIC OPTIMISATION MODEL

5.2.1 MODEL COMPONENTS AND INFORMATION FLOW

Figure 5.1 shows the different components of the bio-economic optimisation model and the information flow between the components. The bio-economic model has a loosely coupled structure, allowing biophysical and economic components to function independently. The main purpose of the Differential Evolution (DE) component is to facilitate information transfer between the components while evolving the irrigation schedules to one with a higher margin above the specified costs (MAS). The structure of the input files and output files necessitates biophysical model-specific procedures to integrate a specific biophysical model (i.e. SWAP and AquaCrop) with the economic model.

The optimisation commences with the DE component generating alternative irrigation timing triggers and indicator values to identify certain irrigation depth options within the crop simulation model. The crop simulation model simulates the impact of the irrigation strategy (timing option and irrigation depth option) on crop yield by translating the irrigation strategy into an irrigation calendar, which shows the calendar day of the irrigation events and the irrigation depths. The simulated crop yield and the irrigation calendar are the only information passed to the economic model to determine the financial performance of the irrigation strategy. The profitability calculation distinguishes between yield and irrigation-dependent costs to better reflect irrigation management decisions on profitability.

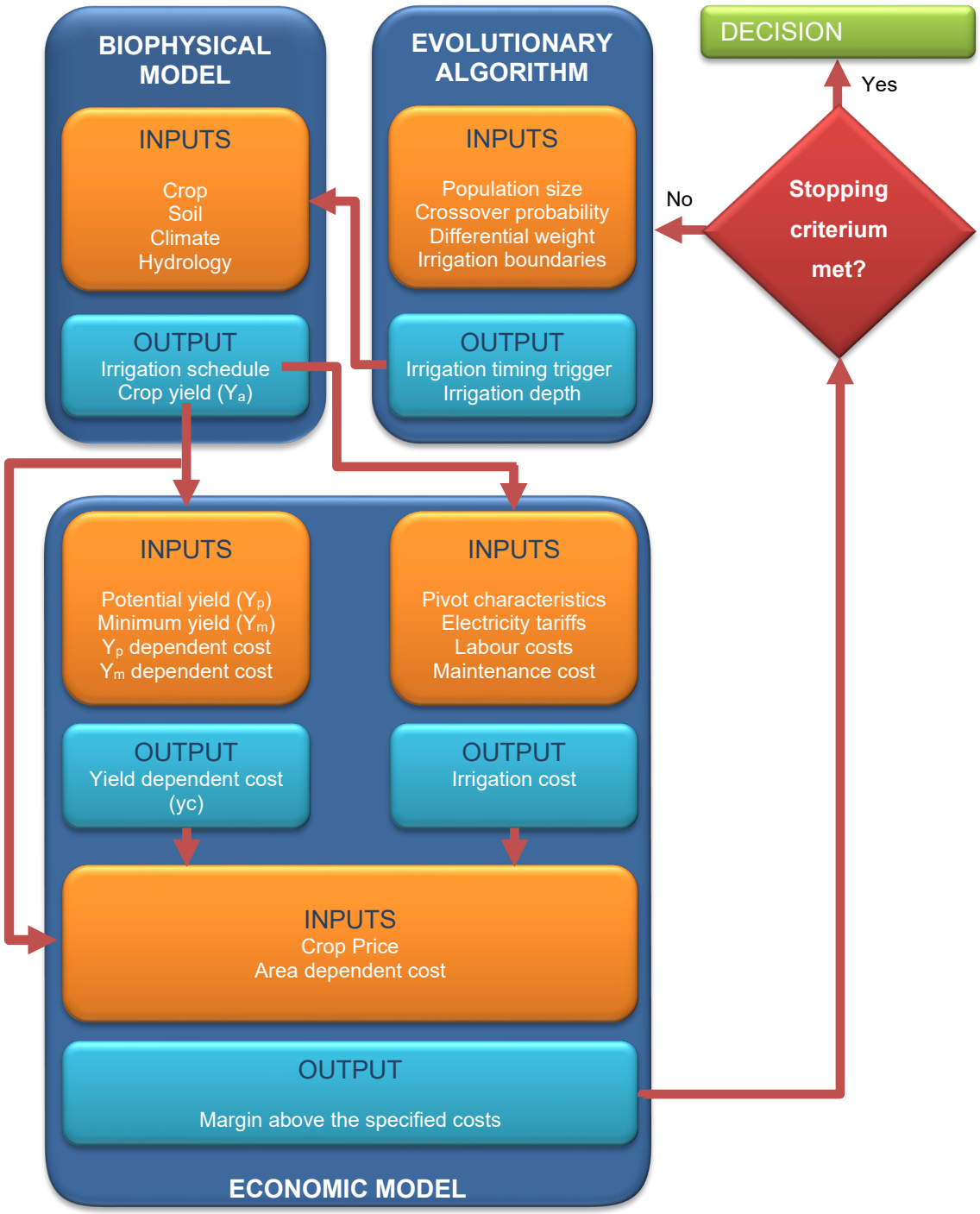

Figure 5.1: Bio-economic optimisation modelling framework showing information flow between different components of the bio-economic optimisation model

The DE algorithm repeats the process by applying mutation, crossover and selection to evolve the candidate population of irrigation schedules to ones with better MAS indicators until the stopping criterium is met.

5.2.2 BIOPHYSICAL MODEL

The modelling framework allows any of the two biophysical models to represent the biophysical component of the bio-economic optimisation model. A bio-economic optimisation model was developed for AquaCrop and SWAP. The details of these models are discussed in Chapter 4.

5.2.3 ECONOMIC MODULE

The economic model calculates the total gross margin above the specified costs for a pivot of 30 ha with an application rate of 12mm/day, which is the key performance indicator for evaluating the profitability of an irrigation schedule. A distinction is made in the model between costs dependent on irrigation applications and costs dependent on crop yield (i.e. fertilizer and harvesting costs). The electricity cost to pump the water represents most of the irrigation-dependent costs. The electricity cost calculations are based on the Ruraflex time of use electricity tariff.

The following equation calculates the MAS associated with a specific irrigation schedule:

$$MAS = p \times Y(i) - ydc \times Y(i) - IDC(i) - ADC \quad (5.1)$$

Where:

MAS	Margin above the specified costs (R ha^{-1})
$Y(i)$	Simulated crop as a function of the irrigation schedule (t ha^{-1})
p	Price of maize (R t^{-1})
ydc	Yield dependent costs (R t^{-1})
$IDC(i)$	Irrigation-dependent cost state-specific irrigation schedule (R ha^{-1})
ADC	Area-dependent cost (R ha^{-1})

The first term (i.e. $p \times Y(i)$) of the MAS calculation calculates the production income as a function of the irrigation schedule by multiplying the simulated maize yield as a function of the irrigation schedule with the selling price of maize. The second term (i.e. $ydc \times Y(i)$) calculates the costs that depend on the simulated crop yield as a function of the irrigation schedule, which was also taken as the yield expectation. Consequently, ydc includes fertilizer costs and harvesting costs. ADC is the only cost component that does not vary as a function of the irrigation schedule and includes costs like fuel, microelements, seed, chemical, harvest, and mechanization costs. The calculation of irrigation-dependent costs (i.e. $IDC(i)$) is not straightforward because it depends on the required irrigation hours to apply a given amount of water. Therefore, the calculation of irrigation-dependent costs is discussed in more detail. Equation 5.2 shows all the costs associated with applying irrigation water.

$$IDC(i) = EC + LC + RMC + WC \quad (5.2)$$

Where:

EC	Variable electricity costs for crop *c* (R ha^{-1})
LC	Total labour costs for crop *c* (R ha^{-1})
RMC	Total repair and maintenance costs for crop *c* (R ha^{-1})
WC	Total water costs for crop *c* (R ha^{-1}) for indirect or direct pricing

The electricity cost calculation does not include fixed costs since fixed electricity costs must be paid whether the irrigator applies water or not. Variable electricity costs are calculated as follows using the Ruraflex electricity tariff:

$$EC_c = \sum_{i,t}\left(ta_{i,t} + rc_{i,t} + dc_{i,t}\right)kWPH_{i,t} + \sum_{i,t} tra_{i,t} kvar\, PH_{i,t} \quad (5.3)$$

Where:

$ta_{i,t}$	Active energy charge on day *i* in timeslot *t* (R kWh^{-1})
$rc_{i,t}$	Reliable energy charge on day *i* in timeslot *t* (R kWh^{-1})
$dc_{i,t}$	Demand energy charge on day *i* in timeslot *t* (R kWh^{-1})
kW	Kilowatt requirement (kW)
$PH_{c,i,t}$	Pumping hours to irrigate crop *c* on day *i* in timeslot *t* (h)
$tra_{i,t}$	Reactive energy charge on day *i* in timeslot *t* (R kVARh^{-1})
$kvar$	Kilovar (kVAR)

The active energy, reliable energy, and demand energy charge are dependent on the kilowatt required to pump irrigation water, while the reactive energy charge is dependent on the kilovar. However, the reliable energy charge is only applicable during the high-demand season. Both active energy and reactive energy consumption are determined by the required pumping hours, which are calculated as follows:

$$RPH_i = \frac{\frac{I_i}{\eta_s} PA \times 10}{q} \quad (5.4)$$

Where:

RPH_i	Required pumping hours on day *i* (h)
η_s	Irrigation system application efficiency (%)
PA	Pivot area (ha)
q	Flow rate (m^3 h^{-1})

Equation 5.4 shows that RPH_i is differentiated for each day and is a function of pivot characteristics (i.e. application efficiency, pivot area, and flow rate). The Ruraflex electricity tariff charges are differentiated into different time-of-use timeslots (i.e. off-peak, standard, and peak) based on the day of the week and time of the day. The irrigator needs to decide during which time-of-use timeslots to irrigate. The assumption is that an irrigator will distribute the

required pumping hours over two consecutive days to facilitate energy management. The following heuristic is used to allocate the required pumping hours to different time-of-use timeslots (Madende, 2017):

$$PH_{i,"off-peak"} = min \begin{vmatrix} RPH_i \\ aph_{i,"off-peak"} \end{vmatrix} \quad (5.5)$$

$$PH_{i,"standard"} = min \begin{vmatrix} RPH_i - PH_{i,"off-peak"} \\ aph_{i,"standard"} \end{vmatrix} \quad (5.6)$$

$$PH_{i,"peak"} = min \begin{vmatrix} RPH_i - PH_{i,"off-peak"} - PH_{i,"standard"} \\ aph_{i,"peak"} \end{vmatrix} \quad (5.7)$$

Where:

$aph_{i,t}$ Total available pumping hours during time-of-use timeslot *t* (i.e. off-peak, standard, and peak) for allocating required pumping hours on day *i* t(h)

$PH_{i,t}$ Day i's required pumping hours allocated to time-of-use timeslot *t* (i.e. off-peak, standard, and peak) when irrigating on day *i* and the next day (h)

The irrigation labour and repair and maintenance costs are calculated using the cost estimation procedures developed by Meiring (1989). Irrigation labour costs are calculated as follows:

$$LC = \sum_i \frac{RPH_i}{24} \times lh \times lw \quad (5.8)$$

Where:

lh Labour hours required per 24 hours of irrigation for a certain pivot size (h)

lw Labour wage rate (R h^{-1})

The total repair and maintenance cost is calculated as follows:

$$RMC_c = \sum_i RPH_{i,c} rt \quad (5.9)$$

Where:

rt Repair and maintenance tariff per 1000 hours pumped for an irrigation system (R/1000 hours)

The assumption is that the water tariff is implemented on a volumetric basis. The total water charge payable to the water user association is calculated as follows:

$$WC_c = cwr_c \times wt \quad (5.10)$$

Where:

cwr_c Crop water requirement as given by WUA for crop *c* (mm)

wt Water tariff (R mm^{-1})

5.2.4 DIFFERENTIAL EVOLUTION ALGORITHM

A DE algorithm was also used to optimise irrigation decisions to improve conjunctive use of surface water and root-accessible water tables. Initial simulations indicated that water table uptake is a function of irrigation applications. Consequently, only the timing of irrigation events and the water applications were considered decision variables. Excluding area irrigated as a decision variable simplifies the algorithm because the irrigation applications could be generated within specified lower and upper bounds. The working of DEOPT (Differential Evolution OPTimisation) is the same as DECAL. However, the objective of DEOPT is to find the irrigation decisions that maximise the MAS. The processing of the data input and output files is also specific to DEOPT.

5.3 BIO-ECONOMIC ANALYSES

Both AquaCrop and SWAP were used in the bio-economic analyses of conjunctive surface and root-accessible water tables. In both cases, optimal conjunctive water use was compared to a baseline situation, representing no information regarding root-accessible water tables. Next, the application of the two models is discussed in more detail.

5.3.1 BASELINE

5.3.1.1 SWAP

A full irrigation strategy represents the baseline whereby the irrigator uses the previous week's observed evapotranspiration and rainfall to calculate the necessary irrigation for the current week. Since the strategy does not consider any soil-water information, the strategy ignores the possible contribution of root-accessible water tables to satisfy the crop's evapotranspiration requirement of the week.

For each state of nature, the cumulative difference between the previous week's crop evapotranspiration demand and rainfall was taken as the irrigation requirement of the current week. The weekly calculated irrigation requirement was scheduled such that irrigation events start on a Friday and consecutively continue until all the water is applied. The reason for starting on a Friday is that it is cheapest to irrigate over weekends, according to the Ruraflex time-of-use timeslots. The maximum daily application was determined according to the application rate of the pivot. The resulting irrigation schedule was used as input in the bio-economic simulation model to quantify the key economic and biophysical performance indicators.

5.3.1.2 AquaCrop

The AquaCrop application baseline was based on farmers' actual water applications. Data collected by Barnard *et al*. (2021) from 19 fields within the Orange-Riet and Vaalharts Irrigation Schemes to investigate the best on-farm water and salt management practices was used to derive the baseline. The irrigation water amounts obtained from the Barnard *et al*. (2021) study were clustered/ grouped into three irrigation schedules that represent the most used irrigation amounts applied during the production season. The irrigation schedules were clustered using the K-means cluster analysis in the IBM SPSS Statistics Program (IBM, 2020). The procedure identifies relatively homogeneous groups of the selected variables by minimising the Euclidean distance from the cluster center. Based on the use of the Elbow rule while conducting a Hierarchical Cluster analysis, it was specified in the K-means procedure that the data be reduced to three clusters. The seasonal water application for the three clusters is 274 mm (cluster 1), 347 mm (cluster 2) and 648 mm (cluster 3). The results from the cluster analysis confirmed that relative to the crop water requirement, some farmers either over- or under-irrigate crops. The seasonal amounts were distributed within the season such that the schedules ensured the optimal irrigation distribution. In other words, the dynamics of crop production and the economic impact of the irrigation timing provided a maximum margin above the specified cost (economic indicator).

5.3.2 CONJUNCTIVE WATER USE OPTIMISATION

Optimising realistic irrigation schedules requires including different weather states to uplift the assumption of perfect foresight. The DEOPT model allows for optimising irrigation decisions while probabilistically representing the state of the soil-crop-atmosphere continuum. Deriving optimal irrigation schedules with DEOPT considers the possible contribution of root-accessible water tables to satisfying crop evapotranspiration requirements because using root-accessible water tables as a potential water source does not come at a cost when the profitability of alternative irrigation schedules is evaluated.

The decision-making framework of Madende and Grové (2020) presented in Figure 3.2 (Chapter 3) is used to guide the optimisation of irrigation decisions to maximise the expected margin above the specified costs irrespective of the state of nature and to maximise the margin above the specified costs in the presence of state-specific unfolding soil-crop-atmosphere information. Next, the application of the decision-making framework for the two objectives is discussed in more detail.

5.3.2.1 Expected outcome maximisation

The first decision tree depicted in Figure 3.2 shows that irrigation decisions are made to maximise the expected outcome (i.e. margin above the specified costs) irrespective of the state of nature occurring for a given irrigation area. Thus, irrigation decisions are made once and for all without considering unfolding information on the state of the soil-crop atmosphere continuum. A separate biophysical model simulation represents each state. The same irrigation decisions apply to all states, and DEOPT evolves the irrigation decisions while considering the contribution of root-accessible water tables through separate biophysical model simulations for each state. Consequently, the optimised irrigation decisions represent the best irrigation water management, regardless of which state of nature unfolds.

The irrigation decisions that maximise the expected outcome regardless of the state of nature were optimised using AquaCrop and SWAP.

5.3.2.2 Unfolding information maximisation

The unfolding information maximisation optimisation recognises that irrigation decisions that maximise expected outcomes irrespective of the state of nature might be suboptimal for a specific state. The second decision tree in Figure 3.2 shows that the irrigator can adjust future irrigation decisions based on the expected future state of the soil-crop-atmosphere continuum, given the past state of the soil-crop-atmosphere continuum is known when the adjustment is made. Consequently, the irrigation decision problem must be solved for each unfolding state of nature, exponentially increasing the problem's dimensionality when including more states. The assumption is that the irrigator is allowed to adjust irrigation decisions weekly.

Therefore, 20 DEOPT optimisations are necessary for each unfolding state of nature. After each optimisation (i.e. one week), the weather file of the biophysical model representing a specific future state of nature is updated with information on the unfolding state of nature. The lower and upper bounds of the irrigation amounts are also fixed in DEOPT to correspond with the optimised irrigation decisions of the previous week. As a result, only future irrigation decisions are optimised.

The unfolding information maximisation analysis was only done for SWAP.

5.4 BIO-ECONOMIC MODEL SETUP AND DATA

5.4.1 SWAP DATA

The SWAP optimisation uses the weather database from SAPWAT (Crosby and Crosby, 1999) to define different weather states. Cluster analysis was used to reduce the dimensionality of the weather database to three clusters containing similar weather patterns. Cluster analysis is a technique focused on classifying homogeneous cases within themselves and heterogeneous between each other (Yim and Ramdeen, 2015).

Cluster analysis was performed on data covering the growing maize season in the Vaalharts area. Two years were considered outliers and removed from the dataset. After the data was organized to fit the simulation period, the reference crop evapotranspiration (ETo) and the rainfall daily amounts were aggregated to weekly averages. After that, the difference between the two was computed and standardized (Jajuga and Walesiak, 2000). The standardized data was used to do a hierarchical cluster analysis using Ward's Linkage method using a statistical software called Statistical Package for the Social Sciences (SPSS) (IBM, 2020). The 48 years of data were reduced to three clusters of 11, 21, and 16 years in each cluster. Only one of the cluster members was used to represent the weather pattern of a cluster. The representative member was chosen based on the mean absolute deviation (MAD).

MAD is a statistic measuring the accuracy of the predictions within a set of quantitative elements and is useful because the prediction errors are in the same unit as the observed data (Khair *et al.*, 2017). The MAD was calculated for each member state within a cluster, translating to 11 MAD calculations for cluster 1, 21 MAD calculations for cluster 2, and 16 MAD calculations for cluster 3. The year with the smallest MAD was chosen to represent the weather pattern of the cluster. The probability that each representative weather state could occur was calculated as the number of years in a cluster divided by the 48 years of data used for the cluster analysis. Consequently, the three states had occurrence probabilities of 33%, 44%, and 23%. The probabilities were used to calculate the expected performance indicators of the irrigation schedules.

The variation in the identified states is depicted in Figure 5.3. As illustrated in Figure 5.3, the differences arose from the main differences between ETo and Rainfall, especially toward the end of the period under simulation (week 20), where State 2 has the largest difference between ETo and Rainfall, meaning that towards the end of the season, the ETo was greater than the rainfall present. In State 1, on the other hand, the difference between ETo and Rainfall in weeks 4 and 20 was similar, while State 3 shows a consistent difference from week 4 up until

week 16. The identified characteristics of each state of nature, measured by ETo and rainfall, set the states apart.

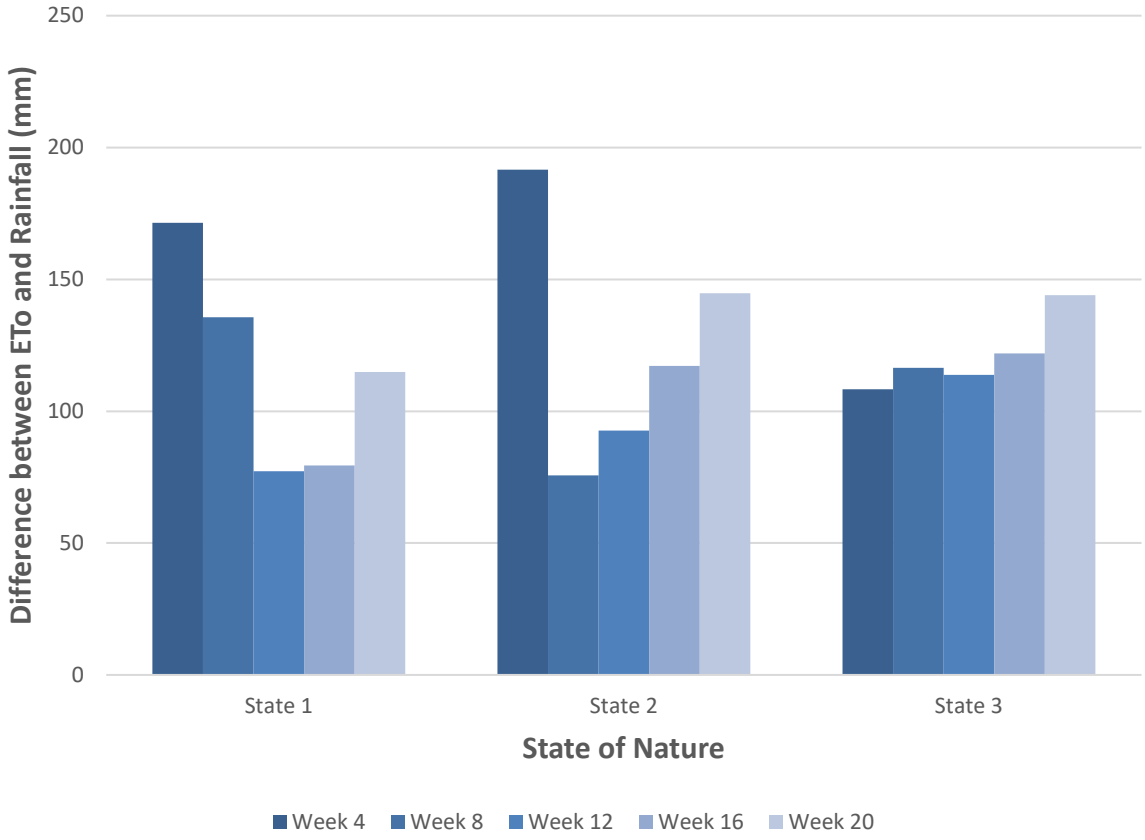

Figure 5.2: Variation of the identified states at various weeks

Source: Own compilation

DECAL estimated SWAP parameters for maize grown on the sandy loam Bainsvlei soil were used in the analyses. The assumption is that the water table depth is 1.5m.

5.4.2 AquaCrop data

The climate files (.TMP, .ET_o and .PLU) were set up using minimum-maximum temperatures ET_o, and rainfall data collected from the automatic weather station at the Orange-Riet weather station for the period 1 January 1983 to 31 December 1994. A default .CO2 file 'MaunaLoa.CO2' was selected to represent the CO_2 concentrations of the farm as the weather station did not measure the CO2 concentrations. The calibrated and validated crop parameters for the Clovelly soil form were used to inform the .CRO, .SOL, .SWO, GWT-files. Aeration stress was activated in the .CRO-file. The implication is that in a shallow groundwater table, the crop could experience stress and thus reduce crop yields when too much irrigation water is applied. The assumption is that the water table depth is 1.5m.

5.4.3 ECONOMIC MODEL DATA

The economic model is generic between the AquaCrop and SWAP applications. The financial calculations are based on a 30.1 ha pivot with an irrigation application rate of 12 mm/day.

The area- and yield-dependent costs for irrigated maize were obtained from the income and cost budgets for the summer crops compiled by BFAP *et al.* (2021), while the variable electricity charges are based on the Ruraflex structure for 2020/2021 (Eskom, 2021). The costs are given in Table 5.1. The estimated maize price was R2 633 t^{-1}.

Table 5.1: Irrigated maize production cost estimates (2021)

Yield dependent costs		
Contracting	R ha^{-1}	1470
Crop insurance	R ha^{-1}	308
Fertiliser	R ha^{-1}	8564
Transport	R t^{-1}	285
Area Dependent costs		
Fuel	R ha^{-1}	926
seed	R ha^{-1}	4975
Weed Control	R ha^{-1}	663
Pest Control	R ha^{-1}	2397
Variable Electricity Charges		
Active Energy Charge		
Off-peak	R kWh^{-1}	0.72
Standard	R kWh^{-1}	1.13
Peak	R kWh^{-1}	1.64
Ancillary Charges		
Off-peak	c kWh^{-1}	0.63
Standard	c kWh^{-1}	0.63
Peak	c kWh^{-1}	0.63
Demand Charges		
Off-peak	R kWh^{-1}	0.41
Standard	R kWh^{-1}	0.41
Peak	R kWh^{-1}	0.41
Other costs		
Labor cost	R/24 hours irrigation	12.58

5.4.4 DIFFERENTIAL EVOLUTION ALGORITHM PARAMETERS

The Differential Evolution algorithm requires the initial population size, maximum number of iterations, mutation factor, crossover probability, and the lower and upper bounds on irrigation applications. The algorithm generated an initial population of 100 irrigation schedules with irrigation events between 6mm and 12mm. The initial population evolved for 500 iterations while applying a mutation factor of 50% and a crossover rate of 10%.

5.5 SWAP RESULTS

5.5.1 BIO-ECONOMIC ANALYSIS WITHOUT CONSIDERING WATER TABLE UPTAKE

The full irrigation management strategy is a strategy where the irrigator, for each state, uses the previous week's observed evapotranspiration and rainfall levels to schedule irrigation for the current week. Thus, the strategy does not use soil-water information to schedule irrigation and ignores the potential contribution of root-accessible water tables. Each state will have an irrigation schedule as it differs in evapotranspiration and rainfall levels.

Table 5.2 shows the bio-economic simulation results for the full irrigation strategy. The full irrigation strategy applications vary by 26mm between a minimum of 557mm (State 1) and a maximum of 583mm (State 2), with an expected application of 574mm. The variation in maize yields was greater when compared to irrigation water applications. Maize yields varied by 3 329kg ha^{-1} between a minimum of 10 733kg ha^{-1} (State 2) and 14 062kg ha^{-1} (State 3) with an expected crop yield of 11 963kg ha^{-1}. The extent of the crop yield variation is attributed to the ability of SWAP to capture the impact of different states of nature on potential non-stressed crop yields since inspection of the crop results file indicated almost no water stress.

Although the full irrigation strategy achieved state-specific potential crop yields, the water use efficiency of the strategy was low as it varies between a minimum of 1.13 (State 3) and a maximum of 1.28 (State 2) with an expected value of 1.19. The water use efficiency results show that the full irrigation strategy is expected to supply 19% more water (i.e. rainfall, irrigation, and root-accessible water tables) than the crop's evapotranspiration requirement. The mismatch between total water supply and crop evapotranspiration requirements results in an expected drainage loss of 92mm, which could be as low as 51mm (State 3) and as high as 143mm (State 2). The order of magnitude of the drainage losses corresponds with the magnitude of the rainfall. The contribution of root-accessible water tables to satisfying crop evapotranspiration requirements was less than 7% in all the states.

The margin above the specified costs of the full irrigation strategy in each state of nature directly results from how the biophysical system responded to the full irrigation strategy. The expected margin above the specified costs for the strategy was R170 291, which varied substantially between R298 022 (State 3) and R94 006 (State 2). The substantial variation in the margin above the specified costs directly results from the yield expectation differences between states of nature and the production income and expenses dependent on crop yield. Expenses dependent on irrigation applications, such as total variable electricity and other

irrigation-dependent costs, varied only with R1 714 (R35 720-R34 006) and R508 (R11 564-R11 056), respectively, for the 30ha pivot.

Table 5.2: Economic and biophysical indicators when applying a state-specific full irrigation strategy without considering root-accessible water table uptake on a 30.1 ha pivot (2021)

		Full irrigation strategy			
	Units	State 1	State 2	State 3	Expected
Probability of occurrence	fraction	0.23	0.44	0.33	
Economic indicators					
Margin above the specified costs	R	132 960	94 006	298 022	170 291
Production income	R	1 218 329	1 156 890	1 515 716	1 289 433
Total variable electricity costs	R	34 006	35 720	34 100	34 791
Active energy charge					
Off-peak	R	12 869	13 477	14 211	13 579
Standard	R	9 030	9 063	8 338	8 816
Peak	R	1 051	1 617	191	1 016
Other variable electricity charges	R	11 056	11 564	11 361	11 380
Other irrigation-dependent costs	R	60 394	63 169	62 064	62 166
Yield dependent costs	R	534 893	507 919	665 455	566 110
Biophysical indicators					
Irrigation application	mm	557	583	573	574
Evapotranspiration	mm	657	643	664	653
Rainfall	mm	146	199	132	165
Water table uptake					
Millimetres	mm	44	39	45	42
Percentage of evapotranspiration	%	7	6	7	6
Drainage	mm	54	143	51	92
Yields	kg ha^{-1}	11 303	10 733	14 062	11 963
Water use efficiency	fraction	1.14	1.28	1.13	1.19

5.5.2 BIO-ECONOMIC ANALYSIS OF CONJUNCTIVE WATER USE

5.5.2.1 Optimal Expected Outcome Irrigation Strategy

DEOPT uses information on the expected state of the soil-crop-atmosphere continuum to devise an irrigation schedule that is the best-performing profit-maximizing schedule irrespective of the state of nature. Consequently, the algorithm also considers root-accessible water tables as a water source to satisfy crop evapotranspiration requirements.

Table 5.3 shows the bio-economic simulation results when the optimized irrigation schedule is applied to each state of nature. The optimal expected outcome irrigation strategy applied only 148mm of irrigation, which is 426mm less than the expected irrigation application of the

full irrigation strategy. The substantial reduction in irrigation application did not impact crop yields in each state of nature much, with absolute deviations from the full irrigation strategy being less than 102kg ha^{-1} across states of nature.

Reducing irrigation applications of the optimal expected outcome strategy improved the expected water use efficiency by 15 percentage points, showing that the strategy uses rainfall and root-accessible water tables more efficiently. Drainage losses associated with overirrigation and ineffective rainfall were reduced to zero in States 1 and 3, while the drainage losses in States 2 were reduced by 86mm. The optimal expected outcome irrigation strategy increased the contribution of root-accessible water tables to substantially satisfy the crop evapotranspiration requirements across all states of nature. Compared to full irrigation, the water table uptake increased by a minimum of 42 percentage points (State 2) and a maximum of 46 percentage points (State 3), with an expected increase of 45 percentage points. When applying the optimal expected outcome irrigation strategy, root-accessible water tables contributed about 51% to satisfy the expected crop evapotranspiration requirement.

The expected margin above the specified costs for the optimal expected outcome irrigation strategy is R 243 553, which is R73 262 higher than that of the full irrigation strategy. The reason for the increase in the expected margin above the specified costs is that the reduction in irrigation application decreased total variable costs and other irrigation-dependent costs, while crop yields were not affected much. The optimal expected outcome irrigation strategy did, however, increase the crop yields in State 2 while compromising crop yield in the other states. The variable electricity costs decreased by a minimum of R25 509 (State 1) and a maximum of R27 223 (State 2), with an expected reduction of R26 294. The other irrigation-dependent costs decreased by a minimum of R44 353 (State 1) and by a maximum of R47 128 (State 2), with an expected decrease of R46 125. Expected production income and expected yield-dependent costs did not change much because crop yields were not affected much by the optimal expected outcome irrigation strategy. Expected production income increased by R1 503 while expected yield-dependent cost increased by R660 compared to the full irrigation strategy.

Table 5.3: Economic and biophysical indicators for the optimal expected outcome strategy considering water table uptake and the changes relative to a state-specific full irrigation strategy for a 30.1 ha pivot (2021)

		Optimal expected outcome irrigation strategy				Change relative to full irrigation strategy			
	Units	State 1	State 2	State 3	Expected	State 1	State 2	State 3	Expected
Probability of occurrence	Fraction	0.23	0.44	0.33		0.23	0.44	0.33	
Economic indicators									
Margin above the specified costs	R	196 655	174 222	368 680	243 553	63 694	80 216	70 658	73 262
Production income	R	1 207 335	1 167 345	1 513 992	1 290 936	- 10 994	10 455	- 1 725	1 503
Total variable electricity costs	R	8 497	8 497	8 497	8 497	- 25 509	- 27 223	- 25 603	- 26 294
Active energy charge									
Off-peak	R	4 197	4 197	4 197	4 197	- 8 672	- 9 280	- 10 014	- 9 382
Standard	R	1 363	1 363	1 363	1 363	- 7 667	- 7 699	- 6 974	- 7 453
Peak	R	0	0	0	0	- 1 051	- 1 617	- 191	- 1 016
Other variable electricity charges	R	2 937	2 937	2 937	2 937	- 8 119	- 8 627	- 8 425	- 8 443
Other irrigation-dependent costs	R	16 042	16 042	16 042	16 042	- 44 353	- 47 128	- 46 022	- 46 125
Yield dependent costs	R	530 066	512 510	664 698	566 770	- 4 827	4 590	- 757	660
Biophysical indicators									
Irrigation application	mm	148	148	148	148	- 409	- 435	- 425	- 426
Evapotranspiration	mm	557	566	620	582	- 100	- 78	- 43	- 71
Rainfall	mm	146	199	132	165	0	0	0	0
Water table uptake									
Millimetres	mm	273	286	329	297	229	248	284	255
Percentage of evapotranspiration	%	49	51	53	51	42*	45*	46*	45*
Drainage	mm	0	56	0	25	- 54	- 86	- 51	- 67
Yields	Kg ha^{-1}	11 201	10 830	14 046	11 977	- 102	97	- 16	14
Water use efficiency	fraction	1.02	1.12	0.98	1.05	-0.12	-0.16	-0.15	-0.15

*The relative change is measured in percentage points.

5.5.2.2 Optimal Sequential Irrigation Strategy

The optimal sequential irrigation strategy allows the irrigator to adjust the irrigator's optimal expected outcome irrigation strategy for the rest of the season weekly based on the unfolding state of nature. The results of the optimal sequential irrigation strategy are given for each state of nature in Table 5.4.

Table 5.4 shows that, contrary to expectation, no substantial adjustments were made to the optimal expected outcome irrigation strategy when the irrigator had the chance to react to unfolding information regarding the soil-crop-atmosphere continuum. In absolute terms, the optimal sequential irrigation strategy does not deviate more than 18mm from the optimal expected outcome irrigation strategy in any state of nature. Irrigation adjustments in all states of nature resulted in higher crop yields. Interestingly, the total irrigation application was increased in State 2 while the applications were reduced in the other two states to increase crop yield. The increases were small, with the highest increase (i.e. 100kg ha^{-1}) in State 1. The relatively small changes in irrigation applications resulted in an increased root-accessible water table contribution in State 1 and State 3 of 14mm and 17mm and a decrease of 7mm in State 2. Accordingly, the water use efficiencies changed by one percentage point in absolute terms.

The margin above the specified costs increased with R8 007 and R3 340 in State 1 and State 3 because irrigation applications were reduced, and crop yields increased in these states of nature. The results for State 2 seem non-optimal because the margin above the specified costs of the optimal sequential irrigation strategy reduced the margin above the specified costs of the optimal expected outcome strategy with R510.

5.5.3 Discussion

The bio-economic simulation results confirm the claims by Barnard *et al.* (2021) that farmers who irrigate to satisfy crop evapotranspiration requirements will have low water use efficiencies. The bio-economic optimization results estimated that 51% of maize's crop evaporation could originate from root-accessible water tables using optimal irrigation management, reducing the irrigation requirements substantially without impacting crop yields. This contribution is in line with findings by Jovanovic *et al.* (2004), who found that the root-accessible water table can potentially contribute about 40% or more to the crop water demand under good (i.e. not optimal as in this research) and Liu *et al.* (2022) who estimate the contribution to be 49%.

Table 5.4: Economic and biophysical indicators for a state-specific sequential strategy considering water table uptake and the changes relative to the optimal expected outcome irrigation strategy for a 30.1 ha pivot (2021)

		Optimal sequential irrigation strategy				Change relative to optimal expected outcome irrigation strategy			
	Units	State 1	State 2	State 3	Expected	State 1	State 2	State 3	Expected
Probability of occurrence	Fraction	0.23	0.44	0.33		0.23	0.44	0.33	
Economic indicators									
Margin above the specified costs	R	204 662	173 712	372 020	246 272	8 007	- 510	3 340	2 719
Production income	R	1 219 299	1 170 902	1 514 746	1 295 502	11 964	3 557	755	4 566
Total variable electricity costs	R	8 069	9 376	7 531	8 467	- 428	879	- 965	- 30
Active energy charge									
Off-peak	R	3 970	4 616	3 568	4 122	- 227	419	- 628	- 75
Standard	R	1 220	1 480	1 384	1 388	- 144	117	20	25
Peak	R	101	46	0	43	101	46	0	43
Other variable electricity charges	R	2 778	3 234	2 775	2 978	- 159	298	- 162	41
Other irrigation-dependent costs	R	15 174	17 667	14 091	15 914	- 867	1 626	- 1 951	- 128
Yield dependent costs	R	535 319	514 071	665 029	568 774	5 253	1 562	331	2 005
Biophysical indicators									
Irrigation application	mm	140	163	130	147	- 8	15	- 18	- 1
Evapotranspiration	mm	567	574	623	589	11	8	3	7
Rainfall	mm	146	199	132	165	0	0	0	0
Water table uptake									
Millimetres	mm	288	280	347	304	14	- 7	17	6
Percentage of evapotranspiration	%	51	49	56	51	2	- 2	3	0
Drainage	mm	0	56	0	25	0	0	0	0
Yields	kg ha^{-1}	11 312	10 863	14 053	12 019	111	33	7	42
Water use efficiency	fraction	1.01	1.12	0.98	1.05	-0.01	0.00	-0.01	0.00

*The relative change in the water table uptake is measured in percentage points

The bio-economic analyses assume the area limiting case (i.e. 30 ha irrigated irrespective of water application rates per hectare). Consequently, the analyses only take into account changes in irrigation water use at the intensive margin (i.e. irrigation water applications per hectare) (Graveline, 2016). According to Graveline (2016), intensive margin changes will create the opportunity to increase the irrigated area (i.e. extensive margin changes) if the production area is not limited. The intensive margin changes in irrigation water use using root-accessible water tables are substantial; therefore, the extensive margin change, if possible, would also be substantial. However, widespread use of root-accessible water tables and extensive margin changes in water use may result in unintended hydro-ecological consequences and the revenues of the water user association responsible for managing irrigation water supply.

The economic benefit of adapting irrigation management decisions was small, contrary to the findings of Madende and Grové (2020), who did not consider root-accessible water tables and included water scarcity in their analyses. The risk of a short supply of irrigation water is reduced in the presence of a shallow groundwater table. Consequently, conjunctive water use strategies considering root-accessible water tables provide substantial economic benefit at the farm level (i.e. optimal expected outcome irrigation strategy), leaving less potential to decrease risk through adaptive decision-making (i.e. optimal sequential irrigation strategy) because a shallow groundwater table neutralizes the impact of insufficient water.

The bio-economic optimization models used a probabilistic representation of the state of the soil-plant-atmosphere when optimizing irrigation water applications. Consequently, when optimizing irrigation application decisions, the optimization procedure has access to all information (i.e. weather states and the cause-and-effect interactions in the SWAP simulation model). No effort was made in this research to devise an information dissemination strategy to facilitate irrigation management considering root-accessible water tables.

Developing sound irrigation strategies should aim to i) manage soil matric (water stress) and osmotic (salinity stress) potential to maintain optimum yields, ii) reduce the amount of irrigation by utilizing rainfall and capillary rise from root-accessible groundwater tables to supplement crop water requirements and iii) minimize salt additions and irrigation-induced drainage and leaching (Barnard et al., 2021). The conjunctive use strategies evaluated did not consider salinity. However, the salt load associated with irrigation and utilization of root-accessible groundwater tables are important. Monitoring of salts in the root zone will be necessary when considering conjunctive water use strategies.

5.6 AQUACROP RESULTS

5.6.1 BIO-ECONOMIC ANALYSIS WITHOUT CONSIDERING WATER TABLE UPTAKE

AquaCrop was used to conduct the economic analysis of applying the farmers' irrigation water strategies of 274 mm, 347 mm and 648 mm in the presence of a shallow groundwater table. However, the differences between the 274 mm and 347 mm strategies are small; therefore, only the results of the 247 mm and 648 mm strategies are discussed.

The expected bio-economic indicators for irrigation applications of 274 mm and 648 mm on a Clovelly soil with a constant water table depth of 1.5 m are given in Table 5.5.

Table 5.5: Expected simulation bio-economic indicators for the baseline irrigation strategies on a Clovelly soil with a 1.5 m constant groundwater table on a 30.1 ha pivot (2023)

		Baseline strategy	
	Units	274 mm	648 mm
Margin above the specified costs	R	398 910 (28 968)	325 994 (34 269)
Gross production income	R	1 605 983 (51 640)	1 586 940 (61 088)
Total variable electricity costs:		16 214	37 911
Off-peak	R	6 986	17 145
Standard	R	3 689	7 908
Peak	R	102	-
Other irrigation costs:			
Water costs	R	28 560	67 543
Yield	t ha^{-1}	14.90 (0.48)	14.72 (0.53)
Groundwater table uptake	mm	256 (61)	140 (38)
Drainage	mm	48 (100)	152 (134)
Evapotranspiration	mm	646 (35)	760 (44)

(Standard Deviation)

Applying 274mm of water results in a crop yield of 14.90 t ha^{-1}. Water table uptake contributes 256 mm (40% of the crop water use) to satisfying crop evapotranspiration requirements, while 48 mm of water is drained from the soil.

The expected gross production calculated for the 274 mm strategy on the 30.1 ha pivot is R1 605 983 with a standard deviation of R51 640 (R1 716 ha^{-1}). The low standard deviation

of the expected gross production income is due to the low standard deviation in the expected crop yield (0.48 t ha^{-1}). The water cost is R28 560. The total electricity cost is R16 214, with a relatively high off-peak electricity cost (R6 986) and a relatively low peak electricity cost (R102).

The 648 mm irrigation strategy results showed an expected crop yield of 14.72 t ha^{-1} with a standard deviation of 0.53 t ha^{-1}. To produce a 14.7 t ha^{-1} crop yield, groundwater uptake of 140 mm (18% of crop water use) is required to meet the evapotranspiration of 760 mm while draining 152 mm. The expected gross margin above the specified costs realised is R325 994. The expected gross production income is R1 586 940 with a standard deviation of R61 088 (R2 030 ha^{-1}). The total variable electricity cost estimated is R37 911. However, interesting to note is that irrigation does not happen during the peak time-of-use period since the peak variable electricity cost is R0. The result could be due to the dynamic of the soil water balance and the timing of when irrigation is necessary for crop production. The water cost is estimated at R67 543.

Compared to the 648 mm strategy, the 274 mm strategy used less irrigation water and recorded lower evaporation (760 mm compared to 646 mm) to produce 0.18 t ha^{-1} more maize yield (14.9-14.72 t ha^{-1}). Because the 274 mm strategy applies less irrigation water, the contribution of groundwater to crop water use is 40% compared to the 18% recorded for the 648 mm strategy. The higher crop yield for the 274 mm strategy resulted in a production income increase of R19 043 and an increase in the expected margin above the specified cost of R72 916. The large difference in the expected margin above the specified cost is due to the reduced production costs.

The 274 mm and 648 mm baseline strategies generally resulted in too much irrigation water being applied to the groundwater table soils. Drainage and runoff occurred to some extent in the drier production years, increased dramatically during higher rainfall years, and were even higher with the application of baseline strategy 648 mm.

5.6.2 BIO-ECONOMIC ANALYSIS OF CONJUNCTIVE WATER USE

The optimal expected outcome irrigation strategy was optimised with the DEOPT algorithm linked to AquaCrop. The expected bio-economic results for the optimal conjunctive water use strategy for the 1 m and 1.5 m groundwater table are given in Table 5.6.

Table 5.6: Expected bio-economic indicators for the optimal irrigation strategies on a Clovelly soil with a 1.5 m constant groundwater table and the changes relative to the baseline strategies of 274 mm and 648 mm on a 30.1 ha pivot (2023)

		Optimal expected outcome irrigation strategy	Changes in the optimal strategies relative to the baseline strategies	
			Baseline strategy	
	Unit		274 mm	648 mm
Margin above the specified costs	R	418 195	19 285	92 201
Gross production Income	R	1 575 587	-30 396	-11 353
Total variable electricity costs:		2 268	-35 644	-24 545
Off-peak	R	1 422	-15 723	-15 723
Standard	R	800	-7 108	-7 108
Peak	R	46	46	46
Other irrigation costs:				
Water costs	R	5 941	-22 619	-61 602
Yield	t ha^{-1}	14.62	-0.28	-0.10
Groundwater table uptake	mm	386	131	247
Drainage	mm	23	-26	-130
Evapotranspiration	%	621	-25	-139

The optimal conjunctive water use strategy for maize production on a 1.5 m constant groundwater table requires 54 mm of irrigation water. Compared to the 274 mm strategy, the optimal strategy results in a 25 mm reduction in evapotranspiration, resulting in a 0.28 t ha^{-1} reduction in crop yield. The water table uptake for the optimal strategy is 131 mm higher compared to the 256 mm estimated for the 274 mm baseline. Drainage decreases by 26 mm from 48 mm. The expected margin above the specified cost for the optimal strategy is R418 1950, which is R19 285 more than for the baseline strategy. Since the crop yield for the optimal irrigation strategy is 0.28 t ha^{-1} lower than for the baseline strategy (274 mm), the reduction in gross production income is R30 396. Due to the decrease in the amount of irrigation water applied from the baseline of 274 mm to the optimal strategy of 54 mm, the reduction in water and total variable electricity cost is R22 619 and R35 644, respectively.

Compared to the 648 mm strategy, the optimal irrigation strategy resulted in a 139 mm decrease in evapotranspiration and a 0.10 t ha^{-1} decrease in the estimated expected crop yield. The reduced irrigation application amount increases by 247 mm in water table uptake while the drainage decreases by 130 mm. The decrease in crop yield resulted in an R11 353 decrease in the gross production income. Meanwhile, the expected margin above the specified costs increased by R92 201. The water and total electricity costs decreased by R61 602 and R24 545, respectively.

5.6.3 DISCUSSION

The results of the baseline strategies (274 mm and 648 mm) showed that producers with root-accessible water tables could over-irrigate their crops when applying irrigation water amounts close to the crop water requirement. The results showed that the 274 mm strategy performed better than the 648 mm strategy regarding irrigation water use efficiency, use of root-accessible water tables, crop production and maximising margin above the specified cost. The application of larger amounts of irrigation water and the high seasonal rainfall in some production years led to waterlogged/ reduced soil aeration conditions, which caused stomatal closure and thus resulted in reduced crop yield (Ren *et al*., 2018). This result is similar to that found by Rizzo *et al*. (2018), who also found that the production season with higher rainfall in combination with higher irrigation water use on shallow groundwater table soils may have a negative impact on crop yield. Still, in dry years, it may contribute to higher yields.

The 247 mm strategy also contributed to a larger groundwater table to crop water use. The estimated groundwater table contribution for production on a 1.5 m groundwater table soil is 40% and 18% when applying 274 mm and 648 mm of water, respectively. The result confirms the argument of Jovanovic *et al*. (2004) and Gao *et al*. (2017) that the upward water flux increases for the same groundwater depth as the irrigation amount becomes smaller.

The results of the optimal conjunctive water use strategy showed a substantial decrease in the optimal amount of irrigation water applied. Even though the reduction in the amount of irrigation water applied is large, the reduction in expected crop yield is less than 0.3 t ha^{-1} because the shallow groundwater table can contribute enough water for crop production (more than 60% of the crop water use) to ensure the minimal reduction in crop yield. The results show that farmers over-irrigated their crops in the presence of root-accessible water tables.

The economic benefits of using conjunctive water use strategies are also reasonably large. Since the optimal strategy applies less irrigation water, there is sometimes a decrease in crop yield and, thus, the gross production income. However, the reduction in gross production income of R30 396 (the decline in production income recorded) is small compared to the potential savings in production costs (saving R35 644 for total variable electricity cost and R22 691 for water costs). The results showed that irrespective of the baseline strategy, the estimated gross margin above the specified costs would be higher for the conjunctive water use strategies.

CHAPTER 6: CONCLUSIONS, SHORTCOMINGS AND RECOMMENDATIONS

6.1 SUMMARY OF RESULTS AND CONCLUSIONS

6.1.1 BIOPHYSICAL MODEL CALIBRATION AND VALIDATION

For AquaCrop, the DECAL calibration process showed good results, especially under non-limiting conditions. The validation results showed that AquaCrop could satisfactorily simulate soil water content, evapotranspiration, water table uptake and grain yield of maize grown on sandy soil. Measurements describing crop phenology, such as canopy cover, were not necessary for calibration using DECAL under these conditions. Instead, soil water content measurements were sufficient, while seasonal above-ground biomass played a crucial role in the objective function. The conclusion is that AquaCrop could be calibrated using inverse modelling when soil water measurements are available.

For SWAP, the results indicated that the calibrated model performed reasonably well, particularly in simulating soil water content and evapotranspiration. However, the validation results showed that there were discrepancies in simulating above-ground biomass and grain yield, especially under shallow groundwater table conditions. This inconsistency might be due to the lack of calibration of soil hydraulic parameters, which were not considered in this study. The conclusion is that more complex models may require simultaneous calibration of soil properties and parameters determining crop water use and crop yield. In this regard, using sensitivity analysis to better understand parameter influences on modelling results can be vital for improving model outputs.

Overall, DECAL proved to be a valuable tool in fine-tuning calibration parameters.

6.1.2 BIO-ECONOMIC ANALYSES

The results of the baseline irrigation applications showed that water table uptake is negligible if the irrigators follow a strategy whereby crop water requirements are satisfied through irrigation and rainfall. The expectation is that such a strategy will result in an overirrigation of 19%. Water table uptake increased on average by 116 mm when water applications were reduced from 648 mm to 274 mm without affecting crop yield much. The maximum expected

outcome irrigation strategy indicated substantial increases in water table uptake and reductions in water applications, which translated to notable increases in profitability (R2433 ha^{-1}) mainly due to increased water use efficiencies. The conclusion is that the magnitude of water table uptake is a function of the decision maker's irrigation management decisions. Consequently, irrigators will forgo profits if they irrigate to satisfy crop evapotranspiration requirements because their conjunctive water use will be sub-optimal. Furthermore, irrigators must thoroughly understand the interrelated linkages between irrigation decisions and the state of the soil-water-atmosphere continuum in the presence of root-accessible water tables to optimise conjunctive water use. Such understanding requires soil water information and a mindset of not refilling the soil water back to field capacity when determining irrigation applications.

Results from the optimal sequential irrigation strategy showed negligible changes in the economic and biophysical indicators because the root-accessible water table acts as a buffer against climatic changes if the irrigation strategy is already devised to consider root-accessible water tables. The conclusion is that root-accessible water tables might be an important risk mitigation strategy in the presence of electricity load shedding and adverse climatic conditions.

6.2 SHORTCOMING

The evolutionary algorithm evaluates the biophysical system's current and possible future states and the time-of-use electricity tariff periods to devise an irrigation schedule (i.e. calendar of irrigations) to maximise expected profits. Since the evolutionary algorithm uses the “prescribed” irrigation scheduling option of the crop simulation model to optimise the irrigation schedule, providing a generic irrigation strategy defined by timing triggers and irrigation amounts is impossible. Consequently, no generic irrigation scheduling guideline could be devised to support better conjunctive water use strategies. However, solving the model recursively every week provides irrigation scheduling decision support for the upcoming week.

6.3 RECOMMENDATIONS

6.3.1 CALIBRATING BIOPHYSICAL MODELS

- Clarity on the objective of the calibration is essential when choosing calibration parameters. Some processes could be calibrated independently, while the parameters of interrelated processes must be calibrated simultaneously. Sensitivity analysis

should target processes to identify the most influential parameters that need calibration.

- Automated calibration is a powerful tool to finetune calibration parameters. However, the calibration objective, selected calibration parameters and the bounds of these parameters need to be carefully considered to produce realistic calibration parameters.

6.3.2 CONJUNCTIVE WATER USE

- Refilling the soil water content to field capacity is detrimental to maximising the contribution of root-accessible water tables to satisfy the evapotranspiration requirements of a crop. Irrigation strategies aimed at maximising the contribution of root-accessible water tables must manage the soil water content so that the capillary fringe extends to its maximum level by leaving the soil dryer.
- Normal irrigation scheduling practices apply during the early stages of crop production while the roots have not reached the capillary fringe.
- Soil water measurements are essential for managing the contribution of root-accessible water tables to satisfy crop water requirements. Preferably, these measurements should include salinity indicators.
- Indirect estimates of crop water requirements (e.g. satellite imagery) must be supplemented with soil water measurements to maximise the contribution of root-accessible water tables to satisfy crop water requirements.
- Spatial monitoring of soil water content and water table depths is necessary to inform the water user association of any unintended hydrological consequences in the large-scale adoption of root-accessible water tables as a water source.

6.3.3 FURTHER RESEARCH

- The underlying information that the evolutionary algorithm uses to devise the optimal irrigation schedules needs to be further analysed using neural networks to develop general guidelines to improve the conjunctive use of surface water and root-accessible water tables.
- The biophysical models' built-in irrigation scheduling options do not cater to irrigation strategies considering the contribution of root-accessible water tables. More research is necessary to develop generic strategies considering root-accessible water tables for these models.
- All indications are that maximising the contribution of root-accessible water tables to satisfy crop water requirements necessitated a lower soil water content. Research is necessary to understand fertiliser uptake and salinity buildup under these conditions.

- The research used Visual Basic for Applications to implement the DE algorithm to calibrate the biophysical models and optimise the contribution of root-accessible water tables to satisfy crop water requirements. The process could be done more efficiently using modern programming languages like Python. Such implementation will also allow capitalising on multithread processing.

REFERENCES

Abedinpour, M., Sarangi, A., Rajput, T.B.S., Singh, M., Pathak, H., Ahmad, T. (2012). Performance evaluation of AquaCrop model for maize crop in a semi-arid environment. Agricultural Water Management 110, 55-66. http://dx.doi.org/10.1016/j.agwat.2012.04.001

Adams, J.E., Arkin, G.F., Ritchie, J.T. (1976). Influence of row spacing and straw mulch on first stage of drying. Soil Science Society of America Journal 40, 436-442.

Ahmadi, S.H., Mosallaeepour, E., Kamgar-Haghighi, A.A., Sepaskhah, A.R. (2015). Modelling maize shield and soil water content with AquaCrop under full and deficit irrigation management. Water Resour. Manag. 29, 2837-2853.

Allen, T.H. (1991). Investigation of curve number procedure. J. Hydraul. Eng. 117, 725-737.

Annandale J.G., Benadé N., Jovanovic N.Z., Steyn J.M. and Du Sautoy (1999) Facilitating Irrigation Scheduling by Means of the Soil Water Balance Model. WRC Report No. 753/1/99, Water Research Commission, Pretoria, South Africa. 285 pp

Awan, U.K., Tischbein, B., Martius, C. (2014). A GIS-based approach for up-scaling capillary rise from field to system level under soil-crop-ground-water mix. Irri. Sci. 32, 449-458.

Ayars, J.E., Christen, E.W., Soppe, R.W. and Meyer W.S. (2006). The resource potential of in-situ shallow ground water use in irrigated agriculture: a review. Irrig Sci 24, 147-160 (2006). https://doi.org/10.1007/s00271-005-0003-y

Barnard, J.H., Matthews, N., du Preez, C.C.,(2021). Formulating and assessing best water and salt management practices: Lessons from non-saline and water-logged irrigated fields. Agric. Water Manag. 247, 106706. https://doi.org/10.1016/j.agwat.2020.106706.

Barnard, J.H., Van Rensburg, L.D., Bennie, A.T.P. (2010). Leaching irrigated saline sandy to sandy loam apedal soils with water of a constant salinity. Irri. Sci. 28, 191-201.

Barnard, J.H., Van Rensburg, L.D., Bennie, A.T.P. and Du Preez C.C. (2017) Water and salt balances of two shallow groundwater cropping systems using subjective and objective irrigation scheduling. WATER SA 43(4):581-594

Basso, B. Sartori, L., Cammarano, D., Fiorentino, C., Grace, P.R., Fountas, S. and Sorensen, C.A. (2012). Environmental and economic evaluation of N fertilizer rates in a maize crop in Italy: A spatial and temporal analysis using crop models. Biosystems Engineering, 113(2), 103-111. https://doi.org/10.1016/j.biosystemseng.2012.06.012

Belhouchette, H., Blanco, M., Wery, J. and Flichman, G. (2012). Sustainability of irrigated farming systems in a Tunisian region: A recursive stochastic programming analysis. Computers and Electronics in Agriculture, 86, 100-110. doi:10.1016/j.compag.2012.02.016

Bennie A.T.P, Coetzee M.J., Van Antwerpen R., Van Rensburg L.D. and Burger R.D. (1988) Water Balance Model for Irrigation Based on Soil Profile Water Supply Rate. WRC Report No. 144/1/88. Water Research Commission, Pretoria, South Africa. 405 pp

Blanco, M. and Flichman, G. (2002). Dynamic optimisation problems: different resolution methods regarding agriculture and natural resource economics. In: Working Paper. Universidad Polite´cnica de Madrid and CIHEAM-Institut Agronomique Mediterraneen de Montpellier, Montpellier, p. 35.

Boisvert, R.Nn and McCarl, B. (1990). Agricultural Risk Modeling Using Mathematical Programming. Bulletin. Department of Agricultural Economics, Cornell University, Agricultural Experiment Station, New York State College of Agriculture and Life Sciences.

Braden, H. (1985). Ein energiehaushalts-und verdunstungsmodell for wasser und stoff-haushaltsuntersuchungen landwirtschaftlich genutzer einzugsgebiete. Mittelungen Deutsche Bodenkundliche Geselschaft 42 (Suppl), 294-299.

Brisson, N., Gary, C., Justes, E., Roche, R., Mary, B., Ripoche, D., Zimmer, D., Sierra, J., Bertuzzi, P., Burger, P., Bussière, F., Cabidoche, Y.M., Cellier, P., Debaeke, P., Gaudillère, J.P., Hénault, C., Maraux, F., Seguin, B., Sinoquet, H. (2003.) An overview of the crop model stics. Eur. J. Agron. 18, 309-332.

Brisson, N., Perrier, A. (1991). A semiempirical model of bare soil evaporation for crop simulation models. Water Resour. Res. 27, 719-727.

Brown, D.R. (2000). A review of bio-economic models. Cornell African Food Security and Natural Resource Management (CAFSNRM) Program.

Bureau for Food and Agricultural Policy (BFAP)., Protein Research Foundation (PRF)., the Oil & Protein Seeds Development Trust / Oilseeds Advisory Committee., and Grain South Africa. (2021). Income & Cost Budgets Summer Crops – 2020/21. October 2020 (Accessed: June 2021)

Confalonieri, R., (2010). Monte Carlo based sensitivity analysis of two crop simulators and considerations on model balance. European Journal of Agronomy 33, 89-93.

Celia, M.A., Bouloutas, E.T., Zarba, R.L. (1990). A general mass-conservative numerical solution for the unsaturated flow equation. Water Resour. Res. 26, 1483-1496.

Crosby, C.T., and Crosby, C.P. (1999). SAPWAT—A Computer Program for Establishing Irrigation Requirements and Scheduling Strategies in South Africa. Report No. 624/1/99. Water Research Commission, Pretoria.

De Jager J.M., Mottram R. and Kennedy JA (2001) Research on a computerised weather based irrigation water management system. WRC Report No. 581/1/01. Water Research Commission, Pretoria, South Africa. 180 pp

Department of Agriculture, Forestry and Fisheries (DAFF) (2015). Irrigation Strategy for South Africa, Pretoria, South Africa , 2015

de Wit, A., Boogaard, H., Fumagalli, D., Janssen, S., Knapen, R., van Kraalingen, D., Supit, I., van der Wijngaart, R., van Diepen, K. (2019). 25 years of the FOFOST cropping system model. Agric. Syst. 168. 154-167.

de Wit, C.T. (1965). Photosynthesis of Leaf Canopies. Technical Report 663. Pudoc, Wageningen.

Ehlers, W., Goss, M., (2003). Water dynamics in plant production. CABI Publishing, Wallingford, Oxon, U.K.

Duncan, W., Loomis, R., Williams, W., Hanau, R. (1967). A model for simulating photosynthesis in plant communities. Hilgardia 38, 181-205.

Dogliotti, S., Rossing, W.A.H. and van Ittersum, M.K. (2003). ROTAT, a tool for systematically generating crop rotations. European Journal of Agronomy 19, 239-250.

Dorward, A. (1999). Modelling embedded risk in peasant agriculture: methodological insights from northern Malawi. Agricultural Economics, 21, 191-203.

Ebrahimi-Mollabashi, E., Huth, N.I., Holzwoth, D.P., Ordóñez, R.A., Hatfield, J.L., Huber, I., Castellano, M.J., Archontoulis, S.V. (2019). Enhancing APSIM to simulate excessive moisture effects on root growth. Field Crop Res. 236, 58-67.

Ehlers, W., Goss, M. (2003). Water dynamics in plant production. CABI Publishing, Wallingford, Oxon, U.K.

Ehlers, L., Barnard, J.H., Dikgwatlhe, S.B., Van Rensburg, L.D., Ceronio, G.M., Du Preez, C.C., Bennie, A.T.P. (2007). Effect of irrigation and water table salinity on the growth and water use of selected crops. Water Research Commission Report No. 1359/1/07, Pretoria, South Africa.

English, M.J. and Raja, S.N. (1996). Review: Perspectives on deficit irrigation. Agric Water Manag 32 (1): 1-14. https://doi.org/10.1016/S0378-3774(96)01255-3

English, M.J., Solomon, K.H. and Hoffman, G.J. (2002). A paradigm shift in irrigation management. Journal of Irrigation and Drainage Engineering, 128(5): 267-277.

Eskom. 2021). Tariffs and charges booklet. Available.at: https://www.eskom.co.za/distribution/wp-content/uploads/2021/07/2020-21.pdf (Accessed: February 2021)

Feddes, R.A., Kowalik, P.J., Zaradny, H. (1978). Simulation of field water use and crop yield. Simulation Monographs. Pudoc. Wageningen.

Finger, R. (2013). Expanding risk consideration in integrated models – The role of downside risk aversion in irrigation decisions. Environmental Modelling and Software, 43: 169-172. DOI:10.1016/j.envsoft.2013.02.001

Finger, J.M., Kreinin, M.E. (1979). A measure of ‘export similarity’ and its possible uses. Econ. J. 905-912.

Flichman, G. (1997). Bio-economic models integrating agronomic, environmental and economic issues with agricultural use of water. Options Méditerranéennes, Sér. A /n"31, 1997 Séminaires Méditerranéens.

Flichman, G., and Allen, T. (2015). Bio-economic modelling: State-of-the-art and key priorities. Food and Agriculture Organization, United Nations. Accessed August 10, 2020. https://www.semanticscholar.org/paper/Bio-economic-modeling%3A-State-of-the-art-and-key-Flichman-Allen/c5dd95bb04313ab8b1954141d124dbd4a6c000a1

GAMS Development Corporation. (2017). GAMS documentation, distribution 24.9. Washington DC, USA

Gao, L., Wang, X., Johnson, B.A., Tian, Q., Wang, Y., Verrelst, J., Mu, X., Gu, X. (2020). Remote sensing algorithms for estimation of fractional vegetation cover using pure vegetation index values: a review. ISPRS J. Photogramm. Remote Sens. 159, 364-377.

Gao, X., Huo, Z., Qu, Z., Xu, X., Huang, G., Steenhuis, T.S. (2017). Modeling contribution of shallow groundwater to evapotranspiration and yield of maize in an arid area. Sc. Rep. 7, 1-12.

Ghahraman B. and Sepaskhah, A. (2004). Linear and non-linear optimization models for allocation of a limited water supply. Irrig Drain 53:39-54. https://doi.org/10.1002/ird.108

Gocht, A., Britz, W. (2010). EU-wide farm types supply in CAPRI – How to consistently disaggregate sector models into farm type models. J. Policy Model. 33, 146-167.

Goosheh, M., Pazira, E., Gholami, A., Andarzian, B., Panahpour, E. (2018). Improving irrigation scheduling of wheat to increase water productivity in shallow groundwater conditions using AquaCrop. Irri. Sci. 67, 738-754.

Graveline, N. (2016). Economic calibrated models for water allocation in agricultural production: A review. Environmental Modelling & Software, 81, 12-25. http://dx.doi.org/10.1016/j.envsoft.2016.03.004

Grové, B. (2019). Improved Water Allocation under Limited Water Supplies Using Integrated Soil-Moisture Balance Calculations and Nonlinear Programming. Water Resources Management, 33, 423-437. https://doi.org/10.1007/s11269-018-2110-6

Grové, B. and M.C. Du Plessis. (2019). Optimising intra-seasonal irrigation water allocation: Comparison between mixed integer nonlinear programming and differential evolution. Water SA, Vol. 45 No. 1, 48-54. https://doi.org/10.4314/wsa.v45i1.06

Guo, D., Olesen, J.E., Pullens, J.W.M., Guo, C., Ma, X. (2021). Calibrating AquaCrop model using genetic algorithm with multi-objective functions applying different weight factors. Agronomy Journal 113, 1420-1438. https://doi-org.ufs.idm.oclc.org/10.1002/agj2.20588

Haj-Amor, Z., Hashemi, H. & Bouri, S. (2017). Soil salinization and critical shallow groundwater depth under saline irrigation conditions in a Saharan irrigated land. *Arab J Geosci* **10**, 301 (2017). https://doi.org/10.1007/s12517-017-3093-y

Han, M., Zhao, C., Šimůnek, J., Feng, G. (2015). Evaluating the impact of groundwater on cotton growth and root zone water balance using HYDRUS-1D coupled with a crop growth model. Agric. Water Manage. 160, 64-75.

Hao, Y., Xu, X., Huang, Q., Huang, G. (2014). Modelling soil water-salt dynamics and maize yield responses to groundwater depths and irrigations. Transactions of the Chinese Society of Agricultural Engineering 20, 128-136.

Hardaker, J.B. and Lien, G. (2010). Probabilities for decision analysis in agriculture and rural resource economics: The need for a paradigm change. Agricultural Systems, 103: 345-350.

Hassanli, M., Ebrahimian, H., Mohammadi, E., Rahimi, A., Shokouhi, A. (2016). Simulating maize yields when irrigating with saline water, using the AquaCrop, SALTMED, and SWAP models. Agricultural Water Management 176, 91-99. http://dx.doi.org/10.1016/j.agwat.2016.05.003

Hazell, P.B.R., Norton, R.D. (1986). Mathematical Programming for Economic Analysis in Agriculture. Macmillan, New York.

He, J., Jones, J.W., Graham, W.D., Dukes, M.D. (2010). Influence of likelihood function choice for estimating crop model parameters using the generalised likelihood un-certainty estimation method. Agricultural Systems 103, 256-264. https://doi.org/10.1016/j.agsy.2010.01.006.

Homayounfar, M., Lai, S.H., Zomorodian, M., Sepaskhah, A.R. and Ganji, A. (2014). Optimal Crop Water Allocation in Case of Drought Occurrence, Imposing Deficit Irrigation with Proportional Cutback Constraint. Water Resour Manage 28, 3207-3225 (2014). https://doi.org/10.1007/s11269-014-0669-0

Hou, L., Zhou, Y., Bao, H., wenninger, J. (2017). Simulation of maize (Zea mays L.) water use with the HYDRUS-1D model in the semi-arid Hailiutu River catchment, Northwest China. Hydrol. Sci. J. 62, 93-103.

Howitt, R.E. (1995). Positive mathematical programming. Am. J. Agric. Econ. 77 (2), 329-342

Howitt, R., Reynaud, A., (2003). Spatial disaggregation of agricultural production data using maximum entropy. Eur. Rev. Agric. Econ. 30 (3), 359-387.

Hsiao, T.C. (1993) Effects of drought and elevated CO2 on plant water use efficiency and productivity. In: Jackson MD Black CR (eds) Global environmental change. Interacting stresses on plants in a changing climate. NATO ASI series. Springer, New York.

Huo, Z., Feng, S., Dai, X., Zheng, Y., Wang, Y. (2012). Simulation of hydrology following various volumes of irrigation to soil with different depths to the water table. Soil Use and Management 28, 229-239. **https://doi.org/10.1111/j.1475-2743.2012.00393.x**

IBM. (2020) IBM SPSS Statistics for Windows, Armonk, NY: IBM Corp.

Jajuga, K., and Walesiak, M. (2000). Standardisation of Data Set under Different Measurement Scales. Wroclaw University of Economics Report. Wroclaw University of Economics, Wroclaw, Poland.

Janssen, S. and van Ittersum, M.K. (2007). Assessing farm innovations and responses to policies: A review of bio-economic farm models. Agricultural Systems, 94, 622-636. doi:10.1016/j.agsy.2007.03.001

Jin, X., Kumar, L., Li, Z., Xu, X., Yang, G., Wang, J. (2016). Estimation of winter wheat biomass and yield by combining the AquaCrop model and field hyperspectral data. Remote Sensing 8, 972. http:// doi:10.3390/rs8120972

Jones, J.W., Antle, J.M., Basso, B., Boote, K.J., Conant, R.T., Foster, I., Charles H., Godfray, J., Herrero, M., Howitt, R.E., Janssen, S., Keating, B.A., Munoz-Carpena, R., Porter, C.H., Rosenzweig, C. and Wheeler, T.R. (2016). Brief history of agricultural systems modeling. Agricultural Systems, 155, 240-254. http://dx.doi.org/10.1016/j.agsy.2016.05.014

Jones, J.W., Antle, J.M., Basso, B.O., Boote, K.J., Conant, R.T., Foster, I., Godfray, H.C.J., Herrero, M., Howitt, R.E., Janssen, S., Keating, B.A., Munoz-Carpena, R., Porter, C.H., Rosenzweig, C., Wheeler, T.R. (2017). Towards a new generation of agricultural system models, data, and knowledge products: state of agricultural systems science. Agric. Syst. 155, 269-288.

Jovanovic, N.Z., Ehlers, L., Bennie, A.T.P., Du Preez, C.C. & Annandale, J.G. (2004). Modelling the contribution of shallow water tables towards crop water requirements. *South African Journal of Plant and Soil*, 21(3): 171-181.

Khair, U., Fahmi, H., Hakim, S.A, and Rahim, R. (2017). Forecasting Error Calculation with Mean Absolute Deviation and Mean Absolute Percentage Error. Journal of Physics: Conference Series, 930: 1-7.

Kanooni, A. and Monem, N.J. (2014). Integrated stepwise approach for optimal water allocation in irrigation canals. Irrig Drain 63:12-21. https://doi.org/10.1002/ird.1798

Kroes, J., Supit, I., van Dam, J., Walsum, P., Mulder, M. (2018). Impact of capillary rise and recirculation on simulated crop yields. Hydrol. Earth Syst. Sci. 22, 2937-2952.

Kroes, J.G., van Dam, J.C., Bartholomeus, R.P., Groenendijk, P., Heinen, M., Hendriks, R.F.A., Mulder, H.M., Supit, I., van Walsum, P. (2017). SWAP Version 4, Theory Description and User Manual. Technical report. Wageningen University.

Kroes, J.G., Van Dam, J.C., Bartholomeus, R.P., Groenendijk, P., Heinen, M., Hendriks, R.F.A., Mulder, H.M., Supit, I., Van Walsum, P.E.V. (2017). SWAP version 4, Theory description and user manual. Wageningen Environmental Research, ESG Report 2780.

Kroes, J.G., van Dam, J.C., Groenendijk, P., Hendriks, R.F.A., Jacobs, C.M.J. (2009). SWAP version 3.2. Theory description and user manual. Alterra report 1649 update 02, Wageningen University and Research centre, Wageningen.

Kruseman, G. (2000). Bio-economic household modelling for agricultural intensification. PhD Thesis, Department of Development Economics, Wageningen Agricultural University, Netherlands.

Lehmann, N. and Finger, R. (2014). Economic and environmental assessment of irrigation water policies: A bio-economic simulation study. Environmental Modelling & Software, 51: 112-122.

Li, J. (1998). Modeling crop yield as affected by uniformity of sprinkler irrigation system. Agric Water Manag 38: 135-146. https://doi.org/10.1016/S0378-3774(98)00055-9

Li, S., Luo, W., Jia, Z., Pan, Y., Wu, D., Zhang, D. (2015). Shallow groundwater use and salinity buildup based on DRAINMOD predicted field hydrology in irrigated areas. Transactions of the Chinese Society of Agricultural Engineering 31, 89-97. doi: 10.11975/j.issn.1002-6819.2015.22.013

Li, S., Luo, W., Jia, Z., Tang, S., Chen, C. (2018). The effect of natural rainfall on salt leaching under watertable management. Land Degrad. Dev. 29, 1953-1961.

Li, X., Zhang, C., Huo, Z. (2020). Optimizing irrigation and drainage by considering agricultural hydrological process in arid farmland with hallow groundwater. J. Hydro. 585, 124785.

Liu, X., Yang, D.W. (2021). Irrigation schedule and optimisation under the different combination of P and ETo using a spatially distributed crop model. Agricultural Water Management 256, 107084. https://doi.org/10.1016/j.agwat.2021.107084

Liu, Z., Wang, X., Huo, Z., Siert Steenhuis, T. (2019). A unique vadose zone model for shallow aquifers: The Hetao irrigation district, China. Hydrol. Earth Syst. Sci. 23, 3097-3115.

Liu, M., Paredes, P., Shi, H., Ramos, T.B., Dou, X., Dai, L., and Perierra, L. S. (2022). Impacts of a Shallow Saline Water Table on Maize Evapotranspiration and Groundwater Contribution using Static Water Table Lysimeters and the Dual Kc Water Balance Model Simdualkc, Agricultural Water Management, 273: 107887.

Louhichi, K., Flichman, G., Zekri, S., (1999). A bio-economic model for analysing the impact of soil and water conservation policies applied to a Tunisian farm. OT: Un modele bio-economique pour analyser l'impact de la politique de conservation des eaux et du sol. Le cas d'une exploitation agricole tunisienne. Economie Rurale 252, 55-64.

Lu, Y., Chibarabada, T.P., McCabe, M.F., De Lannoy, G.J.M. (2021). Glabal sensitivity analysis of crop yield and transpiration from the FAO-AquaCrop model for dryland environments. Field Crops Research 269, 108182. https://doi.org/10.1016/j.fcr.2021.108182

Madende, P. (2017). Risk Efficiency of optimal water allocation within a single and multi-stage decision making framework. MSc (Agricultural Economics) Thesis, Department of Agricultural Economics. University of the Free State, Bloemfontein.

Madende, P. and Grové, B. (2020). Risk efficiency of optimal water allocation within a single- and multi-stage decision-making framework. Agrekon, 59(1), 78-92, DOI:10.1080/03031853.2019.1636668

Maier, H.R., Kapelan, Z., Kasprzyk, J., Kollat, J., Matott, L.S., Cunha, M.C., Dandy, G.C., Gibbs, M.S., Keedwell, E., Marchi, A., Ostfeld, A., Savic, D., Solomtatine, D.P., Vrugt, J.A., Zecchin, A.C., Minsker, B.S., Barbour, E.J., Kuczera, G., Pasha, F., Castelleti, A., Giuliani, M. and Reed, P.M. (2014). Evolutionary algorithms and other metaheuristics in water resources: current status, research challenges and future directions. Environmental Modelling and Software, 62: 271-299.

Matthews, N. and Grové, B. (2017). Modelling Environmental Risk Using the Upper Partial Moment: a Safety-First Approach. Environ Model Assess, 22, 549-562. DOI 10.1007/s10666-017-9556-4

Meiring J.A. (1989). 'n Ekonomiese evaluering van alternatiewe spilpuntbeleggingstrategieë in die Suid-Vrystaat substree met inagneming van risiko. (Afrikaans). M.Sc. Agric. Dissertation. Department of Agricultural Economics. University of the Orange Free State. Bloemfontein. South Africa.

Milly, P.C.D. (1985). A mass conservative procedure for time-stepping in models of unsaturated flow. Adv. Water Resour. 8, 32-36.

Moriasi, D. N., Arnold, J.G., Vazquez-Amábile, G.G. Engel B.A. (2011). ASABE 54, 1705-1711.

National Planning Commission of South Africa (2012). National Development Plan 2030: Our Future – Make It Work. Pretoria, South Africa: National Planning Commission; 2012.

Mwiya, R.,M., Zhang, Z., Zheng, C., Wang, C. (2020). Comparison of approaches for irrigation scheduling using AquaCrop and NSGA-III models under climate uncertainty. Sustainability 12, 7694. https://doi.org/10.3390/su12187694

Niaghi, A.R., Jia, X., Scherer, T.F. (2017). Impact of accurate evapotranspiration estimates on DRAINMOD simulation in North Dakota. American Society of Agricultural and Biological Engineers Annual International Meeting 1701500.

Oosthuizen, H.J. (2014). Modelling the financial vulnerability of farming systems to climate change in selected case study areas in South Africa. Ph.D. thesis, Department of Agricultural Economics, Stellenbosch University, Stellenbosch.

Oosthuizen L.K., Botes J.H.F., Bosch D.J. and Breytenbach P. (1996) Increasing Economic Efficiency of Water Use for Irrigation at Whole-farm Level in the Winterton Area. WRC Report No. 347/2/96. Water Research Commission, Pretoria, South Africa

Ortega, J.F., De Juan, J.A. and Tarjuelo, J.M. (2005). Improved irrigation management: The irrigation advisory service of Castilla – La Mancha (Spain). Agricultural Water Management, 77(1-3): 37-58.

Palosuo, T., Kersebaum, K.C., Angulo, C., Hlavinka, P., Moriondo, M., Olesen, J.E., Patil, R.H., Ruget, F., Rumbaur, C., Takáč, J., Trnka, M., Bindi, M., Çaldağ, B., Ewert, F., Ferrise, R., Mirschel, W., Şaylan, L., Šiška, B., Rötter, R. (2011). Simulation of winter wheat yield and its variability in different climates of Europe: A comparison of eight crop growth models. Europ. J. Agronomy 35, 103-114.

Philip, J.R., De Vries, D.A. (1957). Moisture movement in porous materials under temperature gradients. Eos Trans. Amer. Geophys. Union 38, 222-232.

Ponce, V.M., Hawkins, R.H. (1996). Runoff curve number: has it reached maturity? J. Hydrol. Eng. 1, 11-19.

Raes, D. (2002). BUDGET, a soil water and salt balance model: reference manual. K.U.Leuven, Belgium.

Raes, D., Geerts, S., Kipkorir, E., Wellens, J., Sahli, A. (2006). Simulation of yield decline as a result of water stress with a robust soil water balance model. Agric. Water Manage. 81, 335-357.

Raes, D., Steduto, P., Hsiao, T., Fereres, E. (2017). Chapter 3 calculation procedures. Reference Manual AquaCrop Version 6.0.

Raes, D., Steduto, P., Hsiao, T.C., Fereres, E. (2018). AquaCrop Version 6.0-6.1 Reference manual: Annexes. Food and Agricultural Organization of the United Nations, Rome, Italy.

Raes, D., Steduto, P., Hsiao, T.C., Fereres, E. (2022). AquaCrop 7.0: Chapter 3 Calculation procedures. Food and Agricultural Organization of the United Nations, Rome.

Raes, D., Steduto, P., Hsiao, T.C., Fereres, E. (2009). AquaCrop – The FAO crop model to simulate yield response to water: II. Main algorithms and software description. Agronomy Journal 101, 438-447. https://doi-org.ufs.idm.oclc.org/10.2134/agronj2008.0140s

Raes, D., Van Goidsenhoven, B., Goris, K., Samain, B., De Pauw, E., El Baba, M., Tubail, K., Ismael, J., De Nys, E. (2001). BUDGET, a management tool for assessing salt accumulation in the root zone under irrigation. 4th Inter Regional Conference on Environment-Water, ICID. 27-30 Aug., Fortaleza, Brazil: 244-252.

Reca, J., Roldan, J., Alcaide, M., Lopez, R. and Camacho, E. (2001). Optimisation model for water allocation in deficit irrigation systems I. Description of the model. Agricultural Water Management, 48: 103-116.

Rehman, T. and Romero, C. (1993). The application of the MCDM paradigm to the management of agricultural systems: some basic considerations. Agricultural Systems 41, 239-255.

Ren, D., Xu, X., Hao, Y., Huang, G. (2016). Modeling and assessing field irrigation water use in a canal system of Hetao, upper Yellow River basin: Application to maize, sunflower and watermelon. J. Hydro. 532, 122-139.

Ren, D., Xu, X., Huang, Q., Huo, Z. (2018). Analyzing the Role of Shallow Groundwater Systems in the Water Use of Different Land-Use Types in Arid Irrigated Regions. *Water,* 10(5): 634.

Ritchie, J.T. (1972). Model for predicting evaporation from a row crop with incomplete cover. Water Resour. Res. 8, 1204-1213.

Ritchie, J.T. (1972). Model for predicting evaporation from a row crop with incomplete cover. Water Resour. Res. 8, 1204-1213.

Ritchie, J.T. (1981). Water dynamics in the soil-plant-atmosphere system. Plant Soil 58, 81-96.

Ritzema, H.P., (1994). Subsurface Flow to Drains. Technical Report 16. Wageningen.

Rizzo, G., Edreira, J.I.R., Archontoulis, S.V., Yang, H.S., & Grassini, P. (2018). Do shallow water tables contribute to high and stable maize yields in the US Corn Belt? *Global Food Security,* 18: 27-34.

Robert, M., Dury, J., Thomas, A., Theron, O., Sekhar, M., Badiger, S., Ruiz, L. and Bergez, J. (2016). CMFDM: A methodology to guide the design of a conceptual model of farmers' decision-making processes. Agricultural Systems, 148: 86-94.

Robert, M., Thomas, A., Sekhar, M., Badiger, S., Ruiz, L., Raynal, H. and Bergez, J. (2017). Adaptive and dynamic decision-making processes: A conceptual model of production systems on Indian farms. Agricultural Systems, 157: 279-91.

Sadati, S.K., Speelman, S., Sabouhi, M., Gitizadeh, M., Ghahraman, B. (2014). Optimal irrigation water allocation using a genetic algorithm under various weather conditions. Water 6(10):3068-3084. https://doi.org/10.3390/w6103068

Schaap, M.G. (2004). Graphic user interfaces for pedotransfer functions. In.: Pachepsky, Ya., Rawls, W.J. (Eds), Developments in soil science volume 30. Development of pedotransfer functions in soil hydrology. Elsevier, Amsterdam.

Schütze, N., Paly, M. and Shamir, U. (2012). Novel simulation-based algorithms for optimal open-loop and closed-loop scheduling of deficit irrigation systems. J. Hydroinf. 14 (1) 136-151. https://doi.org/10.2166/hydro.2011.073

Sedaghatdoost, A., Ebrahimian, H. and Liaghat, A. (2019). Water Resour Manage 33: 1383. https://doi.org/10.1007/s11269-019-2191-x

Seidel, S.J., Palosuo, T., Thorburn, P., Wallach, D. (2018). Towards improved calibration of crop models – Where are we now and where should we go? European Journal of Agronomy 94, 25-35. https://doi.org/10.1016/j.eja.2018.01.006

Shelia, V., Šimunek, J., Boote, K., Hoogenbooom, G. (2018). Coupling DSSAT and HYDRUS-1D for simulations of soil water dynamics in the soil-plant-atmosphere system. J. Hydrol. Hydromech. 66, 232-245.

Shirazi, S.Z., Mei, X., Liu, B., Liu, Y. (2021). Assessment of the AquaCrop model under different irrigation scenarios in the North China Plain. Agricultural Water Management 257, 107120. https://doi.org/10.1016/j.agwat.2021.107120

Shrestha, N., Raes, D., Vanuytrecht, E., Sah, S.K. (2013). Cereal yield stabilisation in Terai (Nepal) by water and soil fertility management modeling. Agricultural Water Management 122, 53-62.

Silvestro, P.C., Pignatti, S., Pascucci, S., Yang, H., Li, Z., Yang, G., Huang, W., Casa, R. (2017). Estimating wheat yield in China at the field and district scale from the assimilation of satellite data into the AquaCrop and simple algorithm for yield (SAFY) models. Remote Sensing 9, 509. http:// doi:10.3390/rs9050509

Šimůnek, J., and de Vos, J. A. (1999). Inverse optimization, calibration and validation of simulation models at the field scale. In J. Feyen, & K. Wiyo (Eds.), Modelling of transport processes in soils at various scales in time and space; international workshop of EurAgEng's field of interest on soil and water. Wageningen, Wageningen Pers, 1999 (pp. 431-445)

Šimůnek, J., Hopmans, J.W. (2009). Modeling compensated root water and nutrient up-take. Ecol. Model. 220, 505-521.

Šimůnek, J., van Genuchten, M. Th., Šejna, M. (2012). HYDRUS: Model use, calibration and validation. ASABE 55, 1261-1274.

Singels A. and Smith M.T. (2009) Real Time Irrigation Advice for Small-Scale Sugarcane Production Using A Crop Model. WRC Report No. K5/1576/4. Water Research Commission, Pretoria, South Africa. 147 pp

Skaggs, T.H., Van Genuchten, M.T., Shouse, P.J., Poss, J.A. (2006). Macroscopic approaches to root water uptake as a function of water and salinity stress. Agric. Water Manage. 86, 140-149.

Soil Classification Working Group (1991). Soil classification: a taxonomic system for South Africa. Memoirs on the Agricultural Natural Resources of South Africa No 15. Department of Agricultural Development, Pretoria, South Africa.

Soil Survey Staff (2003). Keys to Soil Taxonomy. United States Department of Agriculture. Natural Resource Conservation Service.

Streuderst, G. (1985). Regressiemodel vir die voorspelling van grondwaterpotensiaal in geselekteerde gronde. M.Sc. dissertation, University of the Free State, Bloemfontein.

SSSA (2008). Glossary of Soil Science Terms 2008. Soil Science Society of America. Soil Science.

Steduto, P., Hsiao, T.C., Fereres, E. (2007). On the conservative behaviour of biomass water productivity. Irri. Sci. 25, 189-207.

Steduto, P., Hsiao, T.C., Raes, D., Fereres, E. (2009). AquaCrop – the FAO crop model to simulate yield response to water: I. Concepts and underlying principles. Agron. J. 101, 426-437.

Steduto, P., Hsiao, T., Fereres, E., Raes, D. (2012). Crop yield response to water. Food and Agriculture Organization of the United Nations, Rome, 2012. FAO irrigation and drainage paper-No. 66, ISBN 978-92-5-107274-5.

Stewart, J.I. and Hagan, R.M. (1973). Function to predict effects of crop water deficits. Journal of the Irrigation and Drainage Division, 99(IR4): 421-439.

Sun, M., Zhang, X., Huo, Z., Feng, S., Huang, G., Mao, X. (2016). Uncertainty and sensitivity assessments of an agricultural-hydrological model (RZWQM2) using the GLUE method. Journal of Hydrology 534, 19-30. https://doi.org/10.1016/j.jhydrol.2015.12.045

Sun, G., Zhu, Y., Ye, M., Yang, J., Qu, Z., Mao, W., Wu, J. (2019). Development and application of long-term root zone salt balance model for predicting soil salinity in arid shallow water table area. Agric. Water Manage. 213, 486-498.

Tenreiro, T.R., García-vila, M., Gómez, J.A., Jimenez-berni, J.A., Fereres, E. (2020). Water modelling approaches and opportunities to simulate space of what the radiations at crop field level. Agric. Water Manage. 240, 106254.

Van Dam, J.C., Feddes, R.A. (2000). Numerical simulation of infiltration, evaporation and shallow groundwater levels with the Richard's equation. J. Hydrol. 233, 72-85.

Van Dam, J.C., Huygen, J., Wesseling, J.G., Feddes, R.A., Kabat, P., Van Walsum, P.E.V., Groenendijk, P., Van Diepen, C.A. (1997). Theory of SWAP Version 2.0: Simulation of Water Flow, Solute Transport and Plant Growth in the Soil-Water-Atmosphere-Plant Environment. Technical report. DLO Winand Staring Centre.

Van Der Laan, M., Annandale, J.G., Bristow, K.L., Du Preez, C.C., Tesfamariam, E. and Stirzaker, R.J. (2009). Modelling the effects of nitrogen and phosphorus stress on crop growth using SWB-Sci: An example using maize. Working Paper. University of Pretoria.

van Genuchten, M.T. (1980). A closed-form equation for predicting the hydraulic conductivity of unsaturated soils. Soil Sci. Soc. Am. J. 44, 892-898.

Van Genuchten, M.T. (1982). A comparison of numerical solutions of the one-dimensional unsaturated-saturated flow and transport equations. Adv. Water Resour. 5, 47-55.

Van Genuchten, M.Th., Leij, F.J., Yates, S.R., (1991). The RETC code for quantifying the hydraulic functions of unsaturated soils, Version 1.0. EPA Report 600/2-91/065, U.S. Salinity Laboratory, USDA, ARS, Riverside, California.

Van Heerden P.S. and Walker S. (2016). Upgrading of SAPWAT3 as a management tool to estimate the irrigation water use of crops. Revised edition. SAPWAT4. WRC Report No: TT 662/16. Water Research Commission, Pretoria, South Africa.

Van Ittersum, M.K., Leffelaar, P.A., van Keulen, H., Kropff, M.J., Bastiaans, L., Goudriaan, J. (2003). On approaches and applications of the Wageningen crop models. Eur. J. Agron. 18, 201-234.

Van Rensburg, L.D., Barnard J.H., Bennie, A.T.P., Sparrow, J.B., Du Preez, C.C. (2012). Managing salinity associated with irrigation at Orange-Riet and Vaalharts Irrigation Schemes. Water Research Commission Report No. 1647/1/12, Pretoria, South Africa.

Vanuytrecht, E., Raes, D., Willems, P. (2014). Global sensitivity analysis of yield output from the water productivity model. Environmental Modelling and Software 51, 323-332. https://doi: 10.1016/j.envsoft.2013.10.017.

Vaux, H.J. and Pruit, W.O. (1983). Crop water production function, in D.I. Hillel (Editor), Advances in Irrigation. Vol. II Academic Press, New York, pp. 61-97.

Venter M., Grové, B. and Van Der Stoep I. (2017) The optimisation of electricity and water use for sustainable management of irrigation farming systems. WRC Report No. TT 717/17. Water Research Commission, Pretoria, South Africa. 186 pp

Villalobos, F.J., Fereres, E. (1990). Evaporation measurements beneath corn, cotton, and sunflower canopies. Agronomy Journal 82, 1153-1159.

von Hoyningen-Huene, J. (1981). Die Interzeption des Niederschlags in land-wirtschaftlichen Pflanzenbeständen. Arbeitsbericht Deutscher Verband für Wasserwirtschaft und Kulturbau, DVWK.

Wagner, M.P., Slawig, T., Taravat, A., Oppelt, N. (2020). Remote sensing data assimilation in dynamic crop models using particle swarm optimisation. International Journal of Geo-Information 9, 105. http:// doi:10.3390/ijgi9020105

Wallach, D., Palosuo, T., Thorburn, P., Hochman, Z., Gourdain, E., Andrianasolo, F., Asseng, S., Basso, B., Buis, S., Crout, N., Dibari, C., Dumont, B., Ferrise, R., Gaiser, T., Garcia, C., Gayler, S., Ghahramani, A., Hiremath, S., Hoek, S., Horan, H., Hoogenboom, G., Huang, M., Jabloun, M., Jansson, P., Jing, Q., Justes, E., Kersebaum, K.C., Klosterhalfen, A., Launay, M., Lewan, E., Luo, Q., Maestrini, B., Mielenz, H., Moriondo, M., Zadeh, H.N., Padovan, G., Olesen, J.E., Poyda, A., Priesack, E., Pullens, J.W.M., Qian, B., Schütze, N., Shelia, V., Souissi, A., Specka, X., Srivastava, A.K., Stella, T., Streck, T., Trombi, G., Wallor, E., Wang, J., Weber, T.K.D, Weihermüller, L., de Wit, A., Wohling, T., Xiao, L., Zhao, C., Zhu, Y., Seidel, S.J. (2021). The chaos in calibrating crop models: Lessons learned from a multi-model calibration exercise. Environmental Modelling and Software 145, 105206. https://doi.org/10.1016/j.envsoft.2021.105206

Wang, X., Yang, J., Yao, R., Yu, S. (2014). Irrigation regime and salt dynamics for rice with brackish water irrigation in coastal region of North Jiangsu province. Transactions of the Chinese Society of Agricultural Engineers 30, 54-63.

Warrick, A.W. (1991). Numerical approximations of darcian flow through unsaturated soil. Water Resour. Res. 27, 1215-1222.

Xu, L.K., Hsiao, T.C. (2004). Predicted vs. measured photosynthetic water use efficiency of crops stands under dynamically changing field environments. J. Exp. Bot. 55, 2395-2411.

Xu, X., Huang, G., Sun, C., Pereira, L.S., Ramos, T.B., Huang, Q., Hao, Y. (2013). Assessing the effects of water table depth on water use, soil salinity and wheat yield: Searching for a target depth for irrigated areas in the upper Yellow River basin. Agric. Water Manage. 125, 46-60.

Xu, X., Huang, G., Zhan, H., Qu, Z., Huang, Q. (2012). Integration of SWAP and MODFLOW-2000 for modelling groundwater dynamics in shallow water table area. J. Hydro. 412-413, 170-181.

Xu, X., Sun, C., Qu, Z., Huang, Q., Ramos, T.B., Huang, G. (2015). Groundwater recharge and capillary rise in irrigated areas of the Upper Yellow River basin assessed by an Agro-hydrological model. Irri. Draing. 64, 587-599.

Xue, J., Huo, Z., Wang, F., Kang, S., Huang, G. (2018). Untangling the effects of shallow groundwater and deficit irrigation on irrigation water productivity in arid region: New conceptual model. Sci. Total Environ. 619-620, 1170-1182.

Yang, Y., Watanabe, M., Zhang, X., Hao, X., Zhang, J. (2006). Estimation of groundwater use by crop production simulated by DSSAT-wheat and DSSAT-maize models in the piedmont region of the North China Plain. Hydrol. Process. 20, 2787-2802.

Yim, O., and Ramdeen, K.T. (2015). Hierarchical Cluster Analysis: Comparison of Three Linkage Measures and Application to Psychological Data. The Quantitative Methods for Psychology, 11(1): 8-21.

Zaidel, J., Russo, D. (1992). Estimation of finite difference interblock conductivities for simulation of infiltration into initially dry soils. Water Resour. Res., 28, 2285-2295.

Zhao, Y., Li, F., Wang, Y., Jiang, R. (2020). Evaluating the effect of groundwater table on summer maize growth using the AquaCrop model. Environ. Model Assess. 25, 343-353.

APPENDIX A: CONSOLIDATED STUDENT CAPACITY BUILDING AND KNOWLEDGE DISSEMINATION

STUDENT CAPACITY BUILDING

Two M.Sc. Agric students majoring in Agricultural Economics from the University of the Free State have worked actively on the project. Both students graduated before the final completion of the project. The abstracts of their research follow.

Erasmus, J.C. (2023).

Bio-economic analysis of the contribution of shallow water tables to irrigated maize production. M.Sc. Agric dissertation, Department of Agricultural Economics, University of the Free State.

ABSTRACT

The main objective of this study is to evaluate the economic benefits of using shallow groundwater as an alternative irrigation water source for two water table scenarios. The bio-economic simulation model was developed to address the main objective of the research. The model includes a calibrated and validated biophysical model that simulates the effect of using surface water in conjunction with shallow groundwater for maize production and an economic module that determines the margin above specified costs when applying the conjunctive water-use irrigation strategies. The bio-economic simulation model was applied on a farm in the Orange-Riet Irrigation Scheme in the Northern Cape to evaluate the economic benefits of using shallow groundwater as an alternative irrigation water source for maize produced on a 1 m and 1.5 m constant groundwater table Clovelly soil. The bio-economic simulation model was used to determine the economics of using farmer irrigation strategies where irrigation water is distributed optimally, and the quantity of water applied is decided without considering the shallow groundwater table. An optimisation component was added to the bio-economic simulation model to determine the economics of conjunctive irrigation management decisions. The results show that the optimal conjunctive-water use irrigation strategies generated for the 1 m and 1.5 m groundwater table Clovelly soils utilised more water from the shallow groundwater tables than the optimised farmer baseline irrigation strategies. The utilisation of the groundwater tables, however, resulted in the following: conjunctive water use strategies would use significantly less irrigation water (24 mm on a 1 m and 54 mm on a 1.5 m groundwater table); yields were slightly lower than obtained with the baseline irrigation strategies (but with no significant difference); drainage was reduced to almost zero in the drier production years and nearly 50% less in the wet production years; far lower water and electricity costs in comparison to the baseline strategies which ultimately resulted in a larger margin above the specified costs for the optimal irrigation strategies. The two main conclusions drawn from the study. Firstly, farmers who do not consider the shallow groundwater table when making irrigation decisions would over-irrigate their crop, which could lead to crop losses. Secondly, shallow groundwater is an economically valuable alternative irrigation source.

Hadebe, M.R. (2023).

The economic value of soil-water information in irrigated maize production with shallow groundwater tables. M.Sc. Agric dissertation, Department of Agricultural Economics, University of the Free State.

ABSTRACT

Due to water scarcity and competing demands, irrigated agriculture (as the bulk user of freshwater resources worldwide and in South Africa) is expected to use water efficiently, which involves exploring the use of Root Accessible Water Tables (RAWT) when scheduling irrigation. Earlier studies have shown that RAWT uptake can potentially contribute about forty percent or more to the crop water demand during the growing season. However, farmers do not consider the information on RAWT uptake when scheduling irrigation, and this was true for the largest and oldest irrigation scheme in South Africa. The main objective of the study was, therefore, to evaluate the economic benefits and improvements in irrigation water use efficiency associated with considering RAWT's contribution to crop water demand in irrigation scheduling decisions in light of unfolding information about the soil-crop-atmosphere continuum for the Vaalharts irrigation scheme. The research first developed a bio-economic simulation model consisting of a crop growth simulation model (SWAP-WOFOST) with dynamic soil water flow calculations and an economic model to simulate the financial implications of the current irrigation practice of satisfying crop water requirements without considering the contribution of RAWT. The developed bio-economic simulation model was then coupled to a Differential Evolutionary (DE) algorithm to optimise irrigation scheduling decisions where the contribution of RAWT to satisfying crop water demand was considered. Research results indicate that the RAWT contribute significantly to crop water demand (expected value of 51%), and when information regarding RAWT uptake is used, there are increases in margins due to the less applied irrigation water, which results in reduced irrigation-dependent costs. The less applied irrigation water will result in significant water savings for large, irrigated areas. Based on the results, the study recommends that irrigators should invest in technology that provides information regarding RAWT uptake. The study further recommends that future research investigate the hydrological impact of large-scale adoption of water use from RAWT.

KNOWLEDGE DISSEMINATION

SANCID Symposium presentation

Grové, B. and Barnard, J.H. (2023). *DECAL: Economic management of conjunctive use of irrigation water and shallow groundwater. Symposium presentation.* South African National Commission on Irrigation and Drainage Symposium on "Research and innovation towards meeting new challenges and a thriving irrigation sector", Tzaneen, 21-23 February 2023.

Scientific paper

Barnard, J.H. and Grové, B. (2023). Calibrating AquaCrop using an evolutionary algorithm with limited measured variables in the objective function. Submitted to *Agricultural Water Management.*

Hadebe, M.R., Grové, B., Matthews, N. and Barnard, J.H. Bio-economic analysis of irrigation scheduling considering shallow groundwater: lessons from South Africa. Submitted to *Science of the Total Environment.*

GWK Farmers Day

Barnard, J.H. and Grové, B. (2023) Importance of considering root accessible soil water in irrigation scheduling

Popular paper

Barnard, J.H., Du Preez, C., Grové, B. and Ceronio, G. (2023) Beste praktyke: lesse van plase in sentraal-Suid-Afrika. Graan SA, Oktober, 2023.

APPENDIX B: DATA ARCHIVING

Prof Bennie Grové
Department of Agricultural Economics
University of the Free State
Bloemfontein
9300
Tel: 051 401-3359
Cell: 0833841987
Email: groveb@ufs.ac.za